UNIVERSITY OF CALIFORNIA, SAN DIEGO

DECELLULARIZED BIOMATERIALS FOR CELL CULTURE AND REPAIR AFTER ISCHEMIC INJURY

A dissertation submitted in partial satisfaction of the requirements for

the degree Doctor of Philosophy

in

Bioengineering

by

Jessica Ann DeQuach

Committee in charge:

Professor Karen L. Christman, Chair
Professor Shu Chien
Professor Adam Engler
Professor Kirk Knowlton
Professor Farah Sheikh

2012

The dissertation of Jessica Ann DeQuach is approved, and it is acceptable in quality and form for publication on microfilm and electronically:

Chair

University of California, San Diego

2012

DEDICATION

For my family.

TABLE OF CONTENTS

LIST OF FIGURES

LIST OF TABLES

ACKNOWLEDGEMENTS

I would like to acknowledge the numerous people that have contributed to this work or who have enhanced my personal and professional development.

First, I would like to thank Dr. Karen Christman, my advisor, who has provided me with such guidance and has allowed me to take creative license with my research. Karen has been a wonderful mentor, and has given me opportunities to grow as a graduate student and as a person. With her support I have been able to explore my research and also consider my path after graduate school. It has also been wonderful to have joined early in the lab, and to watch the lab, and the students grow and develop under Karen's leadership.

My committee members have provided me with their guidance and expertise and helped mold the direction of my research. First, Dr. Shu Chien who is one of the most amazing faculty members that I have ever met, has always made me feel welcome to come and talk in his office. He has always been a constant source of support throughout my graduate career. Dr. Adam Engler has provided great insight into asking questions about my work that has made my research stronger, and has increased my ability to think critically. Dr. Kirk Knowlton has provided the clinical perspective on my committee, also has been great help with my research. Dr. Farah Sheikh has been a wonderful collaborator and has brought her expertise our meetings. And though not officially on my committee, Dr. Sylvia Evans has been on my California Institute of Regenerative Medicine (CIRM) scholarship committee and has listened to me present my work in the early stages, and contributed to my development as a researcher. It has been such an honor to work with each of my committee members at UC San Diego.

I would also like to acknowledge all of the graduate students and post-doctoral students that I have collaborated with while in graduate school. Dr. Ralf Dirschinger patiently taught me everything about stem cell culture and helped me during my first two years in graduate school. I would also like to thank Dr. Valeria Mezzano who has pointed me in the right direction for my skeletal muscle project. Additionally, Dr. Shauna Yuan has been wonderful to work with, and has given me support with my brain matrix project and we have had really great discussions about research together. And I have had a great collaboration with Boris Babenko, on studying the automation of vessel counting and other images, which has ventured into a collaboration in a new field.

Other that I need to acknowledge include Ryan Anderson at the CalIT2 Nano3 Facility for teaching me how to use the critical point dryer and scanning electron microscope, and for answering random technical questions. Additionally, I would like to think Carolina Rogers for her help with the porcine tissue collection, and Dr. Majid Ghassemian for his help with mass spectrometry.

I would like to thank Dr. Robert Sah for his help during my graduate career. He was one of the first faculty members that I met at UC San Diego and encouraged me to join the program when I was debating which graduate school to attend. His continued assistance throughout the years has been wonderful. Additionally, Dr. John Watson, whom I first met during my planning of Bioengineering Day, has been a wonderful mentor who has helped me with my outreach efforts and who I know I can always talk to.

I have also had the pleasure to work with wonderful people in the Bioengineering Department while planning events such as Bioengineering Day, and Graduate Research Symposium. Specifically Lisa Dieu, who has been indispensible for making these events a success and who has become a great friend. I would also like to thank Justin Grevich and

John Rowan for creating the Bioengineering Day website, Cody Noghera for his help with the Corporate Affiliates Program and Steve Lopez for helping out with the event. I would also like to acknowledge my co-chair for both of these events, Angelina Altshuler, who I have thoroughly enjoyed working with while planning these events to bring together faculty, alumni, and students. For planning our heart valve booth to exhibit at the inaugural USA Science and Engineering Festival, I would also like to again thank Angelina Altshuler as well as Carolyn Schutt and Adam Young who were on the planning committee with me.

From the student affairs office, I would like to thank Jan Lenington for always answering my questions. And from the administrative office, I would like to thank Yanna Campen for helping me with reimbursement forms.

I would also like to especially thank the members of the Christman Lab, who I have spent countless of hours with, and who are not just my labmates, but also my friends. First, Dr. Jennifer Singelyn who has taught me so much and who has worked with me at being a better presenter, and I have improved so much with her help. Aboli Rane, who convinced me to join this lab, and who has become one of my closest friends in San Diego. Adam Young who taught me PCR, and who became my conference-attending buddy. Sonya Seif-Naraghi, my shopping pal, who has edited my papers and helped make me into a stronger writer. Stephen Lin, who is a night owl, like me, and who teaches me fun tricks in lab. Nikhil Rao, who introduces me to good music, and who has also helped me with PCR. Todd Johnson, my decellularization partner, and who makes me laugh when we are trying to push up our goggles on the glass of the fume hood. Sophia Suarez and Jean Wang, who have recently joined the lab, and I know they will do great research in the future. I would also like to thank Dr. Airong Song (and his wife Dr. Nina Song,

who have the cutest baby in the world), who has taught me a little bit about chemistry. And Dr. Greg Grover, who I have been collaborating with, has given me career advice and has also made me more comfortable with chemical reactions. Aubrey Smith, who was a visiting CIRM student, was wonderful to work with and mentor. I would also like to acknowledge the visiting scholars that I have interacted with, Denver Faulk, Michael Salvatore, Kristina Javor, and Nadine Leenders.

Pam Schup-Magoffin and Diane Hu, the lab managers and small animal surgeons of the lab, I would like to thank for their help with my animal studies. Diane was absolutely instrumental toward the success of my peripheral artery disease study, and Pam helped me with assessing gelation of the material. I would also like to thank Rebecca Braden, our lab manager, for helping me with her expertise at DNA extraction.

I would like to thank the members of the Engler lab who have helped me with my research. Dr. Yu Suk Choi, Andrew Holle, Gauruv Kaushik, Justin Tse, Ludovic Vincent, and Jennifer Young. I would also thank Angelina Altshuler from Dr. Schmid-Schonbein's lab for teaching me how to run Western Blots. Additionally, I would like to acknowledge Barb Schumacher, Elaine Chan, Eun Hee Han, Michelle Temple, Van Wong and Brad Hansen from Dr. Sah's lab for their help during my rotation.

At this point I would like to thank all of the undergraduate students that I have had the privilege to mentor. In chronological order, Michael Angelo, Amar Miglani, Stephen Lin, Cynthia Cam, Holly Arnold, Joy Lin, Anthony Monteforte, Clifford Mao and Raymond Paseman. You have taught me so much and I hope that you have also learned from me. Additionally, I would like to mention other undergraduate students in the lab who have helped me in one way or another, Dina Ibrahim, Dinah Horn, Vaibhav Bajaj, Jessica Hsieh and Samantha Evans.

I would like to thank Dr. Larry Goldstein and Jennifer Braswell who direct the California Institute for Regenerative Medicine (CIRM) Pre-doctoral Fellowship Program. Also I was the recipient of the Class of 2012 Siebel Scholarship, for which I would like to thank Tom Siebel and the Siebel Foundation, as well Dr. Karen Christman, Dr. Shu Chien, Jenny Hildebrand, and Karen Roter Davis.

Finally, I would like to thank my family, for always believing in me and for encouraging me to strive for excellence in graduate school.

The following chapters are, in part, reprints of the following publications:

Chapter 2, in part, is a reprint of material that is published as: DeQuach, JA, Mezzano V, Miglani A, Lange S, Keller GM, Sheikh F, Christman KL. Simple and high yielding method for preparing tissue specific extracellular matrix coatings for cell culture. PLoS ONE, 2010; 5 (9): e13039.

Chapter 2, in part, is a reprint of material that is published as: Singelyn JM*, DeQuach JA*, Seif-Naraghi SB, Littlefield RB, Schup-Magoffin PJ, Christman KL. Naturally derived myocardial matrix as an injectable scaffold for cardiac tissue engineering. Biomaterials 2009;30(29):5409-16. *Shared first author.

Chapter 2, in part, is in submission as: DeQuach JA, Lin JE, Cam C, Hu D, Salvatore MA, Sheikh F, Christman KL. Injectable skeletal muscle matrix hydrogel promotes neovascularization and muscle cell infiltration in a hindlimb ischemia model.

Chapter 3, in part, is in submission as: DeQuach JA, Lin JE, Cam C, Hu D, Salvatore MA, Sheikh F, Christman KL. Injectable skeletal muscle matrix hydrogel promotes neovascularization and muscle cell infiltration in a hindlimb ischemia model.

Chapter 5, in full, is published as: DeQuach JA, Yuan SH, Goldstein LSB, Christman KL. Decellularized porcine brain matrix for cell culture and tissue engineering scaffolds. Tissue Engineering Part A, accepted with special recognition for the Mary Ann Liebert Inc. Outstanding Student Award.

The author of this dissertation is one of the primary authors or co-author on all publications.

VITA

EDUCATION

March 2012	Ph.D., Bioengineering Department of Bioengineering University of California, San Diego
June 2009	M.S., Bioengineering Department of Bioengineering University of California, San Diego
May 2007	B.S., Biomedical Engineering Department of Biomedical Engineering Case Western Reserve University

AWARDS AND HONORS

Mary Ann Liebert Inc., Outstanding Student Award, Tissue Engineering and Regenerative Medicine International Symposium, 2011
Siebel Scholar, Class of 2012
Student Travel Achievement Recognition Honorable Mention, Society for Biomaterials, 2011
The Grand Challenge Finalist, Telemedicine and Advanced Technology Research Center, 2010
Distinguished Oral Presentation, 10th Annual UC Bioengineering Symposium, 2009
Pre-doctoral Fellowship, California Institute of Regenerative Medicine, 2009

SELECTED PATENTS AND PUBLICATIONS

Karen L. Christman, Jennifer M. Singelyn, **Jessica A. DeQuach**. *Compositions and Methods of Tissue Repair with Extracellular Matrices* (PCT/US09/59015), Submitted.

JM Singelyn*, **JA DeQuach***, SB Seif-Naraghi, RB Littlefield, PJ Schup-Magoffin, KL Christman. *Naturally derived myocardial matrix as an injectable scaffold for cardiac tissue engineering.* Biomaterials, 2009. *Shared first author

ABSTRACT OF THE DISSERTATION

DECELLULARIZED BIOMATERIALS FOR CELL CULTURE AND REPAIR AFTER ISCHEMIC INJURY

by

Jessica Ann DeQuach

Doctor of Philosophy in Bioengineering

University of California, San Diego, 2012

Professor Karen L. Christman, Chair

Ischemic disease, which involves tissue death and dysfunction due to vessel blockage, is one of the largest causes of morbidity and mortality across the world. Ischemia that targets the brain can lead to a stroke, which causes functional impairment. Blockage of the coronary artery can lead to a myocardial infarction (MI) which can eventually lead to heart failure. Ischemia of the vessels in the skeletal muscle causes

peripheral artery disease, which can lead to tissue damage that may necessitate amputation of the affected limb. The severity of the downstream effects of ischemia indicates the need for some sort of treatment to repair the tissue after ischemic attack. Yet, there are few clinical treatments available for patients, creating a need for novel therapies for treating this disease. The use of biomaterials in tissue engineering strategies have recently been studied to alleviate these conditions, however this approach has been met with limited success as many of these therapies require an invasive surgery for delivery to the affected site. Injectable biomaterials offer the advantage of minimally invasive delivery to improve patient outcomes, which would be attractive to reduce patient recovery time. The materials that have been studied often do not mimic the microenvironment of the tissue that it is trying to repair. This is similar to how cells are often cultured on a substrate that do not mimic the *in vivo* environment, which may be important for assessing cellular function.

Thus, the objective of this dissertation was to generate biomaterials derived from decellularized tissue from the brain, skeletal muscle, and cardiac tissue, and test whether they could be used as cell culture platforms that would provide biomimetic substrates and be used as scaffolds for tissue engineering. In this work, I have developed a method to decellularize each tissue leaving behind only the extracellular matrix. The matrix material was then characterized using gel electrophoresis, mass spectrometry, glycosaminoglycan quantification and DNA quantification, indicating that the cellular remnants have been removed, but that the biocomplexity has been retained. These tissue specific biomaterials were tested as a cell culture coating platform *in vitro* and as a potential therapy for ischemia *in vivo*.

The material was enzymatically digested and used as a cell culture coating and compared to conventionally used substrates. It was found that progenitor cells cultured on the tissue-matched coatings display a more mature morphology on the decellularized extracellular matrix (ECM) coatings. For instance, skeletal muscle progenitors differentiate into larger, thicker myotubes, cardiomyocytes derived from human embryonic stem cells localize their intracellular junctions into a more mature organization, and neurons from induced pluripotent stem cells display a clear axon and increased dendritic branching. The maturation of these cell types on the coatings demonstrate a more *in vivo* like phenotype which could be useful for studying cellular behavior and to translate *in vitro* findings into an *in vivo* setting. This material was able to self-assemble upon injection *in vivo*, forming a nanofibrous and porous scaffold that could be used as an injectable biomaterial for ischemic repair. Additionally, *in vitro* assays measuring proliferation and migration show that some of the matrix materials act as a chemoattractant and as a mitogenic agent on cells in culture.

The skeletal muscle matrix has been used in a rat hindlimb ischemia model and compared to a collagen scaffold. It was shown that the skeletal muscle matrix stimulates increased neovascularization, which is important for bringing blood flow to an ischemic region, as well as recruits endogenous muscle progenitor cells into the scaffold. The cardiac matrix is able to gel *in situ* upon injection and has been explored by others in our lab. The brain matrix was also able to self-assemble and form a gel after subcutaneous injection into a mouse, demonstrating proof-of-concept for its use as a tissue engineering scaffold.

To investigate whether the material might be derived from an allogeneic source instead of from porcine origin, the decellularization process was also performed on

human cardiac tissue. It was found that additional steps were needed to fully decellularize the material and render it into a usable form. However, this could provide a potentially allogeneic source for this material.

This work demonstrates that decellularized extracellular matrices derived from various tissues provide a biomimetic platform for cell culture that increases maturation of progenitor and stem cells cultured upon the surface. The maturation of these cells could be important for understanding and regulating cellular processes. The same material can be used as an injectable scaffold that could be delivered through minimally invasive means to treat ischemic damage in the brain, heart and skeletal muscle. When applied in a hindlimb ischemia model, the skeletal muscle matrix is able to increase neovascularization, recruit more muscle progenitor cells, and recruit more proliferating muscle cells when compared to a collagen control. This work shows that decellularized matrices hold great potential for both *in vitro* and *in vivo* applications.

CHAPTER ONE:

Introduction

1.1 Ischemia: general pathophysiology

Ischemic tissue disease is one of the largest causes of morbidity and mortality across the world. Ischemia occurs due to a restriction in blood supply, generally due to occlusion or blockage of the blood vessels [1]. Ischemia may occur due to vasoconstriction, thrombosis or embolism, in these cases a blockage or narrowing of the vessel causes lack of blood flow and hence a shortage of oxygen, glucose and other nutrients in the blood. The resultant lack of blood supply damages the tissue, and if the blood flow is not restored quickly enough, this damage is irreversible. Unfortunately, restoration of the blood flow after a period of ischemia can be as damaging as the initial ischemia itself. The reintroduction of oxygen causes a greater production of damaging free radicals and influx of calcium, which leads to mitochondrial dysfunction[2] and the release of pro-apoptotic proteins that can trigger cell death [3,4]. This is termed reperfusion injury [1,5] which is an important clinical concern to address when the disease state involves the potential for such an injury, such as during heart attack, stroke, free flap transfer, tissue allotransplantation, and peripheral artery disease [6].

The two best-known forms of ischemic attack are strokes and heart attacks. Strokes, or transient ischemic attacks, are due to a blockage of an artery that leads into the brain, and can lead to death of brain tissue. When this occurs in a coronary artery, it causes a myocardial infarction, also called a heart attack or coronary event. Peripheral tissues can also be affected by ischemia – peripheral artery disease affects the skeletal muscle downstream of the artery. If left untreated, this condition can escalate into critical limb ischemia and eventual amputation. With these types of diseases, there usually is long-term degeneration of the tissue after the initial attack, and few therapies can improve functional outcome. Ongoing research in the fields of tissue engineering and biomaterials

attempts to design therapies to restore or improve blood flow to the damaged region and stimulate endogenous repair.

1.2 Peripheral artery disease

Peripheral artery disease (PAD) is a common condition in which blood flow is reduced to the leg and feet [7,8] and affects ~ 27 million people in the Western world[9] [10]. Studies demonstrate that irreversible muscle damage can start after 3 hours of ischemia and is nearly complete at 6 hours, for acute instances [11,12]. With an aging population and prevalence of diabetes mellitus, the incidence of this vascular disease is increasing at an alarming rate [13,14]. Critical limb ischemia (CLI) is the most advanced form of PAD, often leading to amputation of the limb and potential mortality [15,16]. The only current clinical treatment for PAD and CLI is endovascular or surgical revascularization [16], however other strategies to improve limb perfusion are underway. Surgical bypass was the established standard, but recently endovascular therapies such as angioplasty, atherectomy and stenting are used as less-invasive options. However, despite these therapies, CLI continues to carry a major risk of limb amputation, with rates that have not changed significantly in 30 years [17].

1.2.1 Biomaterial therapies for peripheral artery disease

Recently, several clinical trials using cell therapy have demonstrated promising results [18-21], but there are still many questions about which therapeutic cell type to use, quantity of cells, and best route to deliver the cells, as well as a significant problem with poor cell retention and survival [20]. Biomaterials scaffolds have more recently been explored to enhance cell survival by providing a temporary mimic of the extracellular

matrix (ECM) [19,22]. Biomaterials have also been used for delivery of growth factors or their mimics in animal models of PAD and CLI [19,22-24]. However, these scaffolds are composed of fibrin [22], collagen-based matrix [25], gelatin [26], self assembling peptide amphiphiles [24] or alginate [23], which may not provide the proper biomimetic environment for the ischemic skeletal muscle in these conditions. A decellularized skeletal muscle scaffold had been previously explored for replacement of a muscle defect [27], yet this intact scaffold would not be amenable to a minimally invasive method of treating peripheral artery disease.

1.3 Myocardial infarction

Heart failure after a myocardial infarction continues to be the leading cause of death in the western world. Over 7 million people in the United States have suffered a myocardial infarction, and almost 5 million suffer from heart failure [28]. Myocardial infarction is the occlusion of a coronary artery which is often caused by the accumulation of atherosclerotic plaque. The blockage of the artery causes hypoxia downstream and leads to death of cardiomyocytes [29,30], inflammation [31], and degradation of the left ventricular extracellular matrix known as negative left ventricular remodeling[32,33]. Eventually the wall of the ventricle will thin, the infarct will expand [34], scar tissue will form and lead to left ventricular dilatation and decrease in cardiac function [35]. The only current treatments for end stage heart failure are total heart transplantation or the use of a left ventricular assist device. However transplantation is limited by the availability of donor hearts, and assist devices are only able to supplement the function for a limited amount of time.

1.3.1 Biomaterial therapies for myocardial infarction

As a therapy for MI, biomaterial scaffolds can be used in combination with cells, or used alone to recruit endogenous cells into the scaffold. The traditional use of these systems was in the form of cardiac patches [36-41] that would be placed on the epicardial surface of the heart after injury. However, implantation of these materials involves an invasive open chest procedure which requires long recovery times. Injectable biomaterials could allow for minimally invasive delivery directly into the infarcted region [42-46]. Naturally derived materials have been studied such as injectable collagen [25,30,31] and fibrin glue [47], both of which are single protein systems. Christman et al. demonstrated that fibrin glue could induce neovascularization and preserve cardiac function with and without cells [26,30,35,36] . However, the use of this material would require a double-barreled injection system that is not compatible with catheter delivery. As both of these systems contain only single proteins, it would not be a proper mimic of the native microenvironment of the heart. Matrigel, which is a complex mixture of proteins components derived from Engelbreth-Holm-Swarm mouse sarcoma cells, has also been studied for use in cardiac repair. As Matrigel is derived from a mouse cancer cell line, it would not mimic the cardiac extracellular matrix and may also increase potential for tumor formation [48,49] demonstrating that it might not be clinically relevant. Chitosan [42] and alginate [43] have also been used, but are derived from sources that again may not mimic the cardiac matrix environment. Synthetic materials investigated for this purpose includes poly(N-isopropylacrylamide) (PNIPAAM) [29,30] and non-degradable poly(ethylene glycol) (PEG) [50] . However, these therapies have had limited regenerative effect, and while synthetic materials may be tunable, they lack bioactivity which may be

important for cardiac tissue regeneration. This demonstrates that the development of a more biomimetic material may allow for a better environment for cardiac repair.

1.4 Stroke

Ischemia in the brain is a condition in which there is insufficient blood flow in the brain to meet metabolic demand. This leads to hypoxia and thus death of brain tissue or cerebral infarction/stroke which is the third leading cause of death in the United States, and each year approximately 800,000 people suffer a stroke [28]. The ischemia leads to alterations in brain metabolism, reduction in metabolic rates, and energy crisis. While there is an increased incidence of stroke, there is, in contrast, declining mortality, leading to a large increase in the number of disabled stroke patients [51]. Once stroke-induced cell damage has occurred, little can be done to improve functional outcome [52]. While there are some interventions that can be given immediately after stroke that can improve the prognosis of the patient, it must be administered within four and a half hours after onset, which frequently is not achieved [52,53]. Hence, the development of clinically feasible alternatives to repair the brain after the acute injury is important to promote functional restoration [52].

Stem/progenitor cell transplantation shows improvement in behavioral recovery in most preclinical studies. However, direct transplantation of cells into the center of the stroke cavity leads to death of the cells as the tissue is necrotic. But injection to the areas in contact with the damaged tissue may not provide as much functional benefit, and could damage the tissue. The use of an acellular hydrogel scaffold that would allow for cellular infiltration may promote favorable endogenous remodeling at the site of stroke. Minimally invasive delivery would be critical as to prevent damage of the brain tissue

and to implant the scaffold beyond the superficial layer. Tissue engineering may provide promising alternatives for cell transplantation therapy by using biomaterial scaffolds that will degrade as the cells remodel the environment [54].

1.4.1 Biomaterial therapies for stroke

The extracellular matrix of the brain contains relatively small amounts of fibrous proteins such as collagen or fibronectin, but is rich in glycosaminoglycans (GAGs) and proteoglycans [55]. Recently, several groups attempted to recapitulate the physical, chemical and biological properties of brain tissue in culture by using hydrogels of hyaluronic acid, collagen and laminin to provide proteins and GAGs for neural stem cell growth [56] or by studying neural cell response to collagen, fibronectin and GAGs [57]. While these materials are an approximation of the *in vivo* microenvironment, they do not fully mimic the complex native ECM of the brain.

Similarly, a variety of scaffolds have been used *in vivo* to treat traumatic brain injury and other neurological disorders in small animal models. These scaffolds attempt to regenerate or replace damaged brain tissue by providing a platform for neurite growth and axonal alignment. To develop a scaffold for tissue engineering, one approach is to mimic the structure and/or components of the native ECM. Hyaluronic acid [58,59], collagen [60], polycarbonate [60], polycaprolactone [61], and poly(glycolic acid) meshes and gels [62] have been studied as scaffolds in brain lesions in animal models to provide three-dimensional constructs for cellular repopulation or as cell delivery vehicles. Most of these scaffolds need to be implanted requiring major surgery. However, injectable scaffolds of synthetic particles [63], methylcellulose [64], fibrin[51], and a combination of fibronectin/collagen I [65] have been developed, which would allow for minimally invasive delivery. To date, no

scaffolds, which contain the appropriate tissue specific ECM biochemical cues, have been developed for the brain.

1.5 Decellularized Materials

The ECM of each tissue contains similar components; however, each individual tissue is composed of a unique combination of proteins and proteoglycans [66,67]. Recent studies have shown that the ECM of various tissues can be isolated through decellularization and utilized as a tissue engineering scaffold [27,68-72]. The methods for decellularization involve using physical, chemical or enzymatic means to remove the cellular content leaving behind only the extracellular matrix. Through the removal of cellular antigens, the matrix would be able to be used without inducing a foreign body reaction, inflammation, and potential transplant rejection [73]. ECM proteins are generally well conserved among species [74], which would allow for xenogeneic decellularized materials to be tolerated and used clinically[75]. In fact, numerous decellularized ECMs, such as small intestine submucosa (SIS), pericardium, skin, and heart valve, from both bovine and porcine sources are FDA approved and used in the clinic [75]. With the emergence and increasing interest in this technique, guidelines have been published as to how to deem that a material is fully decellularized [76].

Thus, for damage from ischemia, using matrix from the tissue of interest would theoretically provide the best mimic of the native ECM's biochemical cues. Other decellularized ECM materials have been used for a variety of applications for tissue repair [73,76]. These scaffolds are known to promote cellular influx in vivo [77,78]. Their degradation products have angiogenic [79] and chemoattractive [79-82] properties and promote cell migration and proliferation [83]. After removal of the cellular antigens, these scaffolds

are considered biocompatible; both allogeneic and xenogeneic ECM devices have been approved by the FDA and are in clinical use [84]. To date, these decellularized materials have been used exclusively in a patch or intact form, which would not allow for minimally invasive delivery. For these reasons, we sought to develop an injectable hydrogel derived from brain matrix, cardiac matrix, and skeletal muscle matrix that would allow for minimally invasive delivery and treatment of stroke, myocardial infarction, and peripheral artery disease.

1.6 Biomimetic cell culture coatings

The extracellular matrix (ECM) is well known to regulate cell growth [85,86], survival and maturation/differentiation [87,88], as well as play an important role in development [89]. Despite the complex nature of the ECM, *in vitro* studies traditionally assess cell behavior on coatings primarily consisting of single purified protein components or directly on polystyrene tissue culture dishes. These surfaces do not mimic the complexity of the extracellular microenvironment and place further limitations on translating findings from *in vitro* studies to the *in vivo* setting [85,90]. Therefore, it is important to provide a growth platform that will allow cells to not only maintain as much of their native morphology and function as *in vivo,* but also the ability to fully mature, particularly in the case of progenitor and stem cells. Deriving and utilizing the native ECM from specific adult tissues could provide an ideal growth platform since it could more appropriately emulate the mature, tissue specific *in vivo* ECM microenvironment.

Typically, single purified matrix proteins from various animal sources are adsorbed to cell culture substrates to provide a protein coating for cell attachment, which may lead to modifications of cellular behavior as cells lose their normal ECM

microenvironment. More complex coatings have been used, such as combinations of single proteins of various collagens, fibronectin, vitronectin or laminin, and while these combinatorial signals have been shown to affect cell behavior [91,92], they do not completely recapitulate the *in vivo* ECM in terms of the tissue-specific combinations and/or ratios of various proteins and polysaccharides. Cell-derived matrices have also been used, such as fibroblast treated plates [93-97] and Matrigel™ [98] coatings, but they do not mimic any specific native tissue composition. Also, fibroblast pretreated culture platforms have the disadvantage that fibroblasts need to be cultured for several days to deposit matrix [97], and then removed using trypsin prior to using the substrate for cell culture [95,97]. In general, cells tend to maintain better function on cell-derived matrices, thus providing support for a more *in vivo*-like approach. Thus the material that derived from brain matrix, cardiac matrix, and skeletal muscle matrix may also be used as a coating for cellular culture.

1.7 Conclusions

As the extracellular matrix of each tissue has a unique composition specific to that tissue, the ideal biomaterial scaffold would provide an environment that mimics the existing tissue. To this end, scaffolds have been designed that attempt to mimic the composition, structure, or other factors of the tissue that it is trying to repair. Other properties of an ideal scaffold include being biocompatible, able to be remodeled by infiltrating cells, and immunologically inert. Decellularized matrices may provide a better material for tissue engineering scaffolds after ischemia attack, as it would provide a better mimic of the native microenvironment. Similarly, *in vitro* studies should also use a biomimetic platform to mimic the *in vivo* microenvironment to provide the proper cell-

matrix interactions for a better model outside of the body. Again, decellularized matrices may also be used for cellular studies to provide a better growth substrate. Thus, in this work, materials derived from cardiac muscle, skeletal muscle and brain have been developed, characterized and studied for use as cell culture coatings and as injectable scaffolds.

1.8 Scope of the dissertation

The objective of this dissertation was to develop, characterize and study decellularized extracellular matrix from cardiac tissue, brain tissue and skeletal muscle as a clinically relevant biomaterial to alleviate damage due to ischemia, and to utilize the matrix material as a biomimetic cell culture platform. The material should provide a better mimic to the environment seen *in vivo* which would be important for assessing cellular behavior as well for a tissue-specific scaffold for tissue engineering.

Chapter 1 provides an overview of the pathophysiology of ischemia that can affect the brain, heart or skeletal muscle, a summary on biomaterials used to treat these conditions as well as their limitations. This chapter also provides a brief introduction to substrates traditionally used in cellular culture, which may not be a close mimic of the *in vivo* microenvironment.

Chapter 2 describes the development and characterization of decellularized cardiac and skeletal muscle matrix for use as a cell culture coating for muscle progenitor cells. The material demonstrates that it retains complexity after decellularization, and that the material is able to form a cell culture coating and increases maturation of muscle progenitors. Other effects of the material is studied using a mitogenic and migration assay

in vitro, where it was see that the muscle matrix material increases proliferation and has a chemoattractive effect.

Chapter 3 evaluates the effects of the skeletal muscle matrix in a hindlimb ischemia model and studies neovascularization, muscle progenitor and muscle cell infiltration into the injected scaffold. The skeletal muscle matrix was able to form a gel upon injection intramuscularly into the hindlimb and was compared to a collagen scaffold control.

Chapter 4 explores the decellularization process on human cardiac tissue, which may be useful to evaluate whether the material could be taken from an allogeneic source. It was found that decellularization of human cardiac tissue is possible, but requires additional DNA removal and lipid removal steps when compared to the processing of the porcine cardiac matrix.

Chapter 5 describes the development and characterization of decellularized brain matrix for use as a cell culture coating for neural progenitors. The brain matrix was tested whether it could retain complexity and glycosaminoglycan content after processing, and whether the material when used as a coating could affect cell behavior of cultured neurons derived from induced pluripotent stem cells. This work also tested the feasibility of using the material as a minimally invasive delivered scaffold through gelation by testing gelation after subcutaneous injection.

Chapter 6 provides a summary and conclusion, as well as address limitations in studies and future work.

CHAPTER TWO:

Development and characterization of a naturally derived cardiac and skeletal muscle matrices and *in vitro* cellular effects

2.1 Introduction

The extracellular matrix (ECM) is well known to regulate cell growth [85,86], survival and maturation/differentiation [87,88], as well as play an important role in development [89]. Despite the complex nature of the ECM, *in vitro* studies traditionally assess cell behavior on coatings primarily consisting of single purified protein components or directly on polystyrene tissue culture dishes. These surfaces do not mimic the complexity of the extracellular microenvironment and place further limitations on translating findings from *in vitro* studies to the *in vivo* setting [85,90]. Furthermore, the advent of stem cell research has underscored the importance of extracellular cues for the efficient differentiation and maturation of progenitor cells. Therefore, it is important to provide a growth platform that will allow cells to not only maintain as much of their native morphology and function as *in vivo,* but also the ability to fully mature, particularly in the case of progenitor and stem cells. Deriving and utilizing the native ECM from specific adult tissues could provide an ideal growth platform since it could more appropriately emulate the mature, tissue specific *in vivo* ECM microenvironment.

Typically, single purified matrix proteins from various animal sources are adsorbed to cell culture substrates to provide a protein coating for cell attachment, which may lead to modifications of cellular behavior as cells lose their normal ECM microenvironment. More complex coatings have been used, such as combinations of single proteins of various collagens, fibronectin, vitronectin or laminin, and while these combinatorial signals have been shown to affect cell behavior [91,92], they do not completely recapitulate the *in vivo* ECM in terms of the tissue-specific combinations and/or ratios of various proteins and polysaccharides. Cell-derived matrices have also been used, such as fibroblast treated plates [93-97] and Matrigel™ [98] coatings, but they do

not mimic any specific native tissue composition. Also, fibroblast pretreated culture platforms have the disadvantage that fibroblasts need to be cultured for several days to deposit matrix [97], and then removed using trypsin prior to using the substrate for cell culture [95,97]. In general, cells tend to maintain better function on cell-derived matrices, thus providing support for a more *in vivo*-like approach.

While many ECM components are similar, each tissue or organ has a unique composition [66,67,73], and a tissue-specific source could better mimic the extracellular microenvironment, thus allowing for tissue-specific cellular development and maturation. The use of tissue-specific coatings has been recently explored [99,100]; however, limited to no effect was seen on cellular differentiation and morphology when comparing these tissue specific coatings to a conventional collagen coating. In this case, the processing to obtain the material coatings resulted in removal of glycosaminoglycans (GAGs) [99] and potentially other important ECM components. GAGs are sugar residues linked to the core protein of proteoglycans [101], and have been shown to be pivotal for myoblast differentiation [102,103]. Therefore their omission could have resulted in the little differences observed.

We have previously reported the use of tissue derived ECM as an injectable scaffold for myocardial tissue engineering [68]. In this work, we present a simple method to generate abundant tissue-specific substrate coatings, which retain a complex mixture of ECM proteins, peptides, and GAGs. We further demonstrate the biological activity of the ECM coatings to sustain and promote cell differentiation using two cell culture models: differentiation of the C2C12 mouse myoblast cell line and maturation of human stem cell derived cardiomyocytes. Our results show that these coatings promote committed muscle progenitor differentiation and stem cell maturation *in vitro* when compared to cells grown

on traditional cell culture coatings. We also studied other effects of the decellularized muscle matrix on cells *in vitro*. When added to the media at low concentrations, the material is able to act as a mitogenic agent and increases proliferation of cells compared to collagen. Furthermore, when used as a chemoattractant, the material is able to promote increased migration even when compared to known chemoattractants.

2.2 Methods

All experiments in this study were performed in accordance with the guidelines established by the Animal Care and Use Program at the University of California, San Diego and the American Association for Accreditation of Laboratory Animal Care, and were approved by the Institutional Animal Care and Use Committee at UCSD (A3033-01).

2.2.1 Decellularization of skeletal muscle and cardiac tissue for matrix coatings and *in vitro* experiments

Hearts and skeletal muscle from the intercostal muscles were harvested from approximately 30-45 kg pigs, which were anesthetized with ketamine (25 mg/kg) and xylazine (2 mg/kg) followed by euthanasia with Pentobarbital (90 mg/kg). Connective tissue and fat was removed from the skeletal muscle, and the major vessels and atria were removed from the heart. The tissue was then cut into ~1 cm^3 pieces, and decellularized as previously published [68]. Briefly, the tissue was rinsed with deionized water and then stirred in 1% (wt/vol) solution of sodium dodecyl sulfate (SDS) in phosphate buffered saline (PBS) for 4-5 days. Decellularized skeletal muscle and cardiac tissue was stirred overnight in deionized water to remove the detergent. A sample of decellularized matrix

was frozen in Tissue Tek O.C.T. freezing medium, sectioned into 10 μm slices, and stained with hematoxylin and eosin (H&E) to confirm the absence of cells. Following the decellularization protocol, the ECM was lyophilized overnight and milled using a Wiley Mini Mill to create a fine-grained powder.

2.2.2 Preparation of solubilized skeletal muscle and cardiac matrix

In order to obtain a suspension appropriate for coating plates, the milled form of the matrix was solubilized through enzymatic digestion [68,104]. Pepsin (SIGMA, St. Louis, MO) was dissolved in 0.1 M hydrochloric acid (HCl) to make a concentration of 1 mg/ml. Approximately 10 mg of the ECM was digested in 1 mL of pepsin solution under constant stirring. After approximately 48 hours, the matrix was diluted using 0.1 M acetic acid to make a 1-2.5 mg/ml concentration of skeletal muscle and cardiac ECM solutions. These solutions were used to coat tissue culture polystyrene for 1 h at 37°C, followed by rinsing with PBS.

2.2.3 Characterization of skeletal muscle and cardiac matrix

Retained biochemical cues were confirmed using assays for protein and peptide content (SDS-PAGE, mass spectrometry), and polysaccharide content (Blyscan). Solubilized skeletal muscle and cardiac matrix solutions were analyzed by SDS-PAGE and compared to rat tail collagen type I (BD Biosciences, San Jose, CA), as previously described [68]. To determine sulfated glycosaminoglycan (GAG) content, the Blyscan assay (Biocolor, United Kingdom) was used per manufacturer's instructions. Samples were run

in triplicate and averaged. Rat tail collagen served as a negative control for the glycosaminoglycan content determination. To more fully characterize the protein content of the cardiac matrix and skeletal matrix, tandem mass spectroscopy (MS/MS) was performed. Matrix samples were digested using trypsin and analyzed by liquid chromatography (LC)-MS/MS with electrospray ionization. A QSTAR-Elite hybrid mass spectrometer (AB/MDS Sciex) that is interfaced to a nanoscale reversed-phase high-pressure liquid chromatograph (Tempo) using a 10 cm-180 ID glass capillary packed with 5-µm C18 Zorbax™ beads (Agilent). The buffer compositions were as follows. Buffer A was composed of 98% H_2O, 2% acetonitrile (can), 0.2% formic acid, and 0.005% trifluoroacetic acid (TFA); buffer B was composed of 100% ACN, 0.2% formic acid, and 0.005% TFA. Peptides were eluted from the C-18 column into the mass spectrometer using a linear gradient of 5–60% Buffer B over 60 min at 400 ul/min. LC-MS/MS data were acquired in a data-dependent fashion by selecting the 4 most intense peaks with charge state of 2 to 4 that exceeds 20 counts, with exclusion of former target ions set to "360 seconds" and the mass tolerance for exclusion set to 100 ppm. Time-of-flight MS were acquired at *m/z* 400 to 1600 Da for 1 s with 12 time bins to sum. MS/MS data were acquired from *m/z* 50 to 2,000 Da by using "enhance all" and 24 time bins to sum, dynamic background subtract, automatic collision energy, and automatic MS/MS accumulation with the fragment intensity multiplier set to 6 and maximum accumulation set to 2 s before returning to the survey scan. Peptide identifications were made using paragon algorithm executed in Protein Pilot 2.0 (Life Technologies). Proteins were labeled based on at least one identified peptide with the confidence of above 99% for that peptide identification.

2.2.4 Confirmation of cardiac and skeletal muscle matrix adsorption for cell culture coatings

1 mg/ml cardiac matrix, skeletal muscle matrix, or collagen suspended in 0.1 M acetic acid was adsorbed onto tissue culture plastic for 1h at 37°C, followed by rinsing with PBS. The total protein and peptide adsorption content was measured using a micro BCA assay (Pierce, Rockford, IL). The amount of adsorbed protein and peptide was determined by calculating the difference in the coating solutions pre- and post-coating.

The presence of GAGs on the coated tissue culture plastic was confirmed by staining the surfaces with toluidine blue (0.15 mg/mL in 50 mM sodium acetate) for 10 minutes [105]. After incubation with toluidine blue, the cardiac matrix, skeletal muscle matrix, collagen, and uncoated plates were rinsed with PBS and assessed for blue staining with brightfield microscopy.

Time of flight secondary ion mass spectroscopy (ToF-SIMS) was also utilized to confirm adsorption of the complex matrices. Tissue culture dishes were coated with skeletal muscle matrix, cardiac matrix, or collagen at 1 mg/ml for 1 h at 37°C, rinsed twice with dH_20, dried, and then sent to Tascon USA, Inc. (Chestnut Ridge, NY) for analysis. ToF-SIMS spectra were acquired on an ION-TOF ToF.SIMS 5-300 spectrometer with a 25 keV liquid metal ion source using Bi_3^+ primary ions in the bunched mode to achieve high mass resolution (Tascon USA, Inc., Chestnut Ridge, NY). Spectra were acquired for positive secondary ions over a mass range of m/z from 0-800 for evaluation of peak intensities of amino acids fragment ions. The target current used was 0.15 pA, and the area analyzed was approximately 150 x 150 um^2. Mass resolution for a typical spectrum was approximately 6000 at m/z= 44 u ($C_2H_6N^+$). Two reads were performed on two samples for each of the coatings, and two reads were measured on an

uncoated tissue culture plate for reference. To emphasize differences in the coatings, relative peak intensities were normalized to the intensity of C2H3+.

2.2.5 Cell culture

C2C12 skeletal myoblasts (ATCC, Manassas, VA) were maintained on collagen coated plates in growth media consisting of DMEM (Gibco, Grand Island, NY) supplemented with 10% Fetal Bovine Serum (FBS) and 1% penicillin/streptomycin (Gibco, Grand Island, NY), and split 1:8 using trypsin when 80% confluent. Myoblasts were diluted to a concentration of 10^7 cells/ml, and 100 µl was placed in wells in a 96 well plate pre-coated with either skeletal muscle matrix or collagen, in triplicate, to achieve 100% confluency. At 24 h, non-attached cells were removed with a change of growth media. Cells were cultured in growth media for the extent of the experiment in order to analyze differences in differentiation on the surface coating without any induction media.

Human embryonic stem cells (hESCs, HES2, ESI International) were differentiated into beating embryoid bodies as previously described [106] and maintained after Day 18 of differentiation in induction medium (IM) consisting of Stempro34 (Gibco, Grand Island, NY), 1% glutamine, 150 ug/ml transferrin (Roche, Indianapolis, IN), 50 ng/ml L-Ascorbic Acid (SIGMA), 42 ng/ml monothioglycerol (SIGMA), 10 ng/ml hVEGF (R&D systems, Minneapolis, MN), 5mg/ml bFGF (R&D systems, Minneapolis, MN). At 35 and 112 days post differentiation, beating embryoid bodies were dissociated by incubation with collagenase Type I (SIGMA, St. Louis, MO) containing 10 ug/ml DNase (Calbiochem, San Diego, CA) for 1 h, followed by washing in Iscove's Modified Dulbecco's Medium (IMDM) and incubation with trypsin/EDTA

(SIGMA, St. Louis, MO) for 10 min. Trypsin was inactivated with FBS containing 30 mg/ml of DNase. After incubation with these enzymes mechanical dissociation of embryoid bodies was achieved by drawing the cell suspension through a 20-gauge syringe needle 4-5 times. Cells were then washed in IMDM and pelleted at 1500 rpm for 5 min. Cell pellets were resuspended in IM media and plated onto cardiac matrix or gelatin coated plates, in triplicate, at a density of 1-3x10^5 cells per 35 mm dish (0.1% solution of porcine gelatin, SIGMA, St. Louis, MO)

2.2.6 Immunohistochemistry

C2C12 skeletal myoblasts were fixed with 4% paraformaldehyde, incubated with anti-myosin (skeletal, fast) heavy chain (MHC) (1:200, SIGMA, St, Louis, MO), and then stained with a secondary antibody (1:200; Invitrogen, Carlsbad, CA) and Hoechst 33342 (1 μg/ml Invitrogen, Carlsbad, CA). hESC cultures were fixed with 4% paraformaldehyde and incubated with primary antibodies against titin M8 (1:100, kind gift from Dr. M. Gautel, King's College London, UK), sarcomeric a-actinin (1:300, A7811, SIGMA, St. Louis, MO), and desmoplakin (1:100, 2722-5204 AbD Serotec, UK). Cells were then stained with secondary antibodies (1:250; Jackson Immunoresearch, PA) and Hoechst 33342 stain (1 μg/ml, Invitrogen, Carlsbad, CA), followed by visualization of signals by confocal imaging. Image analysis was performed with Axio-Vision image processing software. Percent differentiation of myoblasts was determined as the number of nuclei in MHC positive cells divided by the total number of nuclei. Five evenly spaced measurements were taken along each myotube to determine myotube width. Average number of nuclei per MHC positive myotube was also determined. For hESC derived cardiomyocytes, average cardiomyocyte cluster area was measured by

determining the area of titin M8 positive clusters, and nuclei per cluster was recorded. Average desmoplakin size was determined by measuring pixel area of individual desmoplakin clusters as an indicator of desmosome formation.

2.2.7 *In vitro* proliferation assays

Primary rat aortic smooth muscle cells (RASMC) and C2C12 skeletal myoblasts were maintained on collagen coated plates and split at 1:5 every 2-3 days. Cells between passages 4 and 10 were plated at 750 cells/well in 96 well plates in growth media consisting of DMEM, 10% fetal bovine serum, and 1% pen-strep solution. Twenty-four hours later, the cells were washed with PBS to remove non-adherent cells. Digested skeletal muscle matrix and collagen were brought to a pH of 7.4, and then added to the growth media at concentrations of 0.05 mg/mL. As the ECM was enzymatically digested, pepsin was also included as a control at 0.005 mg/mL. All conditions were run in quadruplicate. Every two days, media was changed and cell proliferation was assessed using the Picogreen® assay (Invitrogen) per manufacturer's directions. Briefly, wells were rinsed in PBS and then incubated with 100 µL of TE buffer. After incubation for 30 minutes at room temperature followed by 5 minutes on a shaker, 100 µL of 1:200 Picogreen reagent was added. Upon covering the plates in foil and shaking them for 30 minutes, double stranded DNA was quantified using a fluorescent plate reader at 630 nm at days 3, 5, and 7.

2.2.8 Migration of cells toward the cardiac matrix

Migration of human coronary artery endothelial cells (HCAECs) and rat aortic smooth muscle cells (RASMCs) was assessed, using a Chemotaxis 96-well Cell

Migration Assay Kit (Chemicon, Billerica, MA) as previously described [107,108], to evaluate the chemoattractive properties of the myocardial matrix as compared to collagen, fetal bovine serum, and pepsin. HCAECs were purchased from Cell Applications, Inc (San Diego, CA) and cultured in MesoEndo Endothelial Cell Media (Cell Applications). RASMCs were isolated from 3 month old Harlan Sprague-Dawley rats, as previously described [109]. Briefly, the aorta was isolated, dissected free from adventitia, and opened longitudinally. Endothelial cells were rinsed off, and the aorta was minced into small pieces. These pieces were weighted under sterile cell strainers in DMEM containing 20% FBS and 1% penicillin/streptomycin. RASMCs grew out from the explants after 2 weeks, and were then cultured and passaged. All cells used in the experiment were below passage 10.

In preparation for the migration assay, cells were serum starved (per manufacturer's instructions) for 15-17 hours in DMEM, containing 0.5% heat-inactivated FBS with no added growth factors. The cells were then harvested with trypsin, and re-suspended to $4x10^5$ cells/mL in serum-free media. The chemoattractant, myocardial matrix, was solubilized and neutralized as described above. Collagen was also neutralized for the study to be used as comparison to the myocardial matrix. 10% FBS in DMEM, a known chemoattractant for both endothelial cells [110] and smooth muscle cells [111], was used as a positive control. As pepsin was used to digest the decellularized ECM, it was tested alone as a control. Thus, pepsin was concurrently stirred in 0.1 M HCl for 48 hours, neutralized, and diluted to match the myocardial matrix concentration. Manufacturer instructions were followed for the assay, where 150 μL of the chemoattractant was added into the feeder tray, and 100 μL of cell suspension was added to the top insert that was separated from the bottom chamber by a 8 μm pore filter. After

a 4 hour incubation at 37°C with 5% CO_2, the cells that migrated toward the chemoattractant remained on the underside of the 8 μm porous membrane. These cells were detached, lysed, stained, and quantified by fluorescence. Fluorescent measurements were performed on a SpectraMax Plate Reader at 483/535 nm. An increase in fluorescence intensity correlates to an increase in the number of cells that migrated through the filter.

2.2.9 Statistical analysis

All data is presented as the mean ± standard error. For the Blyscan assay, samples were run in triplicate and results averaged, and reported using standard deviation. Significance was determined using a two-tailed student's t-test, and reported as $*p < 0.05$ and $**p < 0.01$. With the mitogenic assay, samples were run in quadruplicate and results were averaged.

2.3 Results

2.3.1 Fabrication of matrix materials

In order to fabricate the decellularized matrix coatings, ECM was extracted from adult tissues and then processed to create a solubilized mixture of native ECM components that was adsorbed onto tissue culture plastic for cell culture. Figure 2.1 shows the simplified protocol to achieve solubilized ECM from striated muscle tissue. To isolate the matrix from adult porcine organs, tissues were decellularized using the detergent sodium dodecyl sulfate (SDS). Adult skeletal and cardiac muscle of porcine origin was cut into cubes approximately 1 cm^3, rinsed briefly using deionized water, and

decellularized with 1% SDS in phosphate buffered saline (PBS) until tissue was completely white and then rinsed thoroughly to remove detergents. Tissue sections were frozen, sectioned and then stained using hematoxylin and eosin (H&E), as shown by an absence of nuclei (Figure 2.2a,b). After confirmation of decellularization, the matrix was lyophilized and milled into a fine powder, solubilized through enzymatic digestion using pepsin [68,104], and kept at acidic pH to prevent self-assembly (Figure 2.1).

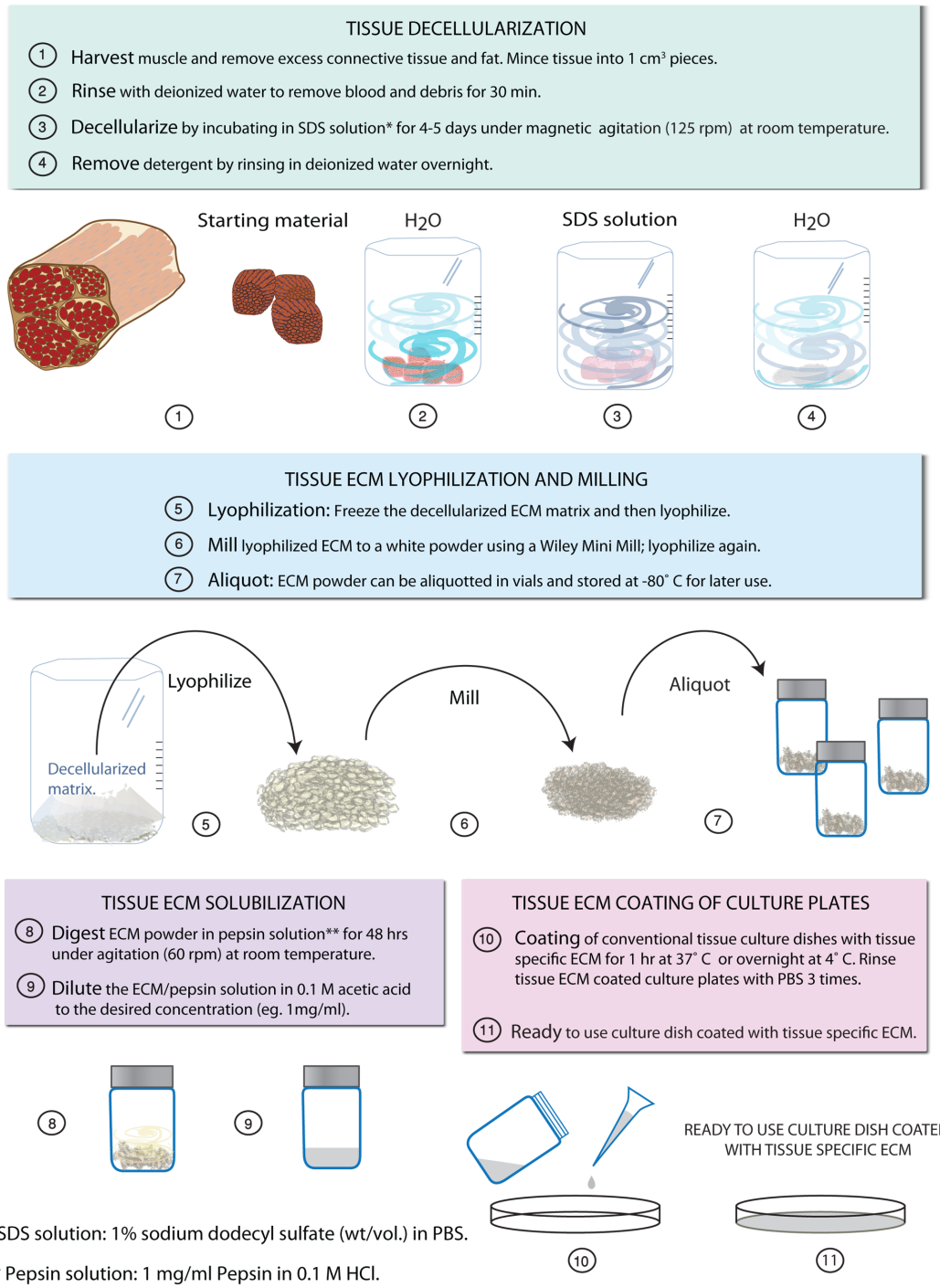

Figure 2.1: Schematic for the generation of tissue-specific muscle ECM coatings for *in* vitro culture.

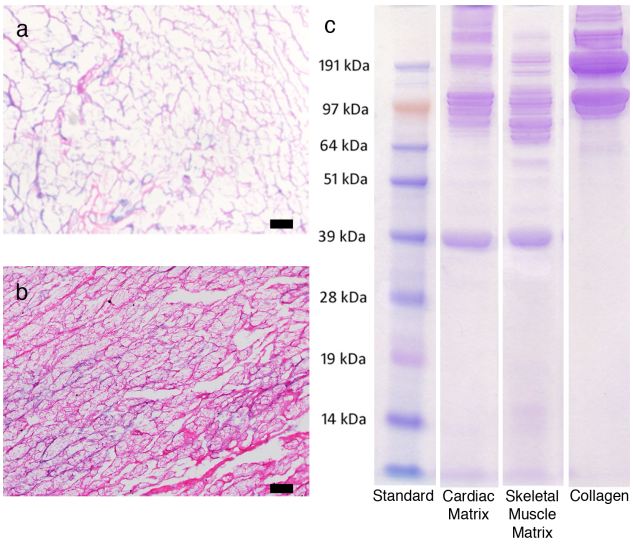

Figure 2.2: Characterization of cardiac and skeletal muscle matrix.
(**a**) H&E section of decellularized cardiac ECM (**b**) H&E section of decellularized skeletal muscle ECM (**c**) PAGE separation of the digested samples compared to collagen I. Note the more complex protein and peptide composition in the muscle matrices.

2.3.2 Characterization of liquid decellularized matrix

Assays for biochemical composition demonstrated that the solubilized muscle matrix coatings retained complex biochemical cues, including proteins, peptides, and polysaccharides. As a first step in demonstrating that the solubilized matrix was composed of a complex milieu of proteins and peptides, we performed PAGE. The solubilized matrices exhibited bands that corresponded to collagen, as expected, in addition to the presence of lower molecular weight bands (Figure 2.2c). We also performed more detailed characterization through mass spectroscopy to identify the components within the material. Interestingly, the results indicated that the components of cardiac matrix originated from a mixture of collagens ranging from collagen I to collagen VI, as well as elastin, fibrinogen, fibronectin and laminin, components expected to be found in the myocardial ECM. In addition, fibrillin-1, a glycoprotein found in

elastic fibers, and lumican, a keratan sulfate proteoglycan, as well as fibulin-3 and -5 were identified (Table 1). Skeletal muscle matrix components contained a mixture of collagen I, II, V, VI, VIII, XI, XII, and XIII. Mass spectroscopy also identified fibrinogen, fibrillin-1, fibulin-5, and the proteoglycans lumican, dermatopontin, and decorin. Proteoglycans can influence cell behavior, and dermatopontin and decorin in particular play a role in matrix assembly, growth factor signaling and myoblast differentiation [112-115]. Furthermore, our solubilized ECM contained heparan sulfate (HS) GAGs, which play an important role in processes such as development and angiogenesis [116,117], and are also implicated in muscle regeneration [102]. However, this methodology is not all-inclusive and, therefore, there may be other extracellular matrix components that were not identified. Using a Blyscan assay we also found that our process allowed for the retention of GAGs, which have been shown to be vital for skeletal myoblast differentiation [102,103]. The solubilized skeletal muscle matrix contained 16.7±0.1 μg GAG per mg of matrix, while the cardiac matrix had approximately 20 μg GAG per mg of matrix as previously reported [68]. The retention of tissue specific components demonstrates that while the 3D structure of the original ECM is lost with this method, many of the original biochemical cues are retained and thus these materials may mimic the subtle complexities of each tissue's ECM.

Table 2.1: Mass spectroscopy composition analysis.

	Cardiac Matrix	Skeletal Muscle Matrix
Collagen I	X	X
Collagen II	X	X
Collagen III	X	
Collagen IV	X	
Collagen V	X	X
Collagen VI	X	X
Collagen VIII		X
Collagen XI		X
Collagen XII		X
Collagen XIII		X
Elastin	X	
Fibrinogen	X	X
Fibronectin	X	
Laminin	X	
Fibrillin-1	X	X
Lumican	X	X
Fibulin-3	X	
Fibulin-5	X	X
Heparan Sulfate		X
Dermatopontin		X
Decorin		X

2.3.3 Surface characterization of ECM coatings

To ensure that the muscle matrices could be adsorbed onto tissue culture plastic, we quantified the amount of protein/peptide adsorbed, verified the presence of GAGs on the surface, and assessed compositional differences using ToF-SIMS. The amount of protein that adsorbed to the tissue culture plastic was measured using a micro BCA assay, which calculates the remaining protein/peptide content in the coating solutions. The difference in total protein/peptide in solution pre- vs. post-adsorption was calculated to be 17.4 ± 1.5 μg/ml for skeletal muscle matrix and 27.4 ± 1.3 μg/ml for cardiac matrix, with collagen measuring at 18.35 ± 0.5 μg/ml. This translates roughly to 0.05-0.09 μg protein adsorbed per mm^2 of tissue culture plastic. Additionally, GAG adsorption to the tissue culture plastic was demonstrated by incubating the coated surfaces with toluidine blue [118]. The cardiac and skeletal matrix coated surfaces remained blue after PBS rinse, whereas the collagen and uncoated dishes were clear (data not shown).

We further employed ToF-SIMS (time of flight secondary ion mass spectroscopy) to analyze cardiac matrix- and skeletal matrix-coated polystyrene dishes compared to collagen-coated and uncoated controls. A previously published peak list [119], which includes peak characteristics of unique amino acid mass fragmentation patterns created from a model of ECM protein surfaces, was chosen for ToF-SIMS. These peaks correspond to amino acids, which are matched to common ECM proteins [119-121] (Table 2). Principal Component Analysis (PCA) was used to highlight any differences in the matrix coatings from the ToF-SIMS data; PCA is a mathematical analysis technique that can be used to characterize the differences between a large set of data by calculating the principal components (PC) [122]. The analysis revealed that there existed distinct differences between the compositions of cardiac matrix-, skeletal muscle matrix-,

collagen-coated surfaces, and the uncoated control due to the clustering of the data when PC2 was graphed against PC1 (Figure 2.3). Most of these differences occurred along PC1 (85%) while PC2 accounted for 6% of the differences. As there was a higher amount of differences seen along PC1, it indicates that the data sets were different from each other.

To further demonstrate that the muscle matrix coatings were more complex than simply collagen and GAGs, we examined individual peaks based on the corresponding amino acid and ECM protein. Both matrix coatings contained peaks associated with amino acids found in fibronectin and laminin as well as collagen (Figure 2.4). Thus, these studies confirmed that the tissue specific coatings adsorbed to the surface of tissue culture plastic, and were more complex than collagen. Moreover, cardiac matrix and skeletal muscle matrix coatings were distinct from each other.

Table 2.2: ToF-SIMS composition analysis.
(adapted from [119-121])

Peak Number	Molecular Fragment	Prevalent Amino Acid	Extracellular Matrix Association
1	CH_4N	Gly	Collagen I
2	C_2H_4NO	Gly	Collagen I
3	C_2H_5S	Met	Collagen I
4	C_4H_6N	Pro	Collagen I
5	C_3H_6NO	Gly	Collagen I
6	$C_3H_5N_2O$	Gly	Collagen I
7	$C_4H_{10}SN$	Met	Collagen I
8	$C_4H_5N_2O_2$	Gly	Collagen I
9	$C_4H_7N_2O_2$	Gly	Collagen I
10	C_5H_9SO	Met	Collagen I
11	C3H3O	Tyr	Fibronectin
12	C2H6NO	Ser	Fibronectin
13	C4H5O	Thr	Fibronectin
14	C3H3O2	Ser	Fibronectin
15	C4H10N	Val	Fibronectin
16	C3H8NO	Thr	Fibronectin
17	C5H7O	Val	Fibronectin
18	C4H6NO	Glu	Fibronectin
19	C7H7O	Tyr	Fibronectin
20	C8H10NO	Tyr	Fibronectin
21	C10H11N2	Trp	Fibronectin
22	C11H8NO	Trp	Fibronectin
23	CH3N2	Arg	Laminin
24	CH5N3	Arg	Laminin
25	C3H4NO	Asn	Laminin
26	C2H7N3	Arg	Laminin
27	C2H6SN	Cys	Laminin
28	C4H4NO2	Asn	Laminin
29	C4H10N3	Arg	Laminin
30	C4H11N3	Arg	Laminin
31	C5H11N4	Arg	Laminin
32	C2H6N	Ala, Cys	
33	C4H5N2	His	
34	C5H10N	Lys	
35	C3H7N2O	Asn, Gly	
36	C3H6NO2	Asp, Asn	
37	C5H7N2	His	
38	C5H8N3	His, Arg	
39	C8H10N	Phe	
40	C6H5N2O	His	
41	C9H8O	Phe	

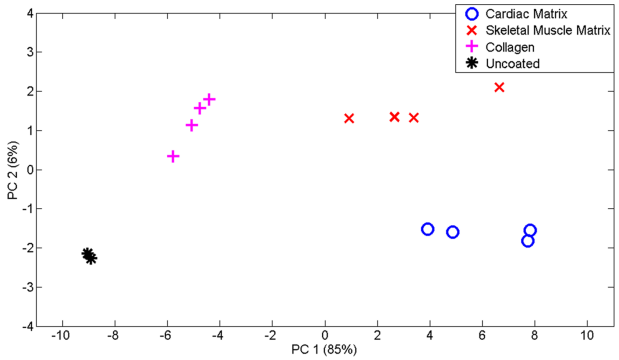

Figure 2.3: Principal component analysis of surface composition differences as detected using ToF-SIMS.
PC1 versus PC2 scores plots for cardiac matrix-, skeletal matrix-coated tissue culture plastic versus collagen coated and uncoated controls. Distinct differences are observed between the coatings as well as the controls, indicating that both of the solubilized muscle matrices adsorbed to the surface.

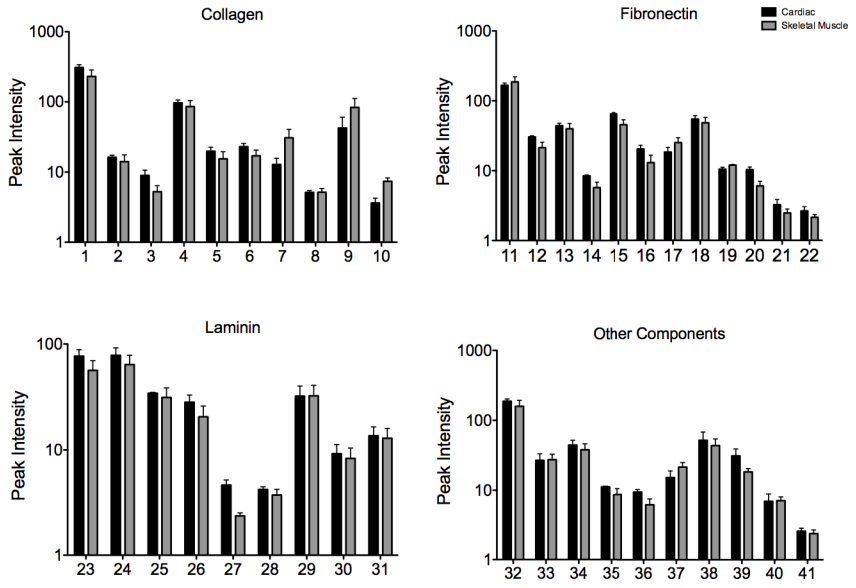

Figure 2.4: Peak value data of functional groups of cardiac matrix and skeletal muscle matrix coatings.
ToF-SIMS peak analysis of cardiac matrix versus skeletal muscle matrix coated tissue culture plastic. The amino acid signatures from the peak values indicate that post adsorption the different matrices retain their complexity with multiple ECM components. See Table 2 for individual peak descriptions.

2.3.4 Enhanced C2C12 cell differentiation on skeletal muscle matrix coating

C2C12 skeletal myoblasts are a well-characterized myogenic cell line capable of differentiation by fusion into multinucleated myotubes [123]. These cells were expanded in growth media, without any components to induce differentiation, and then plated on culture plates coated with either skeletal muscle matrix or collagen. The number of myotubes at 7 days of differentiation was unchanged in cells grown on solubilized native ECM as compared to collagen (data not shown). However C2C12 myoblasts cultured on native ECM differentiated earlier (day 3, $p<0.05$), and had increased fiber diameter and fusion index ($p<0.01$) (Figure 2.5). Figure 2.5 displays images of myotube formation from day 3 after plating. As the main component in both coatings was collagen, the formation of larger, more nucleated myotubes and increased earlier differentiation on the tissue specific matrix illustrates that ECM components other than collagen in the skeletal muscle matrix retained biological activity and have an important effect on C2C12 skeletal myoblast differentiation.

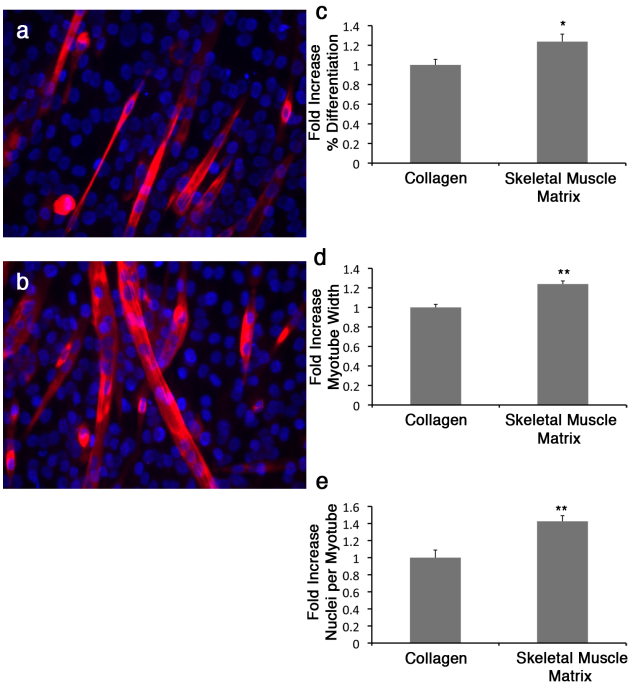

Figure 2.5: C2C12 differentiation/maturation is increased on skeletal muscle matrix coating when compared to standard collagen I.
C2C12 myotube formation is shown at Day 3 on collagen I (**a**) or skeletal muscle matrix (**b**), as labeled by myosin heavy chain (red) staining, and DNA labeled with Hoechst 33342 (blue). Percent differentiation (**c**), myotube width (**d**), and nuclei per myotube (**e**) were significantly increased when myoblasts were grown on the skeletal muscle matrix coating compared to the conventional collagen coating. *p<0.05, **p<0.01.

2.3.5 Enhanced hESC-derived cardiomyocyte cell maturation on cardiac matrix coating

While differentiation of hESCs into cardiomyocytes is routinely achieved, maturation beyond a fetal phenotype has not been readily achieved [124-127]. We therefore pre-committed hESCs to cardiomyocytes and examined whether an adult cardiac matrix coating could further promote maturation of these cells, compared to gelatin. Gelatin was chosen as the comparison coating, as it is the standard substrate for many differentiation

protocols with hESCs [106,128,129]. Of the mixed population, only cells that were positively stained for Titin M8 were assessed, as Titin M8 is a late cardiac muscle-specific marker. Cells were also stained for desmoplakin, and nuclei. Desmoplakin is a cell-cell junction protein that displays a punctate distribution along the sarcolemma during cardiac muscle development, but eventually localizes to the lateral ends of muscle cells at the intercalated disc to form functional intercellular junction structures known as desmosomes, which are important for cell maturation and mechanical and structural integrity [130-132]. Desmosomes also participate in morphogenesis and differentiation [133], and we therefore used desmoplakin, a key component of the desmosomal complex, as a marker to assess whether the cardiac matrix coating would promote a more mature phenotype. hESC-CMs displayed striking differences on the cardiac matrix when compared to gelatin (Figure 2.6), namely an increased multi-cellular organization and maturation. hESC-CMs were found to organize into multi-cellular clusters as indicated by a significant increase in myofibrillar area and number of cardiomyocyte nuclei per cell cluster area when plated on the cardiac matrix compared to gelatin. While there were no differences in the localization of desmoplakin at day 35, at day 112 the immunostaining demonstrated that desmoplakin organized and aggregated to form large localized areas at the lateral/transverse ends between the cardiomyocytes plated on the cardiac matrix, resembling the intercalated disc localization of desmosomal proteins found in fully mature cardiomyocytes *in vivo* [131]. Hence, there was more mature localization of the desmosomal cell-cell junction protein, indicating increased maturation. It should be noted that similar changes in the spatiotemporal patterns of cardiac intercalated disc proteins have been observed during postnatal development and maturation of the human ventricular myocardium [134].

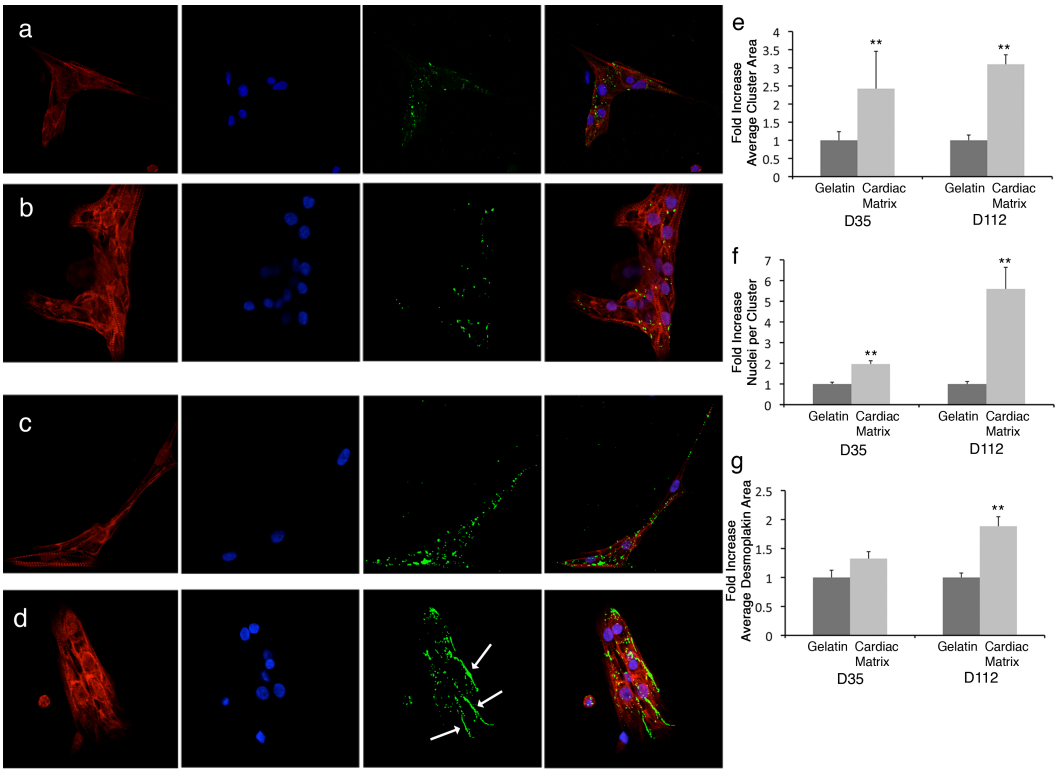

Figure 2.6: Cardiac matrix coatings increase hESC derived cardiomyocyte maturation compared to the standard gelatin substrate.
hESC-derived cardiomyocytes were cultured on gelatin (**a** and **c**) or cardiac matrix (**b** and **d**) and stained for Titin M8 (red), desmoplakin (green), or nuclei (blue). Cell cluster area (**e**), number of nuclei per cluster (**f**), and average desmoplakin positive area (**g**) were measured and compared between the two coatings. Cardiomyocytes had an increased cluster area and number of nuclei at both day 35 and 112. At day 112, the average desmoplakin immunoreactive area was significantly greater on the cardiac matrix, with localization observed at the lateral ends of the cardiomyocytes (arrows), indicating the formation of desmosomes and a more mature phenotype. **p<0.01.

2.3.6 Mitogenic assay

Degradation products of decellularized ECMs have been previously shown to have mitogenic activity [83]. We, therefore, first examined whether the degradation products of the skeletal muscle matrix hydrogel had a mitogenic effect on cells *in vitro*. Proliferation of smooth muscle cells and skeletal myoblasts following exposure to either enzymatically degraded skeletal muscle ECM or collagen was assessed. Pepsin was also

included as a control, as pepsin was utilized to digest the matrix material. A Picogreen assay was used to determine double stranded DNA content at days 3, 5, and 7 in culture to quantify cell proliferation. It was found that both smooth muscle cells (Fig. 2.2A) and myoblasts (Fig. 2.2B), when cultured in media containing degraded skeletal muscle matrix, had a higher rate of proliferation compared to cells cultured in media containing the same concentration of collagen. The increase in cell number was significantly greater at all time points ($p<0.01$). At day 3, there was a 1.85-fold increase in cell number in the skeletal muscle matrix wells compared to collagen for the smooth muscle cells, and a corresponding 2.15-fold increase with the skeletal myoblasts. There was also a 1.3 fold increase for skeletal muscle matrix wells compared to pepsin for both cell types. Thus, the results demonstrate that degradation products of the skeletal muscle matrix are consistent with a higher rate of proliferation in both cell types *in vitro* when compared to collagen or the pepsin control.

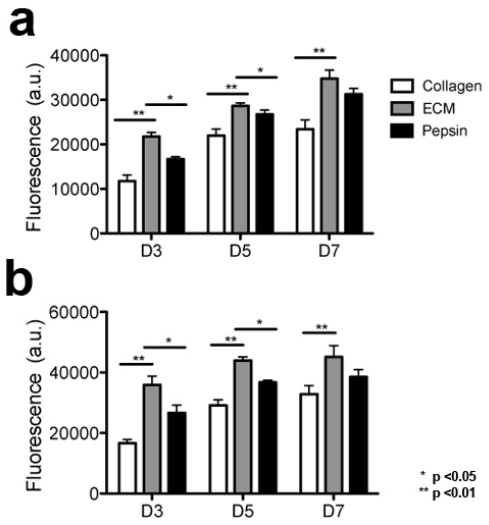

Figure 2.7: *In vitro* mitogenic activity assay.
(A) Rat aortic smooth muscle cells and (B) C2C12 skeletal myoblasts were cultured using growth media with the addition of degraded skeletal muscle matrix, collagen, or pepsin. Proliferation rate was increased for both cell types when cultured in the presence of skeletal muscle matrix degradation products.

2.3.7 Migration of endothelial and smooth muscle cells

Migration of vascular cells towards the myocardial matrix was first tested *in vitro*. A Chemotaxis 96-well Cell Migration Assay Kit was used to quantify the attraction of HCAECs and RASMCs towards the solubilized myocardial matrix, as compared to collagen, FBS, and pepsin. The migration of RASMCs towards the myocardial matrix was significantly greater than all other groups: collagen, FBS, and pepsin ($p < 0.001$) (Figure 2.7). While HCAECs migrated toward the myocardial matrix, the migration was not statistically greater than the other groups per ANOVA. However, there is a noticeable trend similar to that of RASMCs (Figure 2.7). Thus, the matrix was shown to promote migration of both cell types *in vitro*.

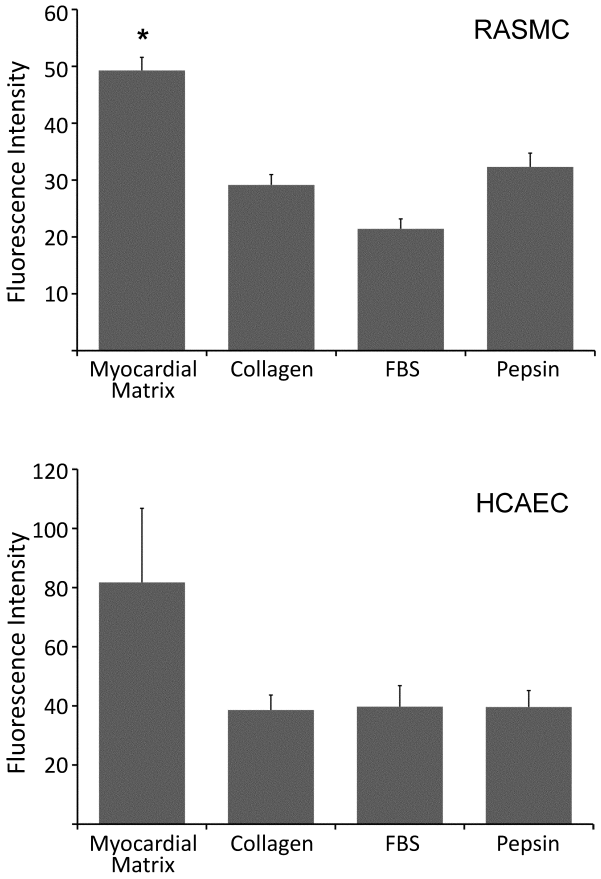

Figure 2.8: Vascular cell migration *in vitro*.
Rat aortic smooth muscle cell (RASMC) and human coronary artery endothelial cell (HCAEC) migration towards solubilized myocardial matrix, collagen, fetal bovine serum (FBS), and pepsin. Fluorescence intensity is proportional to the number of cells that migrated toward each chemoattractant. Both cell types show migration towards the myocardial matrix. Significance from other groups, as determined by an ANOVA with Holm's correction, is indicated (*$p < 0.001$).

2.4 Discussion

There is a compelling need for the development of materials that mimic the native cellular microenvironment for better *in vitro* assays and for the expansion of cells for cell-mediated therapies. In addition, a culture platform where cells are surrounded by an environment that more closely resembles the native ECM niche would improve the assessment of cell behavior in other areas of research such as drug development

applications. There has been a shift of cell culture substrates from single purified proteins, to more complex materials that attempt to mimic the complex native ECM [93]. Combinations of purified proteins have been shown to improve cell proliferation and differentiation, demonstrating that complex coatings are beneficial [93,135]. However, there are many potential combinations, and using a natural matrix would be more physiologically relevant.

In this study, we have presented a method to create matrix coatings derived from porcine adult tissues, performed analysis to determine the components of the solubilized extracellular matrix, and then ensured that the surface composition retained its complexity after adsorption onto tissue culture plastic. We hypothesized that these coatings would have a beneficial effect within 2D muscle culture systems as they more appropriately emulate the native muscle ECM *in vitro*. This culture substrate would thus allow for desirable cell-matrix interactions and provide a better platform for cell phenotype and differentiation, similar to that found *in vivo*. A potential limitation, however, of this approach is that these matrices are of porcine origin, which has the potential for disease transmission and immune recognition. However, the FDA has approved many decellularized xenogeneic ECMs for implantation including porcine dermis, small-intestine submucosa, and heart valves [75] and therefore, we anticipate that these matrices will be a viable option for cell culture. For clinical translation of any cells grown on these coatings, appropriate quality control and testing will of course be essential to ensure lack of pathogens. We have also tested the material to assess any *in vitro* effects of the material, and demonstrate it to be a mitogen for smooth muscle cells and skeletal myoblasts, as well as a chemoattractant for rat aortic smooth muscle cells, and endothelial cells.

The goal of this study was to demonstrate that the simple method for fabricating naturally derived, tissue specific matrix materials could provide a cell culture substrate that emulates the native ECM microenvironment, is readily available, and is as simple to use as conventional protein coatings. Also to study any cellular behavior that could be modified using the material in addition to cell culture media. The ECM plays an important role in directing progenitor and stem cell differentiation and maturation [92,136] and we thus examined the potential for these tissue specific coatings in committed progenitor and stem cell culture. Differentiation of muscle progenitor cells was studied using C2C12 skeletal myoblasts on adult skeletal muscle matrix and compared to a conventional collagen coating I [137]. To examine the potential of the adult myocardial matrix as a coating, we examined its effect on the morphology and maturation of hESC derived cardiomyocytes as compared to the standard gelatin coating typically used in stem cell derived cardiomyocyte cultures [138,139] since we hypothesized that the adult cardiac matrix coating could further promote maturation of these cells. The ECM is also known to regulate cell growth [85,86] and migration, and so the material was also studied as a mitogenic agent and as a chemoattractant. We compared growth of skeletal myoblasts and smooth muscle cells in media containing muscle matrix or collagen, where it was determined that the muscle matrix increased proliferation. To examine the material as a chemoattractant, a migration assay was performed where it was seen that serum-starved cells had increased migration to the muscle matrix even when compared to known chemoattractants.

Our data shows that the native tissue matrix enhanced differentiation of C2C12 skeletal myoblasts and maturation of human embryonic stem cell derived cardiomyocytes when compared to conventional cell culture coatings. Also, that the muscle matrices can

increase proliferation and migration of skeletal myoblasts, endothelial cells and smooth muscle cells. While these extracellular matrix materials contains many biochemical cues of the native environment, one limitation of this study is that it is likely that some ECM components have been lost during processing. However, the remaining matrix components do affect cell differentiation, maturation, proliferation and migration. *S*keletal muscle matrix contains native cues that allowed for increased differentiation and larger myotubes to develop from skeletal myoblasts when compared to a standard single protein coating. The skeletal muscle matrix also increased proliferation of skeletal myoblast and smooth muscle cells when compared to collagen. In addition, the cardiac matrix enhanced the formation and organization of multicellular clusters with intercellular desmosomal like structures resembling the cardiac intercalated disc within hESC derived cardiomyocytes, as well as enhanced migration of smooth muscle cells and endothelial cells. Thus, this report highlights that the cell microenvironment and subtle differences in matrix composition can play an important role on cell phenotype and behavior *in vitro*. We show a method that can allow one to more closely recapitulate this microenvironment in 2D cell culture, which could be applied to any type of *in vitro* assay. Given that the origin of these matrices is adult ECM, it is likely more applicable to terminal differentiation/maturation and adult cell culture. There is also a potential application for cell culture using other cell types, as to date, we have decellularized liver, brain, and other muscle tissue and therefore anticipate that this process can be used to generate substrate coatings from any non-mineralized tissue to present the appropriate cell-matrix interactions. 3D culture systems have recently been highlighted as a better mimic of the *in vivo* environment [140], and similar matrix solutions to those employed here as coatings can self assemble into thin films or gels for 3D cell culture [68,104]. The 3D

environment is not, however, always suitable for all culture studies. Herein, we have developed a simple method to produce decellularized extracellular matrix material that would provide a better approximation of the *in vivo* microenvironment with the added benefit of tissue specificity and complexity. The results of this study show the potential of decellularized, solubilized extracellular matrix materials derived from muscle to promote maturation of committed progenitor and stem cells *in vitro*, increase proliferation and migration, demonstrating this method's applicability to muscle cell culture; however, the general technology has wide ranging implications.

Chapter 2, in part, is a reprint of material that is published as: DeQuach, JA, Mezzano V, Miglani A, Lange S, Keller GM, Sheikh F, Christman KL. Simple and high yielding method for preparing tissue specific extracellular matrix coatings for cell culture. PLoS ONE, 2010; 5 (9): e13039.

Chapter 2, in part, is a reprint of material that is published as: Singelyn JM*, DeQuach JA*, Seif-Naraghi SB, Littlefield RB, Schup-Magoffin PJ, Christman KL. Naturally derived myocardial matrix as an injectable scaffold for cardiac tissue engineering. Biomaterials 2009;30(29):5409-16. *Shared first author.

Chapter 2, in part, is in submission as: DeQuach JA, Lin JE, Cam C, Hu D, Salvatore MA, Sheikh F, Christman KL. Injectable skeletal muscle matrix hydrogel promotes neovascularization and muscle cell infiltration in a hindlimb ischemia model.

The author of this dissertation is one of the primary authors on this publication.

CHAPTER THREE:

Injectable skeletal muscle matrix hydrogel promotes neovascularization and muscle cell infiltration in a hindlimb ischemia model

3.1 Introduction

Peripheral artery disease (PAD) is a common condition in which blood flow is reduced to the leg and feet [7,8]. Critical limb ischemia (CLI) is the most advanced form of PAD, often leading to amputation of the limb and potential mortality [15,16]. The only current clinical treatment for PAD and CLI is endovascular or surgical revascularization [16]. Surgical bypass was the established standard, but recently endovascular therapies such as angioplasty, atherectomy and stenting are used as less-invasive options. However, despite these therapies, CLI continues to carry a major risk of limb amputation, with rates that have not changed significantly in 30 years [17].

Recently, several clinical trials using cell therapy have demonstrated promising results [18-21], but there are still many questions about which therapeutic cell type to use, quantity of cells, and best route to deliver the cells, as well as a significant problem with poor cell retention and survival [20]. Biomaterials scaffolds have more recently been explored to enhance cell survival by providing a temporary mimic of the extracellular matrix (ECM) [19,22]. Biomaterials have also been used for delivery of growth factors or their mimics in animal models of PAD and CLI [19,22-24]. However, these scaffolds are composed of fibrin [22], collagen-based matrix [25], gelatin [26], self assembling peptide amphiphiles [24] or alginate [23], which may not provide the proper biomimetic environment for the ischemic skeletal muscle in these conditions. Moreover, no potential therapies employing only a biomaterial have been explored to date. An acellular, biomaterial only approach may reach the clinic sooner since it has the potential to be an off-the-shelf treatment and does not have the added complications that cells bring, including appropriate source, the need for expansion, or potential disease transmission. Furthermore, a biomaterial that promotes neovascularization and tissue repair on its own

would obviate the need for exogenous growth factors, and the difficulties and expense associated with such a combination product.

The ECM of each tissue contains similar components; however, each individual tissue is composed of a unique combination of proteins and proteoglycans [66,67]. Recent studies have shown that the ECM of various tissues can be isolated through decellularization and utilized as a tissue engineering scaffold [27,68-72]. Thus, for treating critical limb ischemia, using decellularized skeletal muscle matrix would provide the best mimic of the native ECM's biochemical cues. Other decellularized ECM materials have been used for a variety of applications for tissue repair [73,76]. These scaffolds are known to promote cellular influx in a variety of tissues [77,78]. Their degradation products have angiogenic [79] and chemoattractant [79-82] properties, and also promote cell migration and proliferation [83]. After removal of the cellular antigens, these scaffolds are considered biocompatible, and both allogeneic and xenogeneic ECM devices have been approved by the FDA and are in clinical use [84]. A decellularized skeletal muscle scaffold has been previously explored for replacement of a muscle defect [27], yet this intact scaffold would not be amenable to treating peripheral artery disease. We, therefore, sought to develop an injectable hydrogel derived from skeletal muscle matrix that would allow for minimally invasive delivery and treatment of PAD and CLI.

We have recently developed hydrogels derived from decellularized ECMs, including myocardium [68], pericardium [141], and adipose tissue [69], which self-assemble into porous and fibrous scaffolds upon injection *in vivo*. We have recently shown that the injectable hydrogel derived from ventricular ECM promoted endogenous cardiomyocyte survival and preserved cardiac function post-myocardial infarction [142]. In this study, we

developed an analogous tissue specific hydrogel derived from skeletal muscle ECM and examined its potential as a biomaterial only therapy for treating PAD and CLI.

In previous studies, we have shown that a liquid form of skeletal muscle matrix, which forms the hydrogel in this study, was able to promote the differentiation and maturation of C2C12 skeletal myoblast progenitors when used as a cell culture coating [143]. We previously characterized this material, demonstrating its ability to retain a complex mixture of skeletal muscle ECM proteins, peptides, and proteoglycans [143]. In this study, we demonstrate that a liquid form of skeletal muscle matrix can self-assemble into a fibrous scaffold upon injection *in vivo*. The material can also be processed into a lyophilized form that only requires sterile water to resuspend prior to injection, which could provide ease of use in a clinical setting. We show that this injectable skeletal muscle material promotes proliferation of vascular cells and muscle progenitors *in vitro*, and that the hydrogel enhances neovascularization as well as the infiltration of muscle progenitors and proliferating muscle cells *in vivo* in a hindlimb ischemia model, thereby demonstrating its potential for treating PAD and CLI by not only treating ischemia, but also promoting tissue repair.

3.2 Methods

All experiments in this study were performed in accordance with the guidelines established by the Committee on Animal Research at the University of California, San Diego and the American Association for Accreditation of Laboratory Animal Care.

3.2.1 Decellularization of skeletal muscle for matrix preparation

Skeletal muscle from the hindleg was harvested from Yorkshire pigs,

approximately 30–45 kg, immediately after sedation with a ketamine/xylazine combination (25 mg/kg, 2 mg/kg respectively) and euthanasia with beuthanasia (1 mL/5 kg). Fat and connective tissue was removed, and the skeletal muscle was cut into ~1 cm^3 pieces and decellularized as previously published [143]. Briefly, the tissue was rinsed with deionized water and stirred in 1% (wt/vol) solution of sodium dodecyl sulfate (SDS) in phosphate buffered saline (PBS) for 4–5 days. Decellularized skeletal muscle was stirred overnight in deionized water and then agitated rinses under running DI water were performed to remove residual SDS. A sample of decellularized matrix was frozen in Tissue Tek O.C.T. freezing medium, sectioned into 10 μm slices, and stained with hematoxylin and eosin (H&E) to confirm the absence of nuclei. Following the decellularization protocol, the ECM was lyophilized overnight and milled to a fine powder using a Wiley Mini Mill.

3.2.2 Preparation of injectable skeletal muscle matrix and collagen

In order to render the decellularized extracellular matrix (ECM) into a liquid form, the milled form of the matrix was subjected to enzymatic digestion [68,143]. Pepsin (SIGMA, St. Louis, MO) was dissolved in 0.1 M hydrochloric acid (HCl) to make a 1 mg/ml pepsin solution. The ECM at a ratio of 10:1 was digested in the pepsin solution under constant stirring. After approximately 48 hours, the matrix was brought to a physiological pH, and then either diluted for *in vitro* assays or for injection. For *in vivo* studies, the skeletal muscle matrix was brought to a pH of 7.4 through the addition of sodium hydroxide (NaOH) and 10x PBS, and further diluted to 6 mg/ml using 1x PBS [68].

Rat tail collagen (6 mg/mL) was also brought to a physiological pH and salt content using NaOH and PBS, and utilized as a control.

3.2.3 Scanning electron microscopy

Scanning electron microscopy (SEM) was utilized to determine the microstructure of the skeletal muscle matrix gels. These gels were formed *in vivo* by injecting the skeletal muscle matrix subcutaneously in a rat, and excised after 20 minutes. The skeletal muscle matrix gels were harvested and fixed with 2.5% glutaraldehyde for 2 hours, and then dehydrated using a series of ethanol rinses (30-100%). Samples were then critical point dried and coated with iridium using an Emitech K575X Sputter coater. Electron microscopy images were taken using a Phillips XL30 Environmental SEM Field Emission microscope.

3.2.4 *In vivo* gelation test

To prepare for *in vivo* studies, a preliminary test was performed to ensure that the skeletal muscle matrix would be able to gel upon injection. The skeletal muscle matrix was labeled with biotin, and then injected into the hindlimb of healthy Sprague Dawley rats. For biotin labeling, a 10mM solution of EZ link Sulfo-NHS-Biotin (Pierce, Rockford, IL) was prepared and mixed with the liquid skeletal muscle matrix for a final concentration of 0.3 mg of biotin/mg matrix. The mixture was allowed to sit on ice for two hours. The skeletal muscle matrix was then frozen, lyophilized and stored at -80ºC until use. To resuspend the skeletal muscle matrix, sterile water was added at the original volume to bring the material to 6 mg/ml and vortexed. Collagen was also biotinylated using the same protocol.

Female Harlan Sprague Dawley rats (225-250 g) were anesthetized using isoflurane at 5%, intubated, and maintained at 2.5% isoflurane during surgery. In preliminary studies, (n=2) 150 µl of skeletal muscle matrix was injected intramuscularly into healthy rats. The muscle was excised after 20 min, and fresh frozen using Tissue Tek O.C.T.

3.2.5 Hindlimb ischemia model

After confirmation of self-assembly *in vivo*, a rat hindlimb ischemia model was utilized to test the skeletal muscle extracellular matrix. Animals were placed in a supine position and hindlimb ischemia was induced by ligation and excision of the femoral artery. After ligation of the proximal end of the femoral artery, the distal portion of the saphenous artery was ligated and the artery and side branches were dissected free, and then excised as previously described [144,145]. The area was sutured closed and animals were given an analgesic of 0.05 mg/kg of buprenorphine hydrochloride (Reckitt Benckiser Healthcare (UK) Ltd., Hull, England) prior to recovery from anesthesia. One week post-injury, the rats were anesthetized using 5% isoflurane, intubated, and maintained at 2.5% isoflurane for injection. Skeletal muscle matrix and collagen were biotinylated in order to visualize the injection region and 150 µl was injected intramuscularly. Injection was confirmed by a lightening of the muscle at the site of injection. Rats were sacrificed using an overdose of sodium pentobarbital (200 mg/kg) at 3, 5, 7, or 14 days post injection (n=4, except n=3 for 14 day collagen injection), and leg muscles were harvested and frozen in Tissue Tek O.C.T.

3.2.6 Histology and immunochemistry

The excised muscle was cryosectioned into 10 μm slices. Slices were stained with Hematoxylin and Eosin every 1 mm and screened to determine the location of injected material. Adjacent slides were stained for visualization of biotin-labeled skeletal muscle matrix or collagen, to confirm the injection site. Slides were fixed in acetone, incubated with superblock buffer (Pierce), followed by 3% hydrogen peroxide (Sigma), and horseradish peroxidase conjugated neutravidin (Pierce) at room temperature. The reaction was visualized by incubation with diaminobenzidine (DAB, Pierce) for ten minutes.

Five slides evenly spaced within the injection region were then used for immunohistochemistry (IHC). Sections were fixed for 2 min in acetone and blocked with staining buffer for 1 h (2% goat serum and 0.3% Triton X-100 in PBS). Skeletal muscle sections were then assessed for vessel formation using a mouse anti-smooth muscle actin antibody (Dako, Carpinteria, CA; 1:75 dilution) to label smooth muscle cells. After three 5-minute washes with PBS, AlexaFluor 568 anti-mouse (Invitrogen, 1:200 dilution) was used as a secondary. Slides were then mounted using Fluoromount (Sigma). Sections stained with only the primary antibody or secondary antibody were used as negative controls. Images were taken at 100x using Carl Zeiss Observer D.1 and analyzed using AxioVision software. Arterioles were quantified with a visible lumen and a diameter ≥10 μm and normalized over the injection area as previously described [68,146].

In order to assess proliferating muscle cell infiltration into the injection region, sections were stained using a mouse anti-desmin antibody (Sigma; dilution 1:100) and co-stained with a rabbit anti-Ki67 (Santa Cruz Biotech, Santa Cruz, CA; dilution 1:100). AlexaFluor 488 anti-mouse and AlexaFluor 568 anti-rabbit were used for secondary

antibodies (1:200), followed by staining with Hoechst 33342. Slides were mounted with Fluoromount (Sigma) prior to imaging. Additionally, the skeletal muscle tissue was assessed using a rabbit anti-MyoD (Santa Cruz Biotech, Santa Cruz, CA; dilution 1:100), followed by AlexaFluor 488 anti-rabbit as a secondary antibody, and Hoechst 33342. Three 400x images were taken per slide and analyzed using AxioVision software. The number of desmin positive cells, and desmin positive cells that co-localized with Ki67 were counted, averaged and normalized over the area. For the tissue sections analyzed for MyoD, the number of positive cells with MyoD co-localized with nuclei were counted and averaged over the area of injection.

3.2.7 Statistical analysis

All data is presented as the mean ± standard error of mean. Significance was determined using a one-way analysis of variance (ANOVA) with a Bonferroni post-test. A two-tailed Student's t-test was used for all other data and reported as $p<0.05$ and $p<0.001$.

3.3 Results

3.3.1 Injectable skeletal muscle matrix

Skeletal muscle matrix material was derived through decellularization of porcine skeletal muscle tissue (Fig. 3.1A) using previously established methods [143]. The matrix was lyophilized (Fig. 3.1B) and milled into a fine particulate before enzymatic digestion to form a liquid (Fig. 3.1C). At this stage, the liquid skeletal muscle matrix can be diluted and utilized as a coating for cell culture as we have previously reported [143], or can be brought to physiological pH, salt concentration, and temperature, which triggers self-

assembly into a hydrogel (Fig. 3.1D). After raising the pH of the material to 7.4 at room temperature, the material can also be re-lyophilized (Fig. 3.1E) for long-term storage at -80ºC. The material can then be resuspended at a later date using only sterile water (Fig. 3.1F) and utilized for *in vivo* injection.

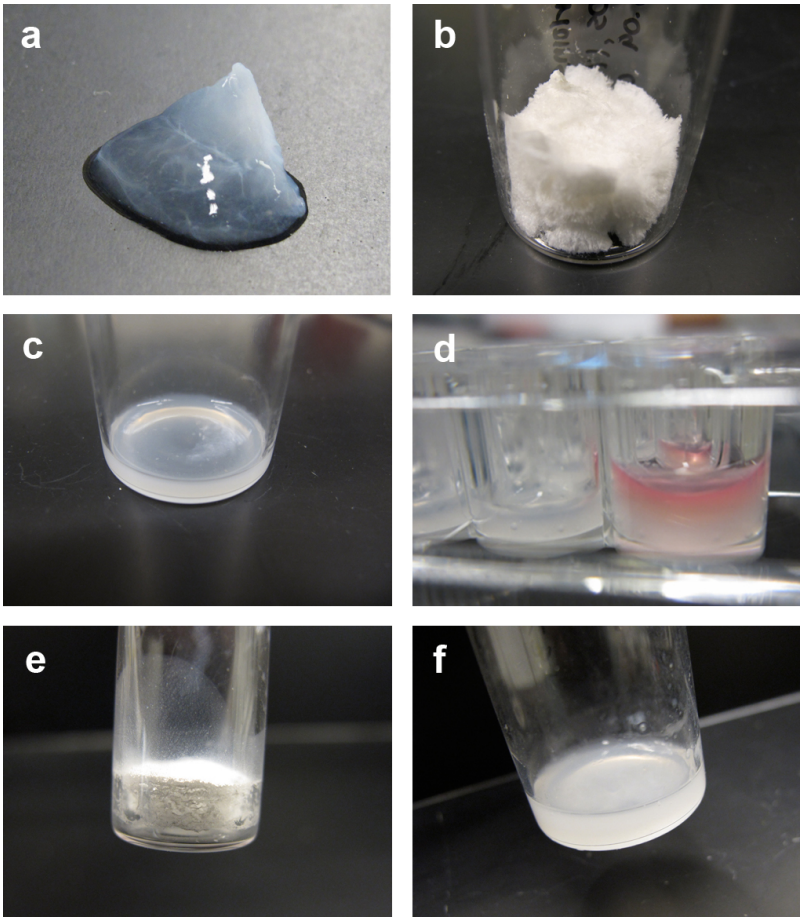

Figure 3.1: Decellularization and tissue processing.
(A) Decellularized skeletal muscle matrix. (B) Lyophilized skeletal muscle matrix prior to milling. (C) Digested skeletal muscle matrix. (D) *In vitro* gel of the skeletal muscle matrix with media on top in right well (E) Skeletal muscle matrix that has been digested and re-lyophilized. (F) Re-lyophilized skeletal muscle matrix resuspended using only sterile water.

3.3.2 Injection and gelation *in vivo*

We initially assessed the ability of the liquid skeletal muscle matrix to form a gel *in situ* by injecting the material into a healthy rat hindlimb. For all *in vivo* studies, we utilized liquid skeletal muscle matrix, which had been biotinylated and re-lyophilized for storage at -80 C. Prior to injection, the material was resuspended in sterile water alone. The skeletal muscle matrix was then loaded into a syringe and injected intramuscularly into a rat hindlimb (Fig. 3.3A). To determine whether the skeletal muscle matrix would self-assemble and form a scaffold, the injection region was excised after 20 minutes. A visible gel, denoted by the white region in Figure 3.3B, was observed within the muscle. Additional matrix injections were cryosectioned and stained to visualize the biotinylated matrix. Similar to our myocardial matrix hydrogel [68], the liquid skeletal muscle matrix self-assembled into a fibrous scaffold once *in vivo* (Fig. 3.3C). To assess the microarchitecture of the skeletal muscle matrix hydrogel, the material was injected subcutaneously, and excised after 20 minutes. Scanning Electron Microscopy (SEM) demonstrated that the matrix forms a porous, fibrous scaffold that is composed of fibers both on the nano- and micro-scale (Fig. 3.4).

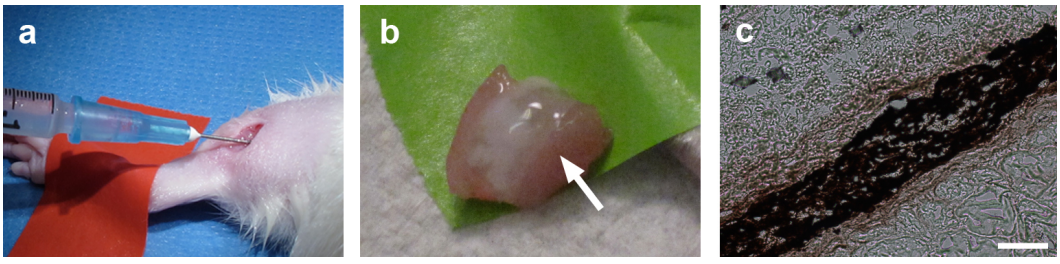

Figure 3.2: Skeletal muscle matrix delivery and gelation *in situ.*
(A) Intramuscular injection of the skeletal muscle matrix material. (B) Gelation of the skeletal muscle matrix *in situ* after 20 minutes as seen after excision of the muscle; arrow denotes the white matrix (C) DAB staining of the biotin-labeled skeletal muscle matrix that gelled within the muscle. Scale bar at 200 µm.

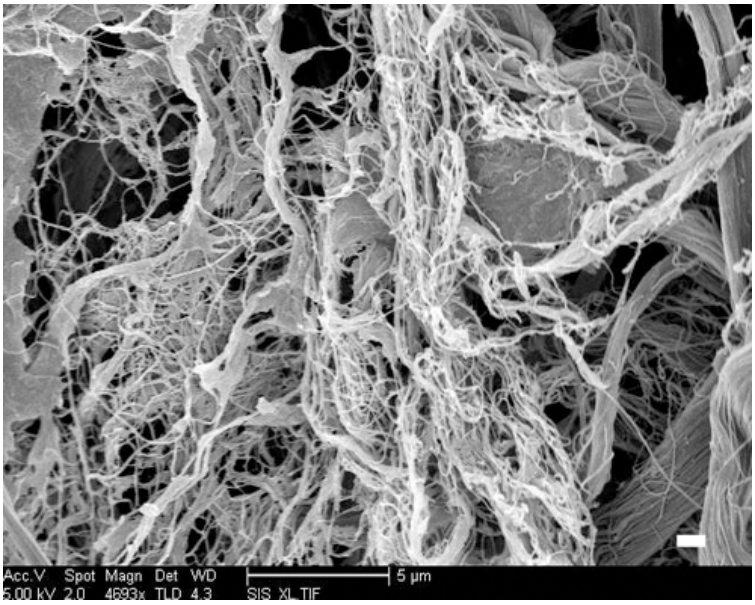

Figure 3.3: Scanning electron microscopy.
Micrograph of a cross-section of excised skeletal muscle matrix scaffold 20 minutes post-subcutaneous injection. Note the formation of the self-assembled fibers on the nano- and micro-scale. Scale bar at 100 µm.

3.3.3 Cellular infiltration and neovascularization

Upon confirmation that the material was able to self-assemble upon injection, we next examined the skeletal muscle matrix hydrogel in a rat hindlimb ischemia model to assess its potential for treating PAD. One week post-hindlimb ischemia, either skeletal muscle matrix or collagen was injected intramuscularly below the site of femoral artery resection. At 3, 5, 7 or 14 days post-injection, the muscle was harvested to determine cellular infiltration. The hydrogel was still present at all time points, although it had significantly degraded by day 14. At each time point, we assessed the amount of neovascularization, which would be critical to treat the ischemic tissue, as well as the

number of muscle cells and muscle progenitors, which could aid in repair of the damaged tissue.

To determine whether the acellular scaffold would support new vessel formation *in vivo*, smooth muscle cells in collagen (Fig. 3.5A) and skeletal muscle matrix (Fig. 3.5B) injected regions were labeled via immunohistochemistry. Arteriole density was significantly greater in the skeletal muscle matrix injection region compared to collagen at 3, 5, and 7 days post-injection (Fig 3.5C), with many of the vessels having an average diameter greater than 25 µm (Fig 3.5D). While not significant, there was still a distinct trend towards an increase in vasculature at day 14 following injection of the skeletal muscle matrix hydrogel.

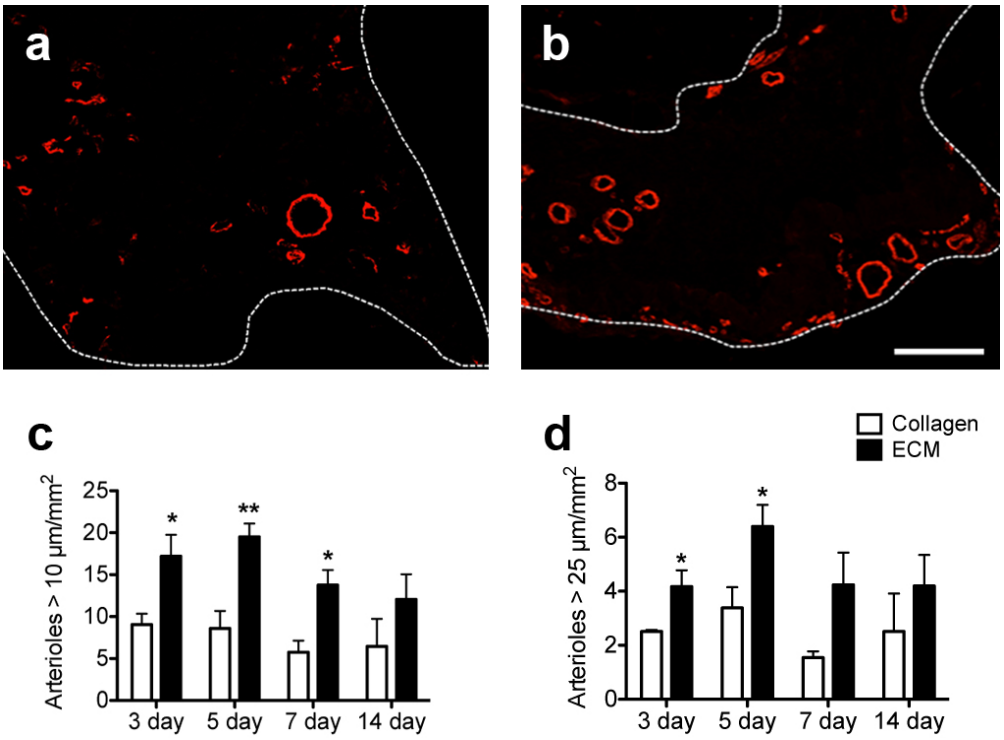

Figure 3.5: Quantification of neovascularization.
(A) Collagen and (B) skeletal muscle matrix injection regions stained with anti-alpha-SMA (red) to determine vessel formation. Vessels with a clear lumen are seen within the injection region within 5 days. Scale bar at 100 µm. Quantification of the vessel density at 3, 5, 7, and 14 days for vessels with a lumen (C) >10 µm or (D) >25 µm demonstrated that the skeletal muscle matrix increased neovascularization. Vessels were, on average, larger in the skeletal muscle matrix when compared to collagen.

In PAD and CLI, patients often suffer from general muscle fatigue and atrophy, and therefore, in addition to increasing vascularization, restoring muscle mass would also be beneficial. We therefore sought to determine whether muscle cells were also recruited to the injection site using staining against desmin (Fig. 3.6A,B). The desmin positive cells were also co-stained for Ki67, a marker for proliferation [147-149], as denoted by the arrows in Figure 3.6. The skeletal muscle matrix recruited significantly more desmin-positive cells when compared to the collagen matrix at 3, 5, and 7 days post-injection, a the trend that continued at day 14 (Fig. 3.6C). Moreover, the majority of cells expressing desmin also were Ki67 positive, indicating proliferating muscle cells were infiltrating the injection region (Fig. 3.6D). The number of Ki67 and desmin positive cells was significantly increased at 3, 5, and 7 days post-injection, with the same trend at day 14. Cell infiltration was further assessed using MyoD as a marker for the potential recruitment of activated satellite cells [150,151]. There was a low number of MyoD positive cells recruited into the injection region of both materials at the examined time points; however, there was a statistically significant increase in MyoD positive cells in the skeletal muscle matrix (Fig. 3.7). The MyoD staining was prevalently perinuclear, which has been shown in other studies [152,153].

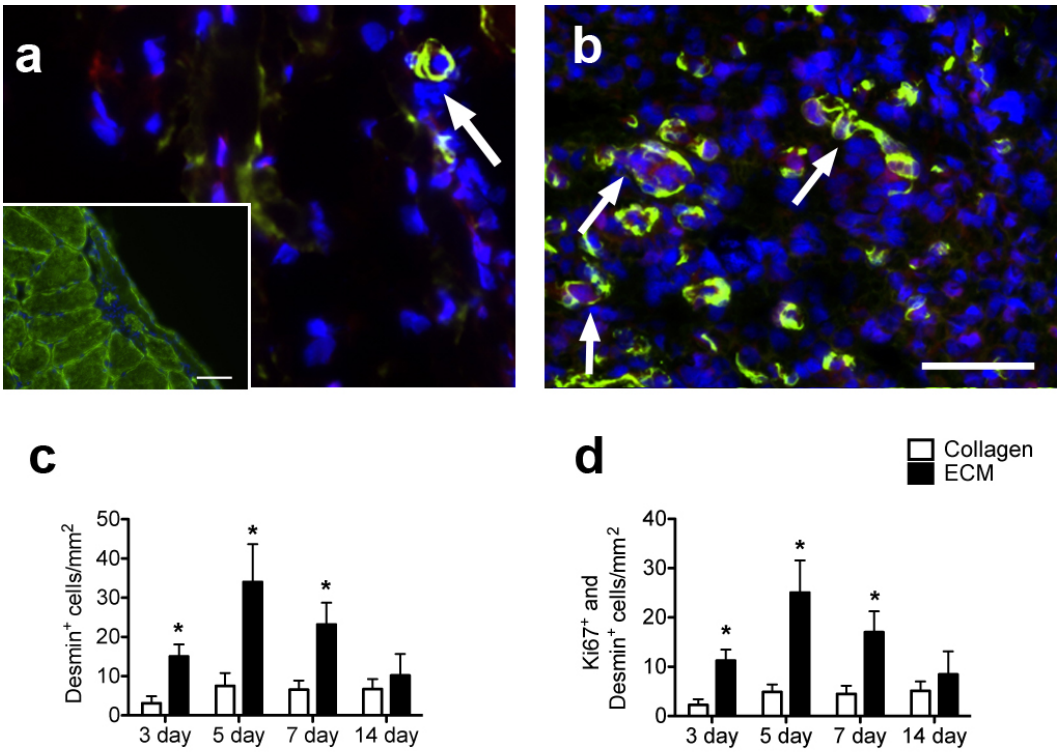

Figure 3.6: Proliferating muscle cell recruitment.
(A) Collagen injection region and (B) skeletal muscle matrix injection region at 5 days with desmin-stained cells (green) co-labeled with Ki67 (red). Arrows denote desmin and Ki67 positive cells. Scale bar at 20 µm. Insert shows positive desmin staining of healthy skeletal muscle, scale bar at 100 µm. (C) Quantification of desmin-positive cells in the skeletal muscle matrix compared to collagen normalized to area. Note that there are significantly more desmin-positive cells in the skeletal muscle matrix. (D) Of these desmin-positive cells, a majority of the cells are proliferating as seen by Ki67 co-labeling.

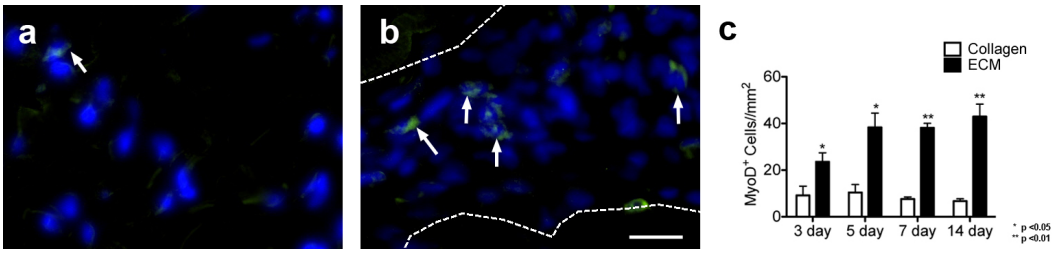

Figure 3.7: Muscle progenitor infiltration.
MyoD positive cells (green) in (A) collagen and (B) skeletal muscle matrix injection regions at 5 days. Area of injection is denoted by the dotted line. Scale bar at 20 µm. (C) Graph of MyoD-positive cells normalized to the area for the injection region. The number of MyoD-positive cells was significantly higher in the skeletal muscle matrix regions at all time points.

3.4 Discussion

Similar to myocardial infarction (MI), which is also a result of atherosclerosis, peripheral artery disease has a large population of affected individuals, with an estimated 27 million suffering from PAD in Europe and North America [154]. Despite recent medical advances and the advent of tissue engineering strategies, revascularization through surgical or endovascular intervention, remains the only treatment. This is further complicated by the fact that approximately 40% of patients with critical limb ischemia, the most severe form of PAD, are not candidates for revascularization procedures [155], and that revascularization has limited benefit when the PAD is diffuse or below the knee. This corresponds to approximately 120,000 leg amputations in the US and 100,000 in the European Union each year [156]. There is therefore a pressing need for the development of new therapies for treating PAD and CLI.

Alternative therapies for PAD and CLI have largely mirrored the attempts for MI and heart failure, including cell transplantation and angiogenic growth factor therapy [17,20,157]. The goal of these therapies has been to increase vascularization of the ischemic limb so that perfusion is sufficient for wound healing to occur, and to resolve pain at rest, thereby also preventing limb amputations. Biomaterial based strategies have recently been explored. Currently, only poly(d,l-lactide-co-glycolide) (PLGA), collagen-fibronectin, alginate, gelatin, fibrin, and peptide amphiphiles have been examined [23,24,26,158-162]. PLGA microspheres in alginate hydrogels have been utilized to deliver vascular endothelial growth factor (VEGF) [158], and alginate hydrogels have been explored for delivery of hepatocyte growth factor (HGF) [23], VEGF [159], and pDNA encoding for VEGF [160]. Alginate microspheres within an injectable collagen matrix have also been used to deliver stromal cell-derived factor-1 (SDF-1) [25], while VEGF loaded alginate

microparticles in a collagen-fibronectin scaffold were used to deliver endothelial cells [161]. Gelatin hydrogels have been employed to deliver basic fibroblast growth factor (bFGF) [26,162], and fibrin scaffolds were utilized to deliver bFGF and granulocyte-colony stimulating factor (G-CSF) along with bone marrow cells. More recently, VEGF-mimetic peptides were delivered using self-assembling peptide amphiphiles [24]. Each of these studies demonstrated enhanced cell transplantation and/or enhanced growth factor/gene delivery with resulting enhancements in neovascularization.

While each of the materials currently explored for treating PAD have been used extensively as tissue engineering scaffolds, they do not mimic the extracellular microenvironment of the skeletal muscle they are intended to treat. The native ECM is a complex combination of fibrous proteins and proteoglycans that can affect many aspects of cellular behavior. Therefore, to regenerate tissue, an ideal scaffold will mimic this native microenvironment. We therefore sought to develop an injectable hydrogel derived from skeletal muscle ECM, which would mimic the native biochemical cues, as well as be amenable to minimally invasive, injectable procedures, which would be advantageous for treating PAD and CLI. We utilized a porcine source of skeletal muscle matrix, as this is the most likely source for a commercial product. Xenogeneic decellularized extracellular matrices have been shown to be biocompatible upon removal of the cellular antigens, and are currently utilized in the clinic for a number of surgical repair applications [163,164].

We found that our liquid version of skeletal muscle matrix was able to form a porous scaffold upon injection, which should promote cellular infiltration to the damaged area [165,166]. We previously assessed the mitogenic properties of the degradation products of this matrix on smooth muscle cells, a relevant cell type for vascularization (Chapter 2).

The skeletal muscle matrix degradation fragments induced a higher proliferation rate compared to collagen. Other studies have also demonstrated mitogenic activity with extracellular matrix degradation products [83]. Care should however be taken when attempting to directly correlate these *in vitro* results to the *in vivo* environment as the majority of these studies, including the study herein, have used pepsin, which would not generate the same ECM degradation products *in vivo*. These *in vitro* studies, however, provided promising evidence that the injectable skeletal muscle matrix scaffold may induce neovascularization *in vivo*. We, therefore, assessed the ability of this new scaffold to induce neovascularization in a rat hindlimb ischemia model compared to collagen, which is the predominant component of the skeletal muscle matrix and a commonly utilized scaffold. Not only was the vessel density higher in the skeletal muscle matrix, but there were significantly more large-diameter vessels greater than 25 μm, indicating maturation of the vasculature. In PAD, the formation of new blood vessels will be critical to treat the ischemic tissue. The presence of more mature vasculature might indicate permanence of the formed vessels, which would be important to getting a vascular supply as quickly as possible to the ischemic region, and to maintain blood flow [167].

In addition to treating the ischemic environment, increasing muscle mass would be beneficial in a therapy for PAD and CLI as patients often suffer with muscle fatigue and atrophy. Previously, we had demonstrated that the liquid form of decellularized skeletal muscle, when utilized as a coating for cell culture (Chapter 2), increased skeletal myoblast differentiation compared to collagen coatings [143], suggesting that this material provides tissue specific biochemical cues to recapitulate the skeletal muscle microenvironment. In this study, we first examined whether the degradation products of the skeletal muscle matrix scaffold would promote proliferation of skeletal myoblasts *in*

vitro. We demonstrated that the degradation products of this scaffold increased myoblast proliferation compared to collagen, (Chapter 2) and therefore, we next sought to assess the infiltration of muscle cells into the scaffold in the hindlimb ischemia model. We measured the number of desmin- and MyoD-positive cells that were recruited into the skeletal muscle matrix scaffold compared to collagen. Desmin, a muscle specific protein, confirms that the cells that infiltrated were from a myogenic origin; however, this may also stain for smooth muscle cells. MyoD, on the other hand, is a specific striated muscle regulatory transcription factor, which coordinates the myogenic program in differentiating myoblasts [168-170]. We found that there were a significantly higher number of muscle cell types (as seen by MyoD and desmin) in the skeletal muscle matrix, and that many of these desmin-positive cells were also proliferating. The MyoD-positive cells also indicate that immature progenitor cell types are recruited to the skeletal muscle matrix. The presence of these MyoD-positive and desmin-positive muscle cells indicate that the skeletal muscle scaffold is recruiting relevant cell types that may aid in the regeneration of the damaged muscle, in addition to treating the ischemic tissue. However, future studies to assess functional benefit, and studies in a large animal model will be critical prior to translation of this therapy to the clinic.

In this study, we demonstrate the potential of an acellular, biomaterial only therapy for treating PAD. Previous biomaterial strategies have only utilized scaffolds to enhance cell or growth factor therapy [23,26,158-162]. However, a lone biomaterial therapy has several benefits, which may allow it to reach patients sooner, including the potential to be an off-the-shelf treatment without the complications that both cells and growth factors can add. To create a material that could be easily prepared in the clinic, we also

developed a method that allowed for long-term storage of the injectable skeletal muscle matrix scaffold, with only sterile water required to resuspend it immediately prior to use.

3.5 Conclusions

The results of this study indicate that an injectable skeletal muscle matrix scaffold may be a potential new biomaterial only therapy for treating PAD. In this study, we demonstrate that decellularized skeletal muscle ECM can be processed to form an injectable matrix material, which self-assembles into a porous and fibrous scaffold *in vivo*. We show that degradation products of the material induce proliferation of smooth muscle cells and skeletal myoblasts *in vitro*. We further observed that the injected scaffold increased neovascularization and infiltration of muscle cells compared to collagen, suggesting that it may improve neovascularization in PAD as well as treat the associated muscle atrophy. Future long-term studies, including those in a larger animal, and studies to assess functional recovery, will be critical prior to translation; however, this study demonstrates proof-of-concept for treating PAD and CLI with an injectable scaffold derived from decellularized skeletal muscle ECM.

Chapter 3, in full, is submitted as: DeQuach JA, Lin JE, Cam C, Hu D, Salvatore MA, Sheikh F, Christman KL. Injectable skeletal muscle matrix hydrogel promotes neovascularization and muscle cell infiltration in a hindlimb ischemia model.

The author of this dissertation is one of the primary authors on this publication.

CHAPTER FOUR:

Decellularized human heart matrix: an allogeneic biomaterial for cardiac repair

4.1 Introduction

Cardiovascular disease remains the leading cause of death in the western world, and total heart transplantation or left ventricular assist devices are the only successful treatment with end stage heart failure. As cardiac tissue has limited ability to regenerate itself, tissue engineering strategies may provide a method to replace the damaged tissue. Biomaterials have been studied to replace the necrotic tissue and stimulate a regenerative response through the use of scaffolds with or without cells. For example, biomaterials have been studied as cardiac patches[36-41,171] which are applied to the epicardial surface of the heart, but require an invasive open-chest surgery for this therapy. Recent cardiac tissue engineering approaches have focused on developing injectable scaffolds that potentially could be delivered through less invasive means. By gelling *in situ*, the material can provide a scaffold that will allow for cellular infiltration and promote regeneration of the tissue, or act as a cell delivery vehicle for transplanted cells. Injectable materials that have been studied include fibrin [146,172], collagen [173], alginate [44], chitosan [174], self-assembling peptide nanofibers[175,176], and Matrigel [177]. However, these materials may not provide as good of a mimic of the native cardiac microenvironment, as the materials are either single component protein systems, derived from a non-tissue specific material, or from a synthetic source. Recently, an injectable material developed from decellularized porcine cardiac matrix has been studied [68]. The injectable porcine cardiac matrix demonstrated preserved function in a rat myocardial infarction model[78], and is intended to provide the correct extracellular milieu to replace degraded-ECM post-myocardial infarction.

As the extracellular matrix in the body is composed of a complex composition of proteins and proteoglycans that affect cellular behavior, decellularized tissue-specific

ECM may provide the best replacement of this complex milieu. It has been shown that decellularized cardiac and skeletal muscle matrix affect cellular morphology, maturation, proliferation and migration *in vitro* (Chapters 2 and 3) [68,143]. Thus, these materials are a promising source for tissue engineering scaffolds. Decellularized materials such as small intestine submucosa (SIS), pericardium, skin, and heart valve, from both bovine and porcine sources are FDA approved and used clinically [75].

However many of the decellularized materials are from a xenogeneic source, mostly of porcine origin. An allogeneic source might be desirable to avoid potential immune response to the alpha-Gal (Galalpha 1,2-Galbeta1,4GlcNAc-R) epitope, which is the major antigen causing hyperacute rejection of porcine material transplantation into primates [178]. Human tissue that has been previously decellularized include fat [69,179], trachea [180,181], amniotic membrane [182-184], pericardium [185], placenta [186,187] larynx, [188] and heart [53]. While heart tissue has been decellularized, it was used as a cardiac patch that would require an open chest procedure to transplant. An injectable form of the human cardiac matrix could be used as a minimally invasive delivery method to regenerate the damaged tissue while preventing the alpha-Gal xenograft immune reaction. With this study, we explore the use of allogeneic cardiac matrix as a potential biomaterial for cardiac repair.

4.2 Methods

All experiments in this study were performed in accordance with the guidelines established by the Committee on Animal Research at the University of California, San Diego and the American Association for Accreditation of Laboratory Animal Care.

4.2.1 Decellularization of human heart matrix

Human hearts from non-cardiac related deaths were received, through a collaboration with the Mayo Clinic. The hearts were trimmed of fat and major vessels and cut into pieces ~ 2-3 mm x 2-3 mm x 2-3 mm. The tissue was rinsed with deionized water for 30 minutes and then stirred in 1% (wt/vol) solution of sodium dodecyl sulfate (SDS) in phosphate buffered saline (PBS) for 4–5 days with solution changes every 24 hours. When the material no longer had color, the material was treated in the following three methods. One section was processed in the method as previously published [68,143], however it was found that the traditionally used methods were unable to completely remove DNA content. One part of the material was first treated with 50 U/mL DNase and 1 U/mL RNase in 50mM tris-hydrochloric acid (HCl), 10 mM magnesium chloride, and 50 mg/mL bovine serum albumin, pH 7.5 salt at 37°C for 24 hours under agitation, and then rinsed using a solution of 1% SDS in PBS for 1 hour. Then the material was stirred in 100% isopropanol (Sigma-Aldrich) for 24 hours and rehydrated in water for 1 hour. To test whether the order of treatment mattered, the last section of material was first treated with the isopropanol for 24 hours then rehydrated in water, and then incubated with DNase/RNase at 37°C followed by a 1 hour SDS/PBS rinse.

Finally, all three sets were treated stirred in 0.01 % Triton X-100 for 1 hour to remove residual SDS, followed by an overnight water rinse. After the overnight water rinse, the matrix was subjected to agitated rinses under running deionized water to test for residual SDS. The material was then stirred in deionized water overnight, followed by freezing and lyophilization.

4.2.2 Characterization of matrix material

A sample of decellularized matrix from each processing step was frozen in Tissue Tek O.C.T. freezing medium, sectioned into 10 μm slices, and stained with hematoxylin and eosin (H&E) to assess for presence of nuclei. Following the decellularization protocol, the ECM was lyophilized overnight and milled to a fine powder using a Wiley Mini Mill. The three types of processing were then assessed using Oil Red O staining for fat content and Hoechst staining for double stranded DNA removal.

The Oil Red O staining was done to determine lipid removal. Briefly, slides were fixed using 4% paraformaldehyde for 1 h and rinsed in deionized water and then 60% isopropanol. Oil Red O Dye (Sigma-Aldrich, St. Louis, MO) was prepared at 5 mg/ml in 100% isopropanol and diluted 3:2 using deionized water as a working solution, and heated at 60°C for 1 hour. Next, the dye was filtered using a 0.22 μm filter to remove particulates. The samples were incubated with Oil Red O for 15 minutes, and then rinsed in 60% isopropanol and rinsed with deionized water, and then mounted with 10% glycerol in 1X PBS. Images were taken using a Carl Zeiss Imager.

Hoechst staining was done by fixing the samples using acetone for 3 minutes. After which the samples were rehydrated in Phosphate Buffered Saline (PBS) and then stained using Hoechst 33342 (Invitrogen), a fluorescent stain for double stranded DNA, at 0.1 μg/mL for 10 minutes. The sections were then rinsed and mounted with Fluoromount (Sigma-Aldrich) and imaged with a Carl Zeiss Observer D1.

4.2.3 Preparation of human cardiac matrix

In order to render the decellularized extracellular matrix (ECM) into a liquid form, the milled form of the matrix was subjected to enzymatic digestion [68,143]. Pepsin (Sigma-Aldrich, St. Louis, MO) was dissolved in 0.1 M hydrochloric acid (HCl) to make a 1 mg/ml pepsin solution, and then added to the human heart matrix at a ratio of 10:1 matrix to pepsin under constant stirring. After approximately 48 hours, the matrix was brought up to a physiological pH of 7.4 using NaOH and HCl and physiological salt concentration using 10X PBS. The material was then diluted to 6 mg/mL using 1X PBS whereupon the material was tested for gelation properties *in vivo*.

4.2.4 Subcutaneous injection to determine gelation

Female Sprague Dawley rats were anesthetized through injection of nembutol, and then kept on heating pads where 100 µl of matrix was injected through a 27-gauge needle subcutaneously in the dorsal region. The material was injected in duplicate at 6 mg/ml on both sides of the back. Fifteen minutes after injection, the rats received an overdose of sodium pentobarbital, and the material was excised from the animal and the formed gels were imaged. One set of formed gels were fresh frozen using TissueTek O.C.T. for histological analysis, and the other set was fixed for Scanning Electron Microscopy imaging.

4.2.5 Scanning electron microscopy of gelled material

Gels formed through *in vitro* and through subcutaneous injections were fixed with 2.5% gluteraldehyde for 2 hours, and the subjected to a series of dehydration steps from 30% EtOH to 100% EtOH. The samples were stored in 100% ethanol until ready for

use. The samples were then critical point dried with a Tousimis Autosamdri 815B and ripped in half. The samples were coated with iridium using an Emitech K575X Sputter Coater. The microscopy images were taken using a Phillips XL30 Environmental SEM Field Emission microscope with images taken at 242 μA, with a working distance of 10 mm and at 10 kV.

4.3 Results

4.3.1 Decellularization of human hearts

Human hearts were collected from patients with non-cardiac related deaths through collaboration with the Mayo Clinic. Immediately it was seen that there was a significant difference in the shape of the heart when compared to the healthy pig hearts. Despite the fact that the hearts were taken from non-cardiac related deaths, there was significant fat content on the human heart when compared to pig hearts (Fig 4.1). To study whether it would be possible to develop an injectable biomaterial from an allogeneic source, human hearts were decellularized using SDS in PBS with antibiotics. Even though the majority of fat was removed from the human hearts, even after decellularization it was seen that the original decellularization method was unable to remove lipids. After lyophilization, it was seen that there were many pieces of the matrix that were yellowed in color, consistent with the appearance of fat or lipids. Interestingly, these yellowed pieces of the decellularized matrix, when pressed on a Kim Wipe exuded oil (Fig 4.2). Thus, a step utilizing isopropanol to remove lipids was added. It was also seen that the original decellularization protocol was not sufficient to remove DNA content, and so an additional DNase and RNase step was added. To determine if the order

mattered, one subset was treated with IPA first and then the enzymes, and the other set of material was treated with DNase/RNase and then followed by the IPA.

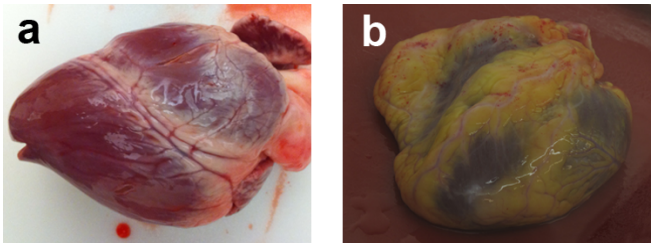

Figure 4.1 Comparison of pig and human heart
(a) porcine heart and (b) human heart prior to processing. Note the human heart contains much more fat content as evidences by the yellow fatty deposits on the epicardial surface of the heart.

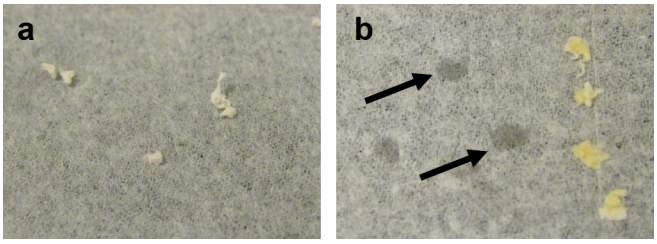

Figure 4.2: Tissue processing inconsistencies
After decellularization, lyophilized samples of the human heart matrix were assessed. It was seen that (a) white pieces of matrix do not leave "oil marks" when pressed whereas (b) yellow pieces of matrix leave oil residue when pressed on a Kim wipe as denoted by the arrows.

Histological samples stained using H&E of the modified decellularization protocol demonstrated a majority of cellular content was removed when compared to fresh tissue (Fig 4.4a). However, the original decellularization protocol showed positive hematoxylin staining (as denoted by the arrow), which could potentially be remnant DNA

(Fig 4.4b). After treatment with DNase and RNase, the material did not have this positive hematoxylin staining (Fig 4.4 c,d).

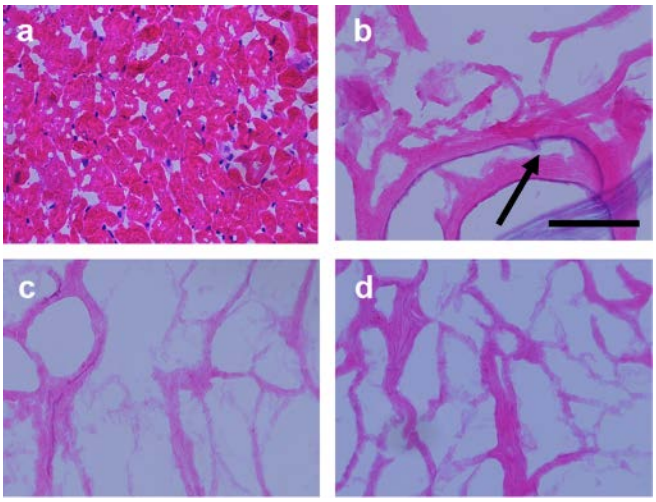

Figure 4.3: Hematoxylin & Eosin staining of human cardiac matrix
(a) staining of Fresh tissue, (b) human heart matrix from original decellularization process (c) matrix after processing first with DNase/RNase then IPA and (d) matrix after processing with IPA and then DNase/RNase. Hematoxylin positive staining is shown after original decellularization protocol (as denoted by arrow). Scale bar at 100 μm.

Staining using Hoechst, which binds directly to double stranded DNA at the minor groove [189], was performed on human heart prior to processing (Fig 4.4 a) where it was seen that the staining is intact and punctuate at the nuclei. The staining of the original decellularization method (Fig 4.4 b), it was seen that the original method was not sufficient to completely remove the DNA content, and so an additional DNase and RNase step was added to the processing. The human heart matrix was additionally processed using DNase/RNase followed by IPA (Fig 4.4 c) or IPA treatment followed by DNase/RNase (Fig 4.4 d). In both instances, it was seen that the DNA content decreased.

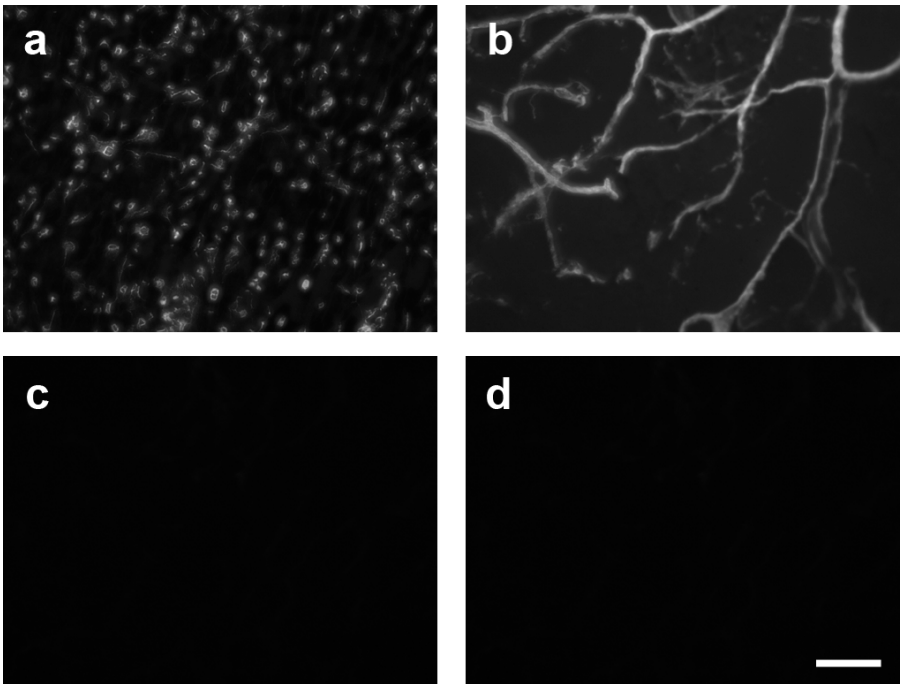

Figure 4.4: Hoechst staining of human cardiac matrix
Hoechst imaging for (a) fresh tissue, (b) human heart matrix from original decellularization process (c) matrix after processing first with DNase/RNase then IPA and (d) matrix after processing with IPA and then DNase/RNase. Note the decreased positive Hoechst staining after treatment with DNase/RNase (c,d). Scale bar at 100 μm.

4.3.2 Lipid removal

Oil Red O staining showed that there is inherent fat content in the non-processed heart tissue (Fig 4.5 a), which remained if using the original decellularization protocol (Fig 4.5 b). However, Oil Red O staining of the decellularized matrix in the new treatments demonstrated that both methods were able to remove lipid content, though the DNase/RNase followed by IPA showed a little positive Oil Red O staining (Fig 4.5 c)

whereas the matrix first treated with IPA then DNase/RNase did not (Fig 4.5 d). The IPA step followed by DNase/RNase may prove to be the better method to remove both DNA and lipid content.

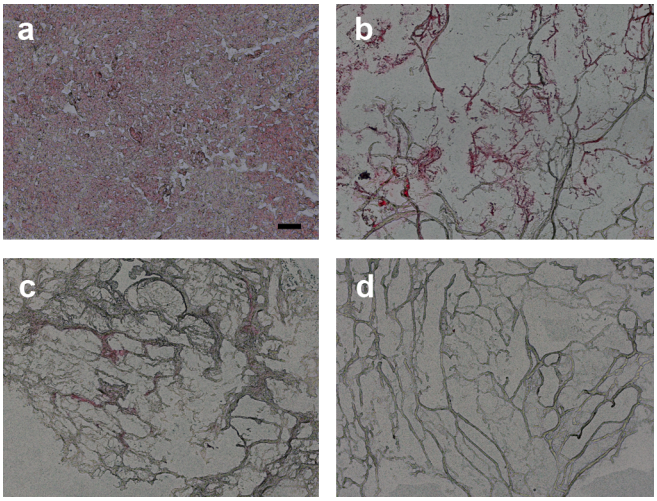

Figure 4.5: Oil Red O staining of histological sections
Sections after Oil Red O incubation for (a) fresh tissue, (b) human heart matrix from original decellularization process (c) matrix after processing first with DNase/RNase then IPA and (d) matrix after processing with IPA and then DNase/RNase. The heart has positive staining for fat content on fresh tissue and on the original protocol. However, there is slight positive staining of the matrix after incubation with DNase/RNase first followed by IPA. However there is no positive staining of the material processed with IP first and then DNase/RNase. Scale bar at 100 μm.

4.3.3 Gelation of the human heart matrix *in vivo*

The material remained a liquid at room temperature, and while on ice. The material was injected subcutaneously into a Sprague Dawley rat to determine whether the material would gel *in vivo*. The matrix was found to be able to self-assemble and form a gel *in situ* after injection within 15 minutes. The formed gel was excised (Fig 4.6), and one set was utilized for histological processing and the other for scanning electron microscopy to assess the microarchitecture of the gel.

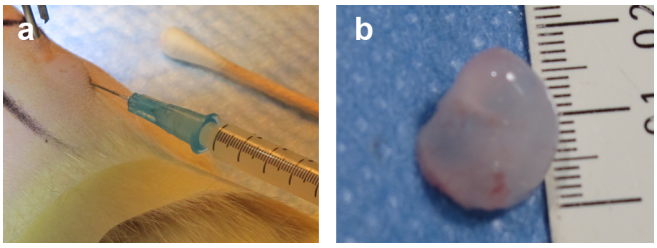

Figure 4.6: Gelation of human heart matrix after subcutaneous injection
(a) The material was brought to physiological pH and salt concentration and diluted down to 6 mg/ml. 100 µl of material was injected subcutaneously and (b) excised after 15 minutes. The material was able to self-assemble and form a gel *in situ* after injection.

4.3.4 Scanning electron microscopy analysis

SEM demonstrated that the self-assembled human heart matrix is able to form a microfibrous and nanofibrous porous scaffold for the *in vivo* formed gels (Fig 4.7).

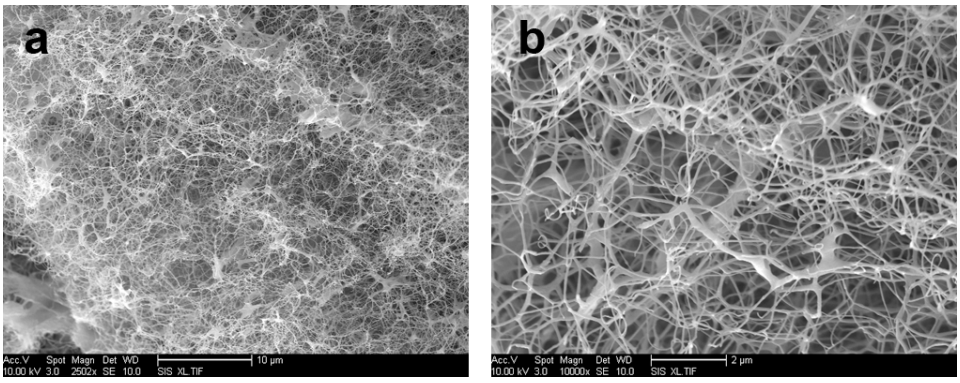

Figure 4.7: Scanning electron microscopy of human cardiac gels
The microarchitecture of the self-assembled human heart matrix gel was studied using scanning electron microscopy. The material forms a microfibrous and nanofibrous scaffold. Scale bar at (a) 10 µm and (b) 2 µm.

4.4 Discussion

In order to repair the myocardium after ischemia injury to prevent negative left-ventricular remodeling effects, a clinically relevant therapy is needed. Cardiac tissue engineering approaches have used a variety of natural and synthetic materials, alone or with cells, as scaffolds to study regeneration of the heart. These materials attempt to provide a microenvironment in which cells could infiltrate or integrate into the host myocardium and repair the damaged tissue. However, many of these materials are not a true mimic of the native ECM in composition and potentially in biochemical cues. Additionally, many of these materials require an invasive open-chest procedure to deliver these scaffolds or patches.

The development and study of injectable decellularized ECM materials has demonstrated the feasibility and attractiveness of minimally invasive therapy, however many of these materials are derived from xenogeneic sources, which may lead to a potential hyperacute immune reaction to the alpha-Gal epitope. This inflammatory reaction is only found in porcine xenotransplantation into primates. The development of an allogeneic source of cardiac matrix may [68] provide a way around this problem, which could be created from donated tissue that does not fit the requirements for whole organ transplantation. However, many factors would need to be considered, such as the age and any potential disease state of the donated cardiac tissue prior to processing into a clinically relevant material.

Thus, this study explored whether an injectable form of human cardiac matrix could be achieved through existing decellularization techniques. The decellularization process was found to need additional steps when compared when the protocol is applied to porcine hearts. However, the porcine tissue was collected from young, healthy, farm

pigs, which have very different visual appearance compared to the aged human hearts. The human hearts contain much more visible fat, and even while the fatty tissue was removed, lipids still remained after decellularization using the original protocol. In addition, the human cardiac matrix still contained significant amounts of DNA, again using the original protocol.

Due to the challenges of removing DNA content and fat content through the original decellularization protocol, two steps were added to the existing protocol, including the addition of a DNase/RNase step and using isopropanol to remove lipid content. To study whether the order of the additional steps were important, one set was first treated with DNase/RNase followed by the IPA, and the second set was treated with IPA and then DNase/RNase. It was seen that the order did matter with IPA treatment first followed by DNase/RNase treatment providing better results.

When it was determined that the tissue has been decellularized and delipidized, the material was then enzymatically digested to create a liquid form of the matrix. This digested human cardiac matrix was then brought to physiological salt and pH content and made into gels upon injection *in vivo.* To test gelation *in vivo*, the 100 µl of matrix was injected subcutaneously into a rat, where self-assembly of the material was identified after 15 minutes post-injection. Future studies are under way to determine whether this material retains any biochemical cues that could enhance neovascularization, decrease fibrosis, and recruit cardiac-relevant cell types *in vivo* and to see whether the cardiac matrix will affect cellular culture *in vitro*. However, the results of this study show the potential to derive allogeneic cardiac matrix material that could be used for many applications in tissue engineering. This material may be able to advance cardiac tissue engineering therapies by providing the proper biomimetic environment, and from an

allogeneic source as to not elicit the alpha-Gal epitope response. However, the source of the heart will play a large role in whether the material will be able to be used clinically. For instance, age, disease, and other factors will be important to identify, and will most likely affect the quality of the cardiac ECM that can be extracted. Further studies are important to determine the effect that the human cardiac ECM will have on cell culture and as a scaffold for tissue engineering, as well as a comparison to the porcine cardiac extracellular matrix.

4.5 Conclusions

We demonstrate that human cardiac tissue can be processed into a decellularized form as a potential allogeneic scaffold for tissue engineering. Additional steps were required to process the material, when compared to cardiac tissue from a porcine origin, as the heart was higher in fat content. The addition of a DNase/RNase and isopropanol step proved to be sufficient to remove lipid and DNA content. Gelation times of the extracellular matrix material from the human heart proved to have similar properties when compared to porcine heart matrix. Further studies are underway to assess cellular effects and response in animal models.

CHAPTER FIVE:

Decellularized porcine brain matrix for cell culture and tissue engineering scaffolds

5.1 Introduction

The extracellular microenvironment has been demonstrated to provide important cues for cellular behavior such as cell migration, differentiation and maturation [85-89]. The extracellular matrix (ECM) is composed of a complex variety of proteins and polysaccharides, and despite its complexity *in vivo*, many studies use purified proteins for cell culture coatings or tissue engineering scaffolds. While many components of the ECM are similar, each tissue contains a unique composition of these proteins and polysaccharides [67,190]. Recently, the use of decellularized matrices for cell culture coatings have been explored for a variety of tissues such as skin, fat, pericardium, heart, skeletal muscle, and liver [99,100,191-193]. These matrices are able to provide a better mimic of native ECM, and have revealed tissue specific effects on cellular behavior [100], including increased maturation of progenitor cell types [191]. To date, no such studies have been performed utilizing decellularized brain ECM.

Brain ECM contains relatively small amounts of fibrous proteins such as collagen or fibronectin, but also includes large amounts of glycosaminoglycans (GAGs) and proteoglycans [55]. It has been shown that neural outgrowth and survival is highly sensitive to surface composition [194,195]. Recently, several groups attempted to recapitulate the physical, chemical and biological properties of brain tissue in culture by using hydrogels of hyaluronic acid, collagen and laminin to provide proteins and GAGs for neural stem cell growth [56] or by studying neural cell response to collagen, fibronectin and GAGs [57]. While these materials are an approximation of the *in vivo* microenvironment, they do not fully mimic the complex native ECM of the brain.

Similarly, a variety of scaffolds have been used *in vivo* to treat traumatic brain injury and other neurological disorders in small animal models. These scaffolds attempt

to regenerate or replace damaged brain tissue by providing a platform for neurite growth and axonal alignment. To develop a scaffold for tissue engineering, one approach is to mimic the structure and/or components of the native ECM. Hyaluronic acid [58,59], collagen [60], polycarbonate [60], polycaprolactone [61], and poly(glycolic acid) meshes and gels [62] have been studied as scaffolds in brain lesions in animal models to provide three-dimensional constructs for cellular repopulation or as cell delivery vehicles. Most of these scaffolds need to be implanted requiring major surgery. However, injectable scaffolds of synthetic particles [63], methylcellulose [64], and a combination of fibronectin/collagen I [65] have been developed, which would allow for minimally invasive delivery. To date, no scaffolds, which contain the appropriate tissue specific ECM biochemical cues, have been developed for the brain.

Here, we report a method to decellularize brain ECM and process the isolated matrix into a form that can be used for cell culture coatings, thereby providing a more *in vivo* like microenvironment for neural cell culture. Additionally, we tested the feasibility of using the solubilized brain matrix as an injectable scaffold for tissue engineering applications.

5.2 Methods

All experiments in this study were performed in accordance with the guidelines established by the Animal Care and Use Program at the University of California, San Diego and the American Association for Accreditation of Laboratory Animal Care, and were approved by the Institutional Animal Care and Use Committee at UCSD (A3033-01).

5.2.1 Decellularization of porcine brains

Brains were removed from female Yorkshire pigs (~30–45 kg), which were anesthetized with ketamine (25 mg/kg) and xylazine (2 mg/kg) followed by euthanasia with Pentobarbital (90 mg/kg). Brains were cut into halves, a small sample was removed for comparison studies, and then decellularized by stirring in 400 mL of 0.1% wt/vol of sodium dodecyl sulfate (SDS) in phosphate buffered saline (PBS) with 1% penicillin/streptomycin. The supernatant containing the cellular remnants was decanted every 24 hours, and refilled to the start volume for 3-4 days until the tissue was decellularized. The slurry was separated into 50 mL conical centrifuge tubes and centrifuged at 10,000 rpm for 5 minutes. To rinse the brain ECM, the conicals were decanted and refilled with deionized water, shaken and centrifuged. This process was repeated between 10-12 times to remove residual SDS. A sample of decellularized brain ECM was frozen in Tissue Tek O.C.T. freezing medium for histological analysis, and the remaining brain ECM was lyophilized and stored at -80°C until further use.

5.2.2 Brain matrix solubilization

Prior to cell culture, the brain matrix was solubilized by enzymatic digestion using previously modified protocols [104,191,196]. Porcine pepsin (Sigma, St. Louis, MO) was dissolved in 0.1 M hydrochloric acid (HCl) at 1 mg/ml and then sterile filtered through a 0.22 μm filter. The pepsin was added to the brain matrix at a ratio of 20:1 for a final concentration of 20 mg/ml for the brain matrix, and then stirred at ~70 rpm for 48 hours.

5.2.3 Characterization of brain matrix material

Fresh frozen decellularized brain ECM was sectioned into 10 µm slices and then stained using hematoxylin and eosin (H&E) to confirm the absence of cells. To quantify DNA removal, a DNeasy assay (Qiagen, Valencia, CA) was performed on lyophilized native brain tissue and decellularized brain ECM in triplicate according to manufacturer's instructions. In brief, samples were digested using the provided Proteinase K, and DNA was separated using a filter trap. After several wash and purification steps, DNA was reconstituted in deionized water and estimated using absorbance readings at 260 nm on a Synergy H4 microplate reader (Biotek, Winooski, VT). Samples were normalized to original dry starting weight. To determine sulfated glycosaminoglycan (GAG) content, the Blyscan assay (Biocolor, United Kingdom) was used per manufacturer's instructions. Samples were run in triplicate and averaged. Rat tail collagen served as a negative control for the glycosaminoglycan content determination. Tandem mass spectrometry (MS/MS) was utilized to more fully characterize the protein content of the brain matrix. Matrix samples were digested using pepsin or trypsin (FASP Protein Digestion Kit, Protein Discovery, Knoxville, TN) and analyzed by liquid chromatography (LC)-MS/MS with electrospray ionization. A QSTAR-Elite hybrid mass spectrometer (AB/MDS Sciex) that is interfaced to a nanoscale reversed-phase high-pressure liquid chromatograph (Tempo) using a 10 cm-180 ID glass capillary packed with 5-µm C18 Zorbax^{TM} beads (Agilent). The buffer compositions were as follows. Buffer A was composed of 98% H_2O, 2% acetonitrile (ACN), 0.2% formic acid, and 0.005% trifluoroacetic acid (TFA); buffer B was composed of 100% ACN, 0.2% formic acid, and 0.005% TFA. Peptides were eluted from the C-18 column into the mass spectrometer using a linear gradient of 5–60% Buffer B over 60 min at 400 ul/min. LC-MS/MS data were acquired in a data-dependent

fashion by selecting the 4 most intense peaks with charge state of 2 to 4 that exceeds 20 counts, with exclusion of former target ions set to "360 seconds" and the mass tolerance for exclusion set to 100 ppm. Time-of-flight MS were acquired at *m/z* 400 to 1600 Da for 1 s with 12 time bins to sum. MS/MS data were acquired from *m/z* 50 to 2,000 Da by using "enhance all" and 24 time bins to sum, dynamic background subtract, automatic collision energy, and automatic MS/MS accumulation with the fragment intensity multiplier set to 6 and maximum accumulation set to 2 s before returning to the survey scan. Peptide identifications were made using paragon algorithm executed in Protein Pilot 2.0 (Life Technologies). Proteins were labeled based on at least one identified peptide with the confidence of above 95% for that peptide identification.

5.2.4 Generation, culture and differentiation of human induced pluripotent stem cells (iPSCs)

Adult human skin biopsies were obtained from healthy volunteers at the Alzheimer's Disease Research Center at the University of California, San Diego. Informed consent procedures were approved by the UCSD IRB and obtained from patients prior to biopsy. Adult human dermal fibroblasts were transduced with retroviruses encoding Oct3/4, Klf4, Sox2, and c-Myc according to previously published protocols [197]. A SDIA (stromal cell-derived inducing activity) with PA6 method was used to induce iPSC to neuroectoderm as described in Zeng et al [198]. Neural progenitor cells (NPC) were prepared from day 12 SDIA induction. NPCs were propagated in DMEM/F12, 1XN2, 1XB27 medium containing 20 ng/ml FGF-2. After NPCs were differentiated for three weeks, neurons were sorted with cell-surface antibodies by

FACSAria (BD Biosciences) using markers recently developed [197], namely $CD184^-$, $CD44^-$, $CD15^{low}$, $CD24^+$.

5.2.5 Culture of hiPSC derived neurons

96 well imaging plates (BD Biosciences) were coated with 20 µg/ml Polyornithine (PO) at 37°C overnight. Next day, the wells were rinsed twice with sterile DI water to remove unattached PO. Plates were coated with the liquid brain matrix diluted to 1 mg/ml using 0.1 M acetic acid for 1 hour at 37°C and rinsed twice with sterile PBS prior to use. Matrigel was diluted to 0.25 mg/ml in DMEM/F12 and incubated for the same period of time. Sorted neurons were plated at 0.625 million cells per cm^2 in neuron differentiation media. Media was changed every 3 days. Cells were fixed and processed at 7 or 14 days.

5.2.6 Immunocytochemistry

Cells were fixed with 4% paraformaldehyde. After blocking with 3% BSA and permeabilizing with 0.3% Triton, cells were labeled with primary antibodies, followed by incubation using secondary antibodies. The following antibodies were used: rabbit anti-GABA 1:200 (Sigma), mouse anti-β-III-tubulin 1:1000 (Covance), rabbit anti-synapsin (Millipore) 1:2500, mouse anti-MAP2a,b 1:500 (Sigma), goat anti-mouse IgG Alexa 488 1:1000, goat anti-rabbit IgG Alexa 568 1:1000 (Invitrogen). Images were taken from a Nikon Axiophot. Synapsin expression was quantified by measuring area of fluorescence using ImageJ. Additionally, to measure dendritic branching, a low density of cells were transfected with pBOS.eGFP [199,200] using Lipofectamine (Invitrogen), as per manufacturer's instructions. Cells were fixed on day 8 for dendrite analysis. Images were

taken from a Nikon Axiophot and primary and secondary branching was counted in ImageJ [201,202].

5.2.7 *In vivo* scaffold feasibility

All animal procedures were performed in accordance with the guidelines established by the Committee on Animal Research at the University of California, San Diego and the American Association for Accreditation of Laboratory Animal Care. Brain matrix was brought to a physiological pH through the addition of sodium hydroxide (NaOH) and 10x PBS, diluted to 16 and 12 mg/ml using 1X PBS, and kept on ice prior to use. Female C57 mice were anesthetized with isoflurane and kept on heating pads whereupon 100 µl of brain ECM was injected through a 27 gauge needle subcutaneously into the dorsal region. Twenty minutes post-injection the mice received an overdose of sodium pentobarbital, the site of injection was excised, and gels were fresh frozen in Tissue Tek O.C.T. for histological analysis or prepared for scanning electron microscopy (SEM).

5.2.8 Characterization of *in vivo* injected brain matrix gels

Frozen brain matrix gels were sectioned to 10 µm slices, and stained using H&E to verify the presence and structure of the gel. Additionally, samples were prepared for SEM analysis by fixation with 2.5% glutaraldehyde for 2h, followed by dehydration in a series of ethanol rinses (30-100%). For comparison, Matrigel and native porcine brain tissue were also prepared for SEM analysis through fixation and dehydration. Samples were critical point dried and coated with iridium using an Emitech K575X sputter coater.

Electron microscope images were taken using a Phillips XL30 Environmental SEM Field Emission microscope.

Immunofluorescent staining was used to identify proteins retained in the brain matrix. Sections of native brain matrix and of brain matrix gels were fixed with acetone and blocked with staining buffer (2% goat serum with 0.3% Triton X-100 in PBS). The following primary antibodies were used: collagen I, collagen III, collagen IV and laminin (1:100, Abcam) and goat anti-rabbit IgG Alexa 568 1:200 (Invitrogen). Only primary or secondary antibodies were used as controls to confirm positive staining. Images were taken using a Carl Zeiss Observer D1.

5.2.9 Statistical analysis

All data are presented as mean ± standard error of the mean. All assays were performed in triplicate and the results averaged.

5.3 Results

5.3.1 Decellularization of brain ECM

The brain matrix material was derived through decellularization of porcine brains using SDS detergent buffered in PBS with antibiotics. Over time, the brain matrix turned white, an indication of cellular removal. The brain matrix material was collected, rinsed, frozen, sectioned and stained with H&E to confirm cellular removal. The absence of intact nuclei in histological sections demonstrated removal of cellular content when compared to native brain tissue (Figure 5.1). The DNeasy assay was used to quantify the DNA removal and it was found that there was a clearance ratio of 95.7% with 0.13±0.02

mg DNA content/mg lyophilized native brain tissue and 0.0069±0.001 µg DNA content/mg in the post-processed brain matrix. A colorimetric Blyscan assay was used to determine sulfated GAG content. The brain matrix material contained 34.7 ± 0.17 µg sulfated GAG/mg dry weight. No sulfated GAGs were found in collagen control. Through mass spectrometry analysis, various extracellular matrix proteins and proteoglycans were identified: collagen I, collagen V, collagen IV, collagen VI, laminin, and perlecan. However, it should be noted that mass spectrometry is not an all-inclusive technique and other proteins may not have been identified.

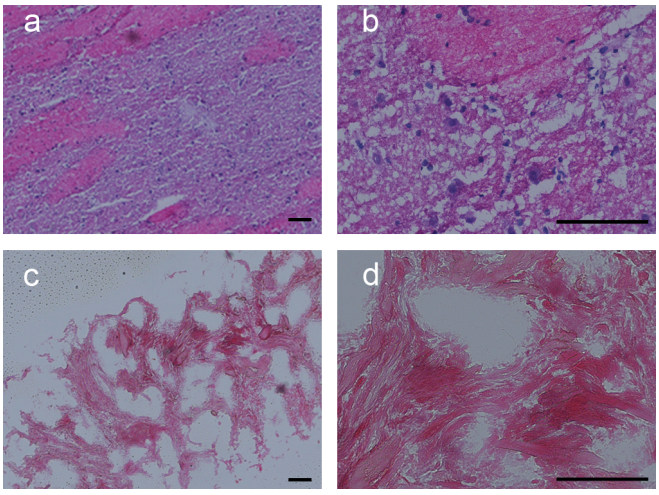

Figure 5.1: Hematoxylin and Eosin stained sections of porcine brain matrix (a,b) compared to decellularized brain matrix (c,d). Scale bars are 100 µm. Note the absence of cells in the decellularized matrix, as compared to native tissue.

5.3.2 *In vitro* culture of iPSC derived neurons on brain matrix

To test brain matrix as a cell culture coating, decellularized brain matrix was solubilized using enzymatic digestion with pepsin. After visual confirmation that the material was solubilized as indicated by the lack of particles in solution, brain matrix was diluted using acetic acid. Imaging plates were coated overnight with polyornithine and then rinsed and incubated with solubilized brain matrix.

Neurons derived from iPSC were sorted by FACS, and then cultured on Matrigel, a standard coating for neurons differentiated from human embryonic or induced pluripotent stem cells [203], and compared to neurons cultured on the decellularized brain matrix. The brain matrix was able to maintain mature neurons, as the iPSC-neurons were able to attach, extend dendritic processes, and were positively stained for the neuronal marker β-III-tubulin (Figure 5.2 a-d). Some neurons cultured on the brain matrix exhibited a distinct morphology with highly complex dendritic processes. These highly arborized dendrites were primarily observed on the brain matrix coated wells, and not on the Matrigel substrates. To quantify the dendritic branching at one week, a low concentration of cells was transfected with eGFP using Lipofectamine. The number of primary dendrites that come directly from the cell body, and secondary dendrites that branch from a primary dendrite were quantified. The neurons cultured on the brain matrix coatings had significantly higher dendritic primary and secondary processes when compared to Matrigel plated neurons (Figure 5.2 e-g).

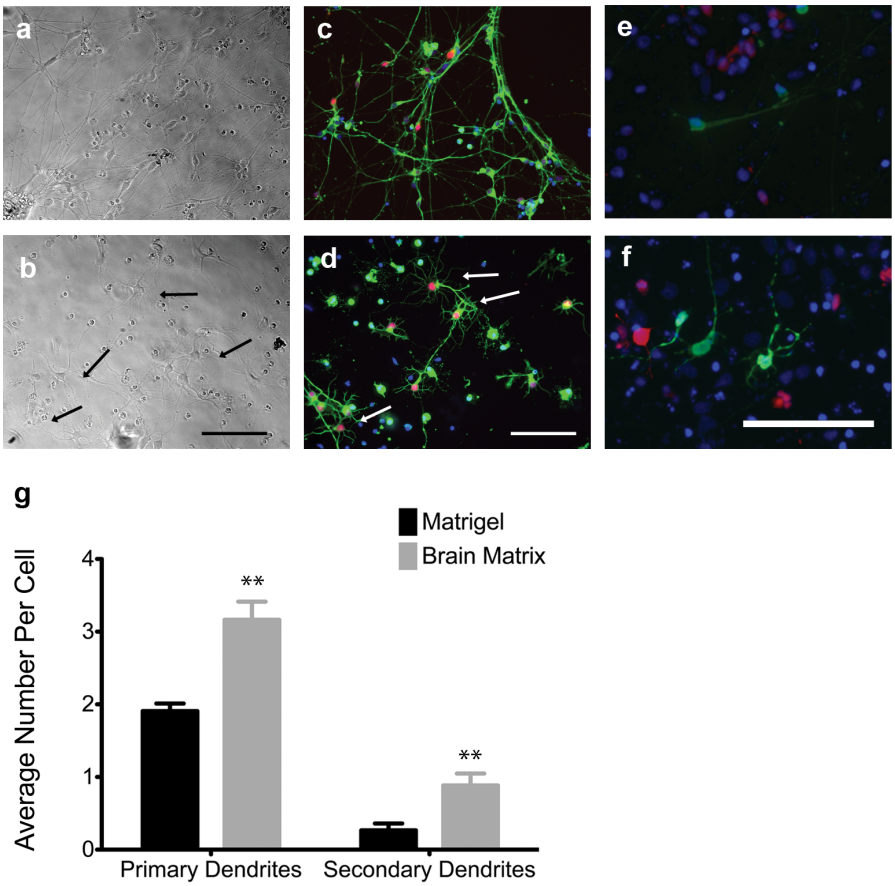

Figure 5.2: Dendritic staining on brain matrix and Matrigel
The brain matrix coating (b, d, f) is able to support neurons derived from induced pluripotent stem cells. Highly branched neurons were identified on the brain matrix, which were not seen in the Matrigel coated wells (a, c, e). Cells were stained (c, d) for β-III-tubulin, a neuronal marker (green) and GABA-ergic neurons were identified through staining for GABA at one week (red). Arrows identify highly branched neurons on the brain matrix coating. eGFP-transfected cells (e, f) were assessed for primary and secondary dendritic branching at 8 days. Quantification of primary dendrites and secondary dendrites indicates a statistically significant increase in dendritic formation on the brain matrix coatings when compared to Matrigel coatings (g). Scale bar at 100 μm. ** $p < 0.01$.

The neurons were able to mature on the brain matrix, as neurons cultured for two weeks polarized and formed dendrites as suggested by MAP2 staining of dendrites, and lack of MAP2 staining of axons (Figure 5.3). Additionally, synapsin, which is a phosphoprotein localized to synapses, increased in expression from one-week cultures to two-week cultures, indicating maturation of the neurons (Figure 5.4). At one week, area

of synapsin was measured to be 178.5 ± 29.4 pixels on Matrigel and 324.0 ± 145.6 pixels on brain matrix. At two weeks, synapsin was measured as 7096.6 ± 2962.7 pixels on Matrigel and 9687.5 ± 1454.2 pixels on the brain matrix. Synapsin expression as measured through immunofluorescence increased over time in both groups with a trend towards increased synapsin expression on the brain matrix, although this was not significant.

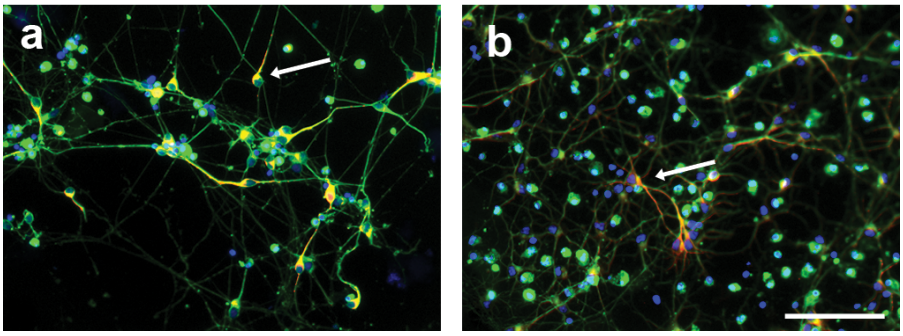

Figure 5.3: Map2 stain of brain matrix and Matrigel
Neurons cultured on Matrigel (a) and brain matrix coatings (b) are able to polarize as evidenced by Map2 localization (red, arrow). Neurons were co-stained for β-III-tubulin, a general neuronal marker (green). Scale bar at 100 μm.

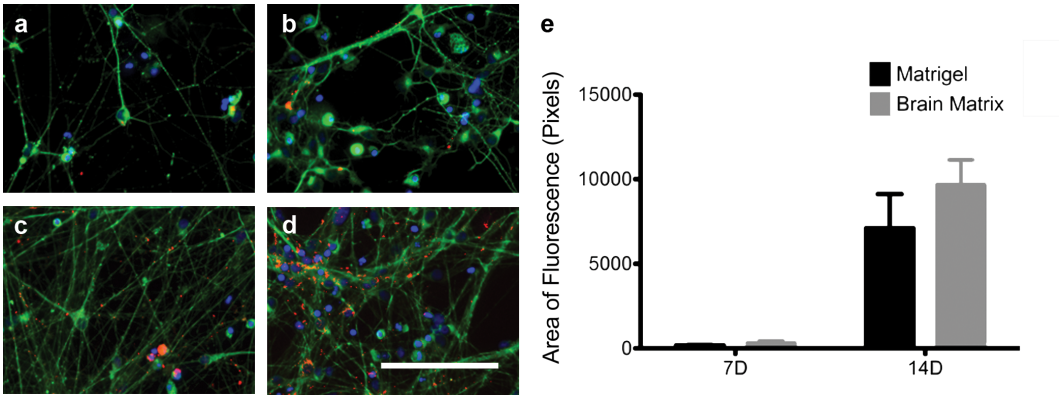

Figure 5.4: Synapsin staining of neurons on brain matrix and Matrigel
Synapsin levels increased in both the Matrigel coated (a, c) and brain matrix coated (b, d) wells over time. Synapsin (red) is co-stained with β-III-tubulin, a general neuronal marker (green). One-week cultures (a, b) demonstrate less synapsin than at two weeks (c, d). Scale bar at 100 μm. Quantification of synapsin expression as area per field of view are shown in (e), and while there is no significance between the coatings, there is a trend of increased synapsin expression on the brain matrix.

5.3.3 Brain matrix scaffold generation *in vivo*

The brain matrix material was able to form a gel *in vivo* when brought to a physiological pH and injected subcutaneously into C57 mice. Solubilized brain matrix remained liquid on ice or at room temperature, but was able to form a gel upon injection at 16 mg/ml, and 12 mg/ml (Figure 5.5). The gel was identified as a large bolus underneath the skin and did not move when gently pressed after 20 minutes post-injection. Immunohistochemistry of sections of the brain matrix gel identified collagen I, collagen III, collagen IV and laminin remaining in the brain matrix hydrogel after injection and did not contain visible amounts of DNA (Figure 5.6). Control sections demonstrated negative staining. To view the structure of the gels, SEM analysis demonstrated that the brain matrix was composed of a series of nanofibrous structures (Figure 5.7). Many of the nanofibers appeared to assemble and form larger microscale fibrils within the gel. For comparison, Matrigel gels and native porcine brain tissue were also imaged using SEM. Matrigel is also able to form a fibrous structure after gelation, but did not form large self-assembled microscale fibers as compared to the brain matrix.

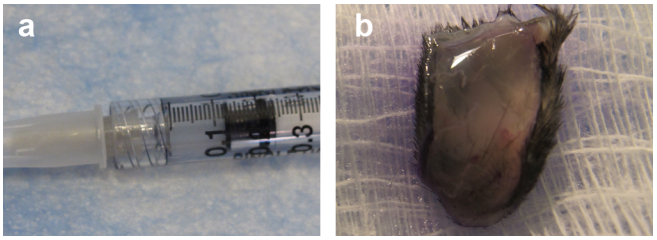

Figure 5.5: Subcutaneous brain matrix gelation
Brain matrix material was loaded into a syringe (a) and injected subcutaneously, whereupon the injected material self assembles into a gel. (b) displays the excised brain matrix hydrogel.

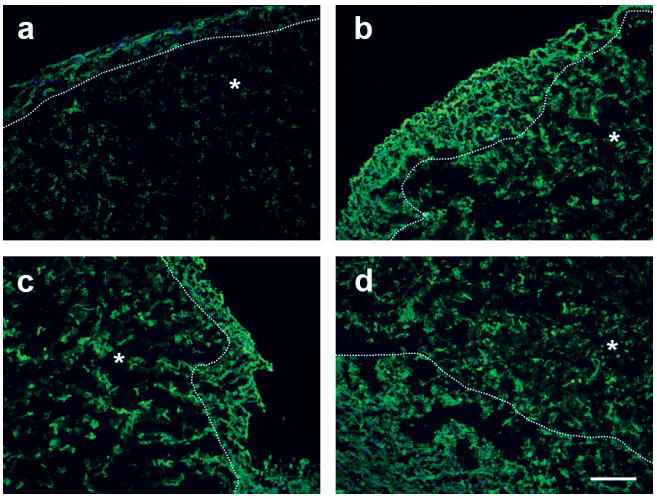

Figure 5.6: Immunohistochemistry of injected brain matrix gels
demonstrates retention of extracellular matrix proteins. A dotted line demarcates the border of the hydrogel, which is denoted by '*'. Collagen I (a), collagen III (b), collagen IV (c) and laminin (d) were observed. Scale bar at 100 μm.

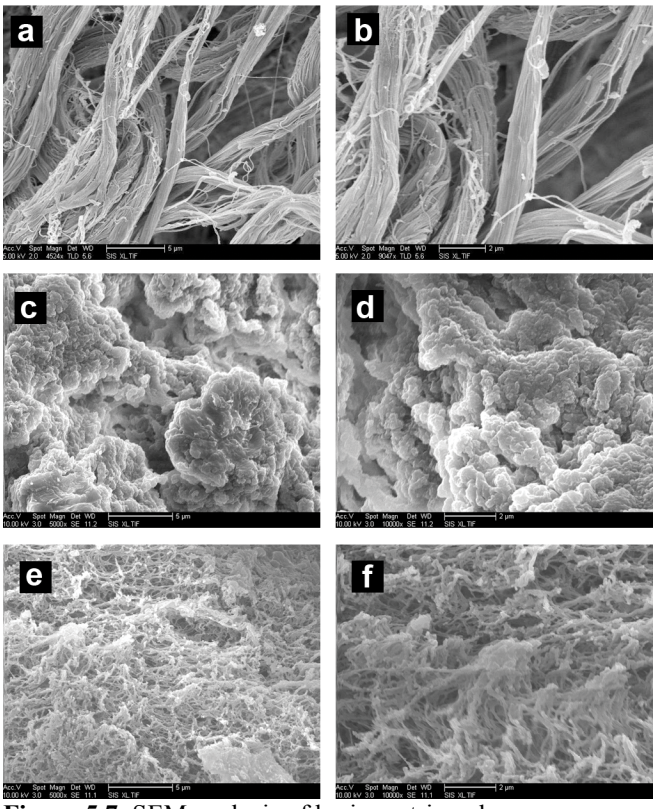

Figure 5.7: SEM analysis of brain matrix gels
SEM analysis was performed on brain matrix gels, native brain tissue, or Matrigel gels. SEM reveals that brain matrix gels formed after subcutaneous injection *in vivo* are composed of a network of nanofibers and microfibers (a,b). This acellular fibrous network is in contrast to the cellular native brain (c, d) and the nanofibrous Matrigel (e, f). Scale bars at 5 μm (a, c, e) and 2 μm (b, d, f).

5.4 Discussion

Extracellular cues play a role in many aspects of neural development *in vivo* [204-206] as well an *in vitro* [206,207]. The substrate chosen for *in vitro* neuron studies is thus highly important as phenotypic, electrophysiological and molecular changes have been identified in neural cells when cultured on various proteins or synthetic coatings [206-208]. Indeed, cell-matrix interactions of neurons derived from human embryonic stem cells were seen to strongly affect differentiation, as neurons demonstrated increased differentiation on laminin-rich substrates, and higher expansion and neurite outgrowth in a dose-dependent manner [209]. As the culture substrate has demonstrated effects on morphology, differentiation and function of neurons, the development of a complex tissue-matched culture substrate may be beneficial for *in vitro* assays and neural growth.

The native ECM is a complex combination of proteins and polysaccharides that play an important role in cellular behavior such as attachment, proliferation, and differentiation. Current cell culture methods and tissue engineering scaffolds conventionally use purified proteins and do not mimic the complexity of the brain extracellular microenvironment. Combinations of purified proteins have been shown to improve cell proliferation and differentiation, which indicates that complex coatings are beneficial, and thus there has been a shift toward more complex materials [91,92]. As there are limitless potential combinations, using a naturally derived matrix may be more physiologically relevant. A variety of tissues have been decellularized and used as cell culture coatings to provide a closer mimic to the *in vivo* microenvironment [99,100,191]. These coatings have shown tissue-specific effects on cellular behavior, and in some instances increased maturation when compared to conventional substrates [100,191].

In this study, we isolated and solubilized extracellular matrix from porcine brain using a detergent decellularization method and processed it to a liquid form using enzymatic digestion. We used SDS detergents to remove cellular content, and though SDS has been shown to denature extracellular matrix proteins [210], others have reported that SDS decellularization was milder than other techniques such as those using Triton X-100 and trypsin [211,212]. Our initial trials attempting to decellularize brain with other detergents such as sodium deoxycholate and Triton X-100 did not remove as much cellular content. We found many differences in developing a decellularization protocol for brain compared to other tissues, as the brain ECM is very weak and the tissue fell apart readily, leading to difficulties in rinsing and recovering the brain matrix. Through this method we were able to isolate brain ECM, but could not maintain the original structure of the brain. The isolated ECM was, however, able to be processed into a cell culture coating and an injectable scaffold. The matrix that was retained in our method was rinsed and processed, and while there were no visible nuclei present in the H&E sections, not all nuclear content was fully removed from the brain matrix material. The remaining DNA content was, however, less than that reported with other decellularization techniques [100].

Overall, brain ECM is composed mostly of glycosaminoglycans and proteoglycans with relatively small amounts of fibrous proteins such as collagen and fibronectin. Our results indicated that the decellularized material contains protein components that are found in the native brain extracellular matrix, and also retains sulfated glycosaminoglycans. Multiple collagen isoforms and laminin as well as the proteoglycan perlecan were retained post processing, though there may be other components that were not identified. The retention of laminin may prove to be important,

as laminin has been shown to increase neurite expansion, survival and outgrowth for neurons [208,209], as well as retinal explant attachment and axonal outgrowth [213]. The decellularization process was able to retain sulfated GAGs, despite the use of SDS, and was found to have one of the highest GAG contents when compared to other reported tissues that have been decellularized [99,100,191,196,210]. GAGs have been shown to have an effect on cell behavior, either alone or through association with other molecules [214]. While our decellularization protocol likely reduces protein and GAG content relative to native tissue, we are still able to retain many of the components while removing over 95% of the cellular content. While there is minor DNA content remaining in our brain matrix, a recent study demonstrated that several commercially available decellularized ECM scaffolds although contained measureable amounts of DNA, could still be used successfully in the clinic [215]. This may indicate that there is a threshold of DNA levels to avoid a negative immune response, or that the detergents may disrupt the structure of DNA so that the immune response will not be triggered.

The brain matrix can be used as an *in vitro* coating and it was shown to support the culture and maturation of neurons. Neurons expressed synapsin, a protein marker that identifies formation of synapses and maturation of the neurons [216]. Synapsin expression increased over time in culture, demonstrating that the neurons matured on the brain matrix coating. Interestingly, extensive dendritic processes were observed on the decellularized brain matrix, supporting complex arborization, but were not seen on Matrigel. Branching complexity has been theorized to have an important effect on the electrophysiology of dendritic neurons [217], though mechanisms controlling dendritic architecture are not fully known.

While there are no clinically used materials for brain tissue reconstruction yet [218], several naturally derived and synthetic materials have been studied as scaffolds in small animal models. None of these scaffolds offer the complexity of native brain ECM, and require major surgery for implantation. Injectable scaffolds [63-65] have been developed for minimally invasive delivery, but again do not recapitulate the composition of the native microenvironment. Thus, we tested proof-of-concept for utilizing our solubilized decellularized brain extracellular matrix as an injectable tissue engineering scaffold. While the brain matrix remains liquid at room temperature, when brought to physiological pH and injected subcutaneously, the material is able to self-assemble into a gel *in vivo*. The advantage of using an injectable hydrogel is that it will allow minimally invasive delivery of the material, injection into multiple sites and could be tailored to fit the size of the brain lesion. Though only injected subcutaneously, this preliminary work offers the potential to use this material as a tissue-matched scaffold. With this work, we demonstrate a method to decellularize and isolate brain ECM, the development of cell culture coatings derived from brain ECM, and *in vivo* feasibility of a brain matrix scaffold for tissue engineering applications.

Chapter 5, in full, is published as: DeQuach JA, Yuan SH, Goldstein LSB, Christman KL. Decellularized porcine brain matrix for cell culture and tissue engineering scaffolds. Tissue Engineering Part A, accepted with special recognition for the Mary Ann Liebert Inc. Outstanding Student Award.

The author of this dissertation is one of the primary authors on this publication.

CHAPTER SIX:

Summary and future work

6.1 Summary and conclusions

The ECM is composed of a complex variety of proteins and polysaccharides, that is unique to each tissue [67,190]. And this extracellular microenvironment has been well-known to influence cellular behavior such as attachment, survival, migration, proliferation and differentiation [66,84,135,219-221]. Despite its complexity *in vivo*, many studies use purified proteins for cell culture coatings or tissue engineering scaffolds, which may not provide the correct biomimetic environment. Thus, to properly study cellular behavior, and to regenerate tissue, a biomimetic platform would provide the proper biochemical cues. Previously studied materials in tissue engineering applications to treat stroke, myocardial infarction, and peripheral artery disease include single protein scaffolds such as collagen, fibrin, and self-assembling peptides which would not provide a mimic of the complexity of the *in vivo* microenvironment. Additionally, combination materials such as collagen-fibrin, or hyaluronan-hybrids have been utilized, but again do not provide a complex platform. Materials derived from non-mammalian sources such as chitosan and alginate have been used. And synthetic materials such as PEG have also been utilized. An example of materials that have been studied that are complex include Matrigel which is derived from a mouse sarcoma cell line, and small intestine sub-mucosa or bladder matrix which again do not mimic any specific tissue.

Hence, we have developed decellularized biomaterials from porcine brain, skeletal muscle, and cardiac tissue that can be used as a cell culture substrate, for *in vitro* assays, or as an injectable biomaterial that could be used after ischemic damage to prevent the debilitating downstream effects. The importance of choosing a biomimetic substrate for cellular culture could be important for functional studies and for drug development testing, especially as the use of human embryonic stem cells or using one's

induced pluripotent stem cells for disease modeling and personalized medicine is on the horizon. For instance, with this work we demonstrate that progenitor cells maintain more mature phenotype when cultured on the decellularized biomaterial when compared to conventional substrates. Each tissue has its own unique ECM, which is created by the cells of that tissue, which indicate that the choice of tissue ECM may be important [84,222]. A comparison of decellularized dermal, fat, and sarcoma tissue reveal that the ECM composition is different between the tissues, and disease state [220]. Thus for cellular culture and for biomaterials for tissue engineering, it suggests that using the ECM from that same tissue would provide the best environment for cell-ECM interactions.

The development of biomaterials from decellularized porcine tissues are explored and tested as a cell culture coating (Chapter 2 and 5). The matrix materials from brain, skeletal muscle and tissue were characterized using mass spectrometry and glycosaminoglycan analysis and it was determined that the material is able to retain ECM proteins and polysaccharides. Cardiomyocytes, skeletal muscle, and neural progenitors all demonstrate a more mature morphology when cultured on the tissue-matched matrix when compared to conventional coatings. The muscle matrix was also studied in mitogenic and migration *in vitro* assays, in order to determine whether the matrix materials would have an effect on cellular behavior. It was found that the muscle matrices are able to increase proliferation and migration when compared to commonly used materials. These studies demonstrate that the decellularized extracellular matrix materials have potential to provide a microenvironment that is able to affect multiple cellular activities.

Scaffolds were formed to study the decellularized matrix as a biomaterial for tissue engineering to treat ischemic injury. Upon injection, the materials are able to self-

assemble into a porous nanofibrous scaffold (Chapter 3, 4, and 5) that may provide a conducive environment for cellular infiltration for tissue engineering. The skeletal muscle matrix was then explored to alleviate ischemia in a femoral hindlimb ischemia model where it was found that the material is able to recruit vessels and muscle cells to the site of injury (Chapter 3). As the previously studied materials have been from a xenogeneic source, an allogeneic tissue source is explored (Chapter 4) from human cardiac tissue.

With this work, we demonstrate that through decellularization of brain, skeletal muscle, and cardiac tissue that we are able to develop a material that can be used as a biomimetic cell culture platform as well as an injectable scaffold for tissue engineering. As a cell culture coating, the cells demonstrate a more mature morphology, a closer mimic to how primary cells appear after isolation. For example, muscle progenitor cells fuse into larger, thicker myotubes, which is a process that mimics the formation of muscle fibers in the body during development. Cardiomyocytes derived from human embryonic stem cells appear striated, and display a more mature formation of the intracellular junction protein desmoplakin. And neurons that were differentiated from induced pluripotent stem cells exhibit a clearly defined axon and increased dendritic branching when compared to standard coatings. Additionally, we find that materials can be injected to form a self-assembling scaffold *in situ* that could be used as a tissue engineering scaffold, and can be derived from allogeneic sources with further processing. The decellularized extracellular matrix is a robust platform technology that can be used to further elucidate cell-matrix interactions and be translated as a clinically relevant material used to patients suffering from ischemic attack.

6.2 Limitations and future work

There are some limitations in design of the studies presented in this dissertation, as well opportunities for future work.

Future studies would include the study of cell-matrix interactions to see if there is any functional change in addition to changes in cellular morphology. For instance, with the cell culture studies presented in this work in Chapter 2 and 5, only morphological changes were studied. Additionally, these studies were only performed on coatings, as opposed to 3-D systems such as using cell encapsulation. However, many of these studies are underway through collaborations at other institutions.

A more rigorous characterization of the decellularized material would provide additional information about why the decellularized biomaterials had an effect on the maturation of stem and progenitor cells when compared to conventional coatings. While it is extremely difficult to study the composition of the material using a high-throughput method, we chose to use mass spectrometry as it could provide information of the composition without the need to characterize each individual peptide. However, as a technique, mass spectrometry has its limitations, as it is non-quantitative and not all-inclusive. With samples as heterogeneous and complex as the decellularized materials, better methods will need to be developed to study the composition of these materials.

Another limitation is potential batch-to-batch variability of the material. As with many biologically derived materials, there is likely to be variability as the source material is highly complex and naturally derived. While efforts were made to limit the variability in the studies performed, it is still an issue that affects materials that are biologically derived materials.

In Chapter 3, one limitation to the hindlimb ischemia model study was that comparison to a non-tissue specific scaffold would also be of interest. While the study compared the skeletal muscle matrix to a commonly used material, collagen, which is an important control. However to answer whether the material needs to be derived from a tissue-specific source, comparison of the skeletal muscle matrix to a non-tissue matched source would also provide important information. Further limitations include the fact that effects were only studied in the biomaterial, and not in the surrounding tissues. Future studies to assess functional benefit, and studies in a large animal model will be critical prior to translation of this therapy to the clinic. For instance, regional injection sites might play an important role for functional benefit, and multiple injections might be needed. A limitation of using a small animal model is that the 150 µl injection spreads through most of the tissue, and information about the importance of injection location could not be determined from the study, but could be better studied in a large animal model.

In Chapter 4, additional studies are underway to determine whether the allogeneic tissue source will demonstrate any effect on cardiac-relevant cell types as seen with the porcine cardiac matrices. Further characterization of the human cardiac matrix will be needed, and compositional and behavioral comparison to porcine matrix would be useful. *In vivo* applications need further studying, to test whether an allogeneic source would induce less immune reaction than a porcine source of the cardiac matrix.

References

1. Chen FC, Ogut O. Decline of contractility during ischemia-reperfusion injury: actin glutathionylation and its effect on allosteric interaction with tropomyosin. American journal of physiology. Cell physiology 2006;290(3):C719-27.

2. Griffiths EJ, Halestrap AP. Mitochondrial non-specific pores remain closed during cardiac ischaemia, but open upon reperfusion. The Biochemical journal 1995;307 (Pt 1):93-8.

3. Green DR, Reed JC. Mitochondria and apoptosis. Science 1998;281(5381):1309-12.

4. Toledo-Pereyra LH, Lopez-Neblina F, Toledo AH. Reactive oxygen species and molecular biology of ischemia/reperfusion. Annals of transplantation : quarterly of the Polish Transplantation Society 2004;9(1):81-3.

5. Wang WZ, Baynosa RC, Zamboni WA. Therapeutic interventions against reperfusion injury in skeletal muscle. The Journal of surgical research 2011;171(1):175-82.

6. Wang WZ, Fang XH, Stephenson LL, Khiabani KT, Zamboni WA. Ischemia/reperfusion-induced necrosis and apoptosis in the cells isolated from rat skeletal muscle. Journal of orthopaedic research : official publication of the Orthopaedic Research Society 2008;26(3):351-6.

7. Manzi M, Palena L, Cester G. Endovascular techniques for limb salvage in diabetics with crural and pedal disease. J Cardiovasc Surg (Torino) 2011;52(4):485-92.

8. Stansby G, Williams R. Angioplasty for treatment of isolated below-the-knee arterial stenosis in patients with critical limb ischemia. Angiology 2011;62(5):357-8.

9. Hackam DG, Goodman SG, Anand SS. Management of risk in peripheral artery disease: recent therapeutic advances. American heart journal 2005;150(1):35-40.

10. Hirsch AT, Haskal ZJ, Hertzer NR, Bakal CW, Creager MA, Halperin JL, Hiratzka LF, Murphy WR, Olin JW, Puschett JB and others. ACC/AHA 2005 guidelines for the management of patients with peripheral arterial disease (lower extremity, renal, mesenteric, and abdominal aortic): executive summary a collaborative report from the American Association

for Vascular Surgery/Society for Vascular Surgery, Society for Cardiovascular Angiography and Interventions, Society for Vascular Medicine and Biology, Society of Interventional Radiology, and the ACC/AHA Task Force on Practice Guidelines (Writing Committee to Develop Guidelines for the Management of Patients With Peripheral Arterial Disease) endorsed by the American Association of Cardiovascular and Pulmonary Rehabilitation; National Heart, Lung, and Blood Institute; Society for Vascular Nursing; TransAtlantic Inter-Society Consensus; and Vascular Disease Foundation. Journal of the American College of Cardiology 2006;47(6):1239-312.

11. Blaisdell FW. The pathophysiology of skeletal muscle ischemia and the reperfusion syndrome: a review. Cardiovascular surgery 2002;10(6):620-30.

12. Ahmad TS, Musa G, Lee JK. A review of free flap failures in the University Hospital, Kuala Lumpur. Annals of the Academy of Medicine, Singapore 1997;26(6):840-3.

13. Comerota AJ. Endovascular and surgical revascularization for patients with intermittent claudication. The American journal of cardiology 2001;87(12A):34D-43D.

14. Manzi M, Palena L, Cester G. Endovascular techniques for limb salvage in diabetics with crural and pedal disease. The Journal of cardiovascular surgery 2011;52(4):485-92.

15. Chan YC, Cheng SW. Drug-eluting stents and balloons in peripheral arterial disease: evidence so far. Int J Clin Pract 2011;65(6):664-8.

16. Dattilo PB, Casserly IP. Critical limb ischemia: endovascular strategies for limb salvage. Prog Cardiovasc Dis 2011;54(1):47-60.

17. Tongers J, Roncalli JG, Losordo DW. Therapeutic angiogenesis for critical limb ischemia: microvascular therapies coming of age. Circulation 2008;118(1):9-16.

18. Alev C, Ii M, Asahara T. Endothelial progenitor cells: a novel tool for the therapy of ischemic diseases. Antioxid Redox Signal 2011;15(4):949-65.

19. Kawamoto A, Katayama M, Handa N, Kinoshita M, Takano H, Horii M, Sadamoto K, Yokoyama A, Yamanaka T, Onodera R and others. Intramuscular transplantation of G-CSF-mobilized CD34(+) cells in patients with critical limb ischemia: a phase I/IIa, multicenter, single-blinded, dose-escalation clinical trial. Stem Cells 2009;27(11):2857-64.

20. Menasché P. Cell therapy for peripheral arterial disease. Curr Opin Mol Ther 2010;12(5):538-45.

21. Gupta R, Losordo DW. Cell therapy for critical limb ischemia: moving forward one step at a time. Circ Cardiovasc Interv 2011;4(1):2-5.

22. Layman H, Rahnemai-Azar AA, Pham SM, Tsechpenakis G, Andreopoulos FM. Synergistic angiogenic effect of codelivering fibroblast growth factor 2 and granulocyte-colony stimulating factor from fibrin scaffolds and bone marrow transplantation in critical limb ischemia. Tissue Eng Part A 2011;17(1-2):243-54.

23. Ruvinov E, Leor J, Cohen S. The effects of controlled HGF delivery from an affinity-binding alginate biomaterial on angiogenesis and blood perfusion in a hindlimb ischemia model. Biomaterials 2010;31(16):4573-82.

24. Webber MJ, Tongers J, Newcomb CJ, Marquardt KT, Bauersachs J, Losordo DW, Stupp SI. Supramolecular nanostructures that mimic VEGF as a strategy for ischemic tissue repair. Proceedings of the National Academy of Sciences of the United States of America 2011;108(33):13438-43.

25. Kuraitis D, Zhang P, Zhang Y, Padavan DT, McEwan K, Sofrenovic T, McKee D, Zhang J, Griffith M, Cao X and others. A stromal cell-derived factor-1 releasing matrix enhances the progenitor cell response and blood vessel growth in ischaemic skeletal muscle. European cells & materials 2011;22:109-23.

26. Layman H, Spiga MG, Brooks T, Pham S, Webster KA, Andreopoulos FM. The effect of the controlled release of basic fibroblast growth factor from ionic gelatin-based hydrogels on angiogenesis in a murine critical limb ischemic model. Biomaterials 2007;28(16):2646-54.

27. Merritt EK, Hammers DW, Tierney M, Suggs LJ, Walters TJ, Farrar RP. Functional assessment of skeletal muscle regeneration utilizing homologous extracellular matrix as scaffolding. Tissue Eng Part A;16(4):1395-405.

28. Lloyd-Jones D, Adams R, Carnethon M, De Simone G, Ferguson TB, Flegal K, Ford E, Furie K, Go A, Greenlund K and others. Heart disease and stroke statistics -- 2009 update: a report from the American Heart Association Statistics Committee and Stroke Statistics Subcommittee. Circulation 2009;119(3):480-6.

29. Weisman HF, Bush DE, Mannisi JA, Weisfeldt ML, Healy B. Cellular mechanisms of myocardial infarct expansion. Circulation 1988;78(1):186-201.

30. Narula J, Haider N, Virmani R, DiSalvo TG, Kolodgie FD, Hajjar RJ, Schmidt U, Semigran MJ, Dec GW, Khaw BA. Apoptosis in myocytes in end-stage heart failure. N Engl J Med 1996;335(16):1182-9.

31. Deten A, Volz HC, Briest W, Zimmer HG. Cardiac cytokine expression is upregulated in the acute phase after myocardial infarction. Experimental studies in rats. Cardiovasc Res 2002;55(2):329-40.

32. Thomas CV, Coker ML, Zellner JL, Handy JR, Crumbley AJ, 3rd, Spinale FG. Increased matrix metalloproteinase activity and selective upregulation in LV myocardium from patients with end-stage dilated cardiomyopathy. Circulation 1998;97(17):1708-15.

33. Tyagi SC, Campbell SE, Reddy HK, Tjahja E, Voelker DJ. Matrix metalloproteinase activity expression in infarcted, noninfarcted and dilated cardiomyopathic human hearts. Mol Cell Biochem 1996;155(1):13-21.

34. Hutchins GM, Bulkley BH. Infarct expansion versus extension: two different complications of acute myocardial infarction. Am J Cardiol 1978;41(7):1127-32.

35. Jeremy RW, Hackworthy RA, Bautovich G, Hutton BF, Harris PJ. Infarct artery perfusion and changes in left ventricular volume in the month after acute myocardial infarction. J Am Coll Cardiol 1987;9(5):989-95.

36. Kellar RS, Shepherd BR, Larson DF, Naughton GK, Williams SK. Cardiac patch constructed from human fibroblasts attenuates reduction in cardiac function after acute infarct. Tissue Eng 2005;11(11-12):1678-87.

37. Leor J, Aboulafia-Etzion S, Dar A, Shapiro L, Barbash IM, Battler A, Granot Y, Cohen S. Bioengineered cardiac grafts: A new approach to repair the infarcted myocardium? Circulation 2000;102(19 Suppl 3):III56-61.

38. Zimmermann WH, Didie M, Wasmeier GH, Nixdorff U, Hess A, Melnychenko I, Boy O, Neuhuber WL, Weyand M, Eschenhagen T. Cardiac grafting of engineered heart tissue in syngenic rats. Circulation 2002;106(12 Suppl 1):I151-7.

39. Fujimoto KL, Tobita K, Merryman WD, Guan J, Momoi N, Stolz DB, Sacks MS, Keller BB, Wagner WR. An elastic, biodegradable cardiac patch induces contractile smooth muscle and improves cardiac remodeling

and function in subacute myocardial infarction. J Am Coll Cardiol 2007;49(23):2292-300.

40. Robinson KA, Li J, Mathison M, Redkar A, Cui J, Chronos NAF, Matheny RG, Badylak SF. Extracellular matrix scaffold for cardiac repair. Circulation 2005;112(suppl I):I-135-143.

41. Badylak SF, Obermiller J, Geddes L, Matheny R. Extracellular matrix for myocardial repair. The Heart Surgery Forum 2002;6(2):E20-26.

42. Lu WN, Lu SH, Wang HB, Li DX, Duan CM, Liu ZQ, Hao T, He WJ, Xu B, Fu Q and others. Functional Improvement of Infarcted Heart by Co-Injection of Embryonic Stem Cells with Temperature-Responsive Chitosan Hydrogel. Tissue Eng Part A 2008.

43. Leor J, Tuvia S, Guetta V, Manczur F, Castel D, Willenz U, Petnehazy O, Landa N, Feinberg MS, Konen E and others. Intracoronary injection of in situ forming alginate hydrogel reverses left ventricular remodeling after myocardial infarction in Swine. J Am Coll Cardiol 2009;54(11):1014-23.

44. Landa N, Miller L, Feinberg MS, Holbova R, Shachar M, Freeman I, Cohen S, Leor J. Effect of injectable alginate implant on cardiac remodeling and function after recent and old infarcts in rat. Circulation 2008;117(11):1388-96.

45. Dai W, Wold LE, Dow JS, Kloner RA. Thickening of the infarcted wall by collagen injection improves left ventricular function in rats: a novel approach to preserve cardiac function after myocardial infarction. J Am Coll Cardiol 2005;46(4):714-9.

46. Christman KL, Fok HH, Sievers RE, Fang Q, Lee RJ. Fibrin glue alone and skeletal myoblasts in a fibrin scaffold preserve cardiac function after myocardial infarction. Tissue Eng 2004;10:403-9.

47. Christman KL, Vardanian AJ, Fang Q, Sievers RE, Fok HH, Lee RJ. Injectable fibrin scaffold improves cell transplant survival, reduces infarct expansion, and induces neovasculature formation in ischemic myocardium. J Am Coll Cardiol 2004;44(3):654-60.

48. Albini A, Melchiori A, Garofalo A, Noonan DM, Basolo F, Taraboletti G, Chader GJ, Gavazzi R. Matrigel promotes retinoblastoma cell growth in vitro and in vivo. Int J Cancer 1992;52(2):234-40.

49. Yue W, Brodie A. MCF-7 human breast carcinomas in nude mice as a model for evaluating aromatase inhibitors. J Steroid Biochem Mol Biol 1993;44(4-6):671-3.

50. Dobner S, Bezuidenhout D, Govender P, Zilla P, Davies N. A synthetic non-degradable polyethylene glycol hydrogel retards adverse post-infarct left ventricular remodeling. J Card Fail 2009;15(7):629-36.

51. Zhong J, Chan A, Morad L, Kornblum HI, Fan G, Carmichael ST. Hydrogel matrix to support stem cell survival after brain transplantation in stroke. Neurorehabilitation and neural repair 2010;24(7):636-44.

52. Wei L, Keogh CL, Whitaker VR, Theus MH, Yu SP. Angiogenesis and stem cell transplantation as potential treatments of cerebral ischemic stroke. Pathophysiology : the official journal of the International Society for Pathophysiology / ISP 2005;12(1):47-62.

53. Godier-Furnemont AF, Martens TP, Koeckert MS, Wan L, Parks J, Arai K, Zhang G, Hudson B, Homma S, Vunjak-Novakovic G. Composite scaffold provides a cell delivery platform for cardiovascular repair. Proceedings of the National Academy of Sciences of the United States of America 2011;108(19):7974-9.

54. Osanai T, Kuroda S, Yasuda H, Chiba Y, Maruichi K, Hokari M, Sugiyama T, Shichinohe H, Iwasaki Y. Noninvasive transplantation of bone marrow stromal cells for ischemic stroke: preliminary study with a thermoreversible gelation polymer hydrogel. Neurosurgery 2010;66(6):1140-7; discussion 1147.

55. Novak U, Kaye AH. Extracellular matrix and the brain: components and function. J Clin Neurosci. Volume 7; 2000. p 280-90.

56. Suri S, Schmidt CE. Cell-laden hydrogel constructs of hyaluronic acid, collagen, and laminin for neural tissue engineering. Tissue Eng Part A. Volume 16; 2010. p 1703-16.

57. Carbonetto S, Gruver MM, Turner DC. Nerve fiber growth in culture on fibronectin, collagen, and glycosaminoglycan substrates. J Neurosci. Volume 3; 1983. p 2324-35.

58. Wang T-W, Spector M. Development of hyaluronic acid-based scaffolds for brain tissue engineering. Acta biomaterialia. Volume 5; 2009. p 2371-84.

59. Cui FZ, Tian WM, Hou SP, Xu QY, Lee I-S. Hyaluronic acid hydrogel immobilized with RGD peptides for brain tissue engineering. J Mater Sci Mater Med. Volume 17; 2006. p 1393-401.

60. Eagle KS, Chalmers GR, Clary DO, Gage FH. Axonal regeneration and limited functional recovery following hippocampal deafferentation. J Comp Neurol. Volume 363; 1995. p 377-88.

61. Wong DY, Krebsbach PH, Hollister SJ. Brain cortex regeneration affected by scaffold architectures. J Neurosurg. Volume 109; 2008. p 715-22.

62. Park K, Teng… Y. The injured brain interacts reciprocally with neural stem cells supported by scaffolds to reconstitute lost tissue. Nature biotechnology; 2002.

63. Mahoney MJ, Saltzman WM. Transplantation of brain cells assembled around a programmable synthetic microenvironment. Nat Biotechnol. Volume 19; 2001. p 934-9.

64. Tate M, Shear D, Hoffman S, Stein… D. Biocompatibility of methylcellulose-based constructs designed for intracerebral gelation following experimental traumatic brain injury. Biomaterials; 2001.

65. Tate M, Shear D, Hoffman… S. Fibronectin promotes survival and migration of primary neural stem cells transplanted into the traumatically injured mouse brain. Cell …; 2002.

66. Lutolf MP, Hubbell JA. Synthetic biomaterials as instructive extracellular microenvironments for morphogenesis in tissue engineering. Nat Biotechnol 2005;23(1):47-55.

67. Uriel S, Labay E, Francis-Sedlak M, Moya ML, Weichselbaum RR, Ervin N, Cankova Z, Brey EM. Extraction and assembly of tissue-derived gels for cell culture and tissue engineering. Tissue Eng Part C Methods 2009;15(3):309-21.

68. Singelyn JM, DeQuach JA, Seif-Naraghi SB, Littlefield RB, Schup-Magoffin PJ, Christman KL. Naturally derived myocardial matrix as an injectable scaffold for cardiac tissue engineering. Biomaterials 2009;30(29):5409-16.

69. Young DA, Ibrahim DO, Hu D, Christman KL. Injectable hydrogel scaffold from decellularized human lipoaspirate. Acta biomaterialia 2011;7(3):1040-9.

70. Uygun BE, Soto-Gutierrez A, Yagi H, Izamis ML, Guzzardi MA, Shulman C, Milwid J, Kobayashi N, Tilles A, Berthiaume F and others. Organ reengineering through development of a transplantable recellularized liver graft using decellularized liver matrix. Nature medicine 2010;16(7):814-20.

71. Ott HC, Matthiesen TS, Goh SK, Black LD, Kren SM, Netoff TI, Taylor DA. Perfusion-decellularized matrix: using nature's platform to engineer a bioartificial heart. Nature medicine 2008;14(2):213-21.

72. Valentin JE, Turner NJ, Gilbert TW, Badylak SF. Functional skeletal muscle formation with a biologic scaffold. Biomaterials 2010;31(29):7475-84.

73. Gilbert TW, Sellaro TL, Badylak SF. Decellularization of tissues and organs. Biomaterials 2006;27(19):3675-83.

74. Bernard MP, Chu ML, Myers JC, Ramirez F, Eikenberry EF, Prockop DJ. Nucleotide sequences of complementary deoxyribonucleic acids for the pro alpha 1 chain of human type I procollagen. Statistical evaluation of structures that are conserved during evolution. Biochemistry 1983;22(22):5213-23.

75. Badylak SF, Freytes DO, Gilbert TW. Extracellular matrix as a biological scaffold material: Structure and function. Acta Biomater 2009;5(1):1-13.

76. Crapo PM, Gilbert TW, Badylak SF. An overview of tissue and whole organ decellularization processes. Biomaterials 2011;32(12):3233-43.

77. Numata S, Fujisato T, Niwaya K, Ishibashi-Ueda H, Nakatani T, Kitamura S. Immunological and histological evaluation of decellularized allograft in a pig model: comparison with cryopreserved allograft. The Journal of heart valve disease 2004;13(6):984-90.

78. Rieder E, Nigisch A, Dekan B, Kasimir MT, Muhlbacher F, Wolner E, Simon P, Weigel G. Granulocyte-based immune response against decellularized or glutaraldehyde cross-linked vascular tissue. Biomaterials 2006;27(33):5634-42.

79. Li F, Li W, Johnson S, Ingram D, Yoder M, Badylak S. Low-molecular-weight peptides derived from extracellular matrix as chemoattractants for primary endothelial cells. Endothelium 2004;11(3-4):199-206.

80. Badylak SF, Park K, Peppas N, McCabe G, Yoder M. Marrow-derived cells populate scaffolds composed of xenogeneic extracellular matrix. Exp Hematol 2001;29(11):1310-8.

81. Zantop T, Gilbert TW, Yoder MC, Badylak SF. Extracellular matrix scaffolds are repopulated by bone marrow-derived cells in a mouse model of achilles tendon reconstruction. J Orthop Res 2006;24(6):1299-309.

82. Beattie AJ, Gilbert TW, Guyot JP, Yates AJ, Badylak SF. Chemoattraction of Progenitor Cells by Remodeling Extracellular Matrix Scaffolds. Tissue Eng Part A 2008.

83. Reing JE, Zhang L, Myers-Irvin J, Cordero KE, Freytes DO, Heber-Katz E, Bedelbaeva K, McIntosh D, Dewilde A, Braunhut SJ and others. Degradation products of extracellular matrix affect cell migration and proliferation. Tissue Eng Part A 2009;15(3):605-14.

84. Badylak SF. The extracellular matrix as a biologic scaffold material. Biomaterials 2007;28(25):3587-93.

85. Koochekpour S, Merzak A, Pilkington GJ. Extracellular matrix proteins inhibit proliferation, upregulate migration and induce morphological changes in human glioma cell lines. Eur J Cancer 1995;31A(3):375-80.

86. Williams CM, Engler AJ, Slone RD, Galante LL, Schwarzbauer JE. Fibronectin expression modulates mammary epithelial cell proliferation during acinar differentiation. Cancer Res 2008;68(9):3185-92.

87. Bosnakovski D, Mizuno M, Kim G, Takagi S, Okumura M, Fujinaga T. Chondrogenic differentiation of bovine bone marrow mesenchymal stem cells (MSCs) in different hydrogels: influence of collagen type II extracellular matrix on MSC chondrogenesis. Biotechnol Bioeng 2006;93(6):1152-63.

88. Chastain SR, Kundu AK, Dhar S, Calvert JW, Putnam AJ. Adhesion of mesenchymal stem cells to polymer scaffolds occurs via distinct ECM ligands and controls their osteogenic differentiation. J Biomed Mater Res A 2006;78(1):73-85.

89. Simon-Assmann P, Kedinger M, De Arcangelis A, Rousseau V, Simo P. Extracellular matrix components in intestinal development. Experientia 1995;51(9-10):883-900.

90. Everitt EA, Malik AB, Hendey B. Fibronectin enhances the migration rate of human neutrophils in vitro. J Leukoc Biol 1996;60(2):199-206.

91. Brafman DA, Shah KD, Fellner T, Chien S, Willert K. Defining Long-Term Maintenance Conditions of Human Embryonic Stem Cells With Arrayed Cellular Microenvironment Technology. Stem Cells Dev 2009.

92. Flaim CJ, Teng D, Chien S, Bhatia SN. Combinatorial signaling microenvironments for studying stem cell fate. Stem Cells Dev 2008;17(1):29-39.

93. Cooper ST, Maxwell AL, Kizana E, Ghoddusi M, Hardeman EC, Alexander IE, Allen DG, North KN. C2C12 co-culture on a fibroblast substratum enables sustained survival of contractile, highly differentiated myotubes with peripheral nuclei and adult fast myosin expression. Cell Motil Cytoskeleton 2004;58(3):200-11.

94. Luo Y, Kobler JB, Zeitels SM, Langer R. Effects of growth factors on extracellular matrix production by vocal fold fibroblasts in 3-dimensional culture. Tissue Eng 2006;12(12):3365-74.

95. Radisic M, Park H, Martens TP, Salazar-Lazaro JE, Geng W, Wang Y, Langer R, Freed LE, Vunjak-Novakovic G. Pre-treatment of synthetic elastomeric scaffolds by cardiac fibroblasts improves engineered heart tissue. J Biomed Mater Res A 2008;86(3):713-24.

96. Ueno H, Nakamura F, Murakami M, Okumura M, Kadosawa T, Fujinag T. Evaluation effects of chitosan for the extracellular matrix production by fibroblasts and the growth factors production by macrophages. Biomaterials 2001;22(15):2125-30.

97. VanWinkle WB, Snuggs MB, Buja LM. Cardiogel: a biosynthetic extracellular matrix for cardiomyocyte culture. In Vitro Cell Dev Biol Anim 1996;32(8):478-85.

98. Kleinman HK, Martin GR. Matrigel: basement membrane matrix with biological activity. Semin Cancer Biol 2005;15(5):378-86.

99. Stern MM, Myers RL, Hammam N, Stern KA, Eberli D, Kritchevsky SB, Soker S, Van Dyke M. The influence of extracellular matrix derived from skeletal muscle tissue on the proliferation and differentiation of myogenic progenitor cells ex vivo. Biomaterials 2009;30(12):2393-9.

100. Zhang Y, He Y, Bharadwaj S, Hammam N, Carnagey K, Myers R, Atala A, Van Dyke M. Tissue-specific extracellular matrix coatings for the promotion of cell proliferation and maintenance of cell phenotype. Biomaterials 2009;30(23-24):4021-8.

101. Prydz K, Dalen KT. Synthesis and sorting of proteoglycans. J Cell Sci 2000;113 Pt 2:193-205.

102. Casar JC, Cabello-Verrugio C, Olguin H, Aldunate R, Inestrosa NC, Brandan E. Heparan sulfate proteoglycans are increased during skeletal muscle regeneration: requirement of syndecan-3 for successful fiber formation. J Cell Sci 2004;117(Pt 1):73-84.

103. Olguin HC, Santander C, Brandan E. Inhibition of myoblast migration via decorin expression is critical for normal skeletal muscle differentiation. Dev Biol 2003;259(2):209-24.

104. Freytes DO, Martin J, Velankar SS, Lee AS, Badylak SF. Preparation and rheological characterization of a gel form of the porcine urinary bladder matrix. Biomaterials 2008;29(11):1630-7.

105. Uygun BE, Stojsih SE, Matthew HWT. Effects of immobilized glycosaminoglycans on the proliferation and differentiation of mesenchymal stem cells. Tissue Engineering Part A. Volume 15; 2009. p 3499-512.

106. Yang L, Soonpaa MH, Adler ED, Roepke TK, Kattman SJ, Kennedy M, Henckaerts E, Bonham K, Abbott GW, Linden RM and others. Human cardiovascular progenitor cells develop from a KDR+ embryonic-stem-cell-derived population. Nature 2008;453(7194):524-8.

107. Reing JE, Zhang L, Myers-Irvin J, Cordero KE, Freytes DO, Heber-Katz E, Bedelbaeva K, McIntosh D, Dewilde A, Braunhut SJ and others. Degradation Products of Extracellular Matrix Affect Cell Migration and Proliferation. Tissue Eng Part A 2008.

108. Akahane T, Akahane M, Shah A, Connor CM, Thorgeirsson UP. TIMP-1 inhibits microvascular endothelial cell migration by MMP-dependent and MMP-independent mechanisms. Exp Cell Res 2004;301(2):158-67.

109. San Antonio JD, Karnovsky MJ, Ottlinger ME, Schillig R, Pukac LA. Isolation of heparin-insensitive aortic smooth muscle cells. Growth and differentiation. Arterioscler Thromb 1993;13(5):748-57.

110. Lau YT, Ma WC. Nitric oxide inhibits migration of cultured endothelial cells. Biochem Biophys Res Commun 1996;221(3):670-4.

111. Di Luozzo G, Pradhan S, Dhadwal AK, Chen A, Ueno H, Sumpio BE. Nicotine induces mitogen-activated protein kinase dependent vascular smooth muscle cell migration. Atherosclerosis 2005;178(2):271-7.

112. Okamoto O, Fujiwara S, Abe M, Sato Y. Dermatopontin interacts with transforming growth factor beta and enhances its biological activity. Biochem J 1999;337 (Pt 3):537-41.

113. Droguett R, Cabello-Verrugio C, Riquelme C, Brandan E. Extracellular proteoglycans modify TGF-beta bio-availability attenuating its signaling during skeletal muscle differentiation. Matrix Biol 2006;25(6):332-41.

114. Cabello-Verrugio C, Brandan E. A novel modulatory mechanism of transforming growth factor-beta signaling through decorin and LRP-1. J Biol Chem 2007;282(26):18842-50.

115. Brandan E, Cabello-Verrugio C, Vial C. Novel regulatory mechanisms for the proteoglycans decorin and biglycan during muscle formation and muscular dystrophy. Matrix Biol 2008;27(8):700-8.

116. Vlodavsky I, Miao HQ, Medalion B, Danagher P, Ron D. Involvement of heparan sulfate and related molecules in sequestration and growth promoting activity of fibroblast growth factor. Cancer Metastasis Rev 1996;15(2):177-86.

117. Lin X, Buff EM, Perrimon N, Michelson AM. Heparan sulfate proteoglycans are essential for FGF receptor signaling during Drosophila embryonic development. Development 1999;126(17):3715-23.

118. Makovitzky J, Richter S. The relevance of the aldehyde bisulfite toluidine blue reaction and its variants in the submicroscopic carbohydrate research. Acta Histochem. Volume 111; 2009. p 273-91.

119. Brown BN, Barnes CA, Kasick RT, Michel R, Gilbert TW, Beer-Stolz D, Castner DG, Ratner BD, Badylak SF. Surface characterization of extracellular matrix scaffolds. Biomaterials 2009;31(3):428-37.

120. Canavan HE, Graham DJ, Cheng X, Ratner BD, Castner DG. Comparison of native extracellular matrix with adsorbed protein films using secondary ion mass spectrometry. Langmuir. Volume 23; 2007. p 50-6.

121. Lhoest J, Wagner M, Tidwell C. Characterization of adsorbed protein films by time of flight secondary ion mass spectrometry. Journal of biomedical …; 2001.

122. Wold S, Esbensen, E., Geladi, P. Principal Component Analysis. Chemometrics and Intelligent Laboratory Systems 1987;2(1-3):37-52.

123. Rios R, Carneiro I, Arce VM, Devesa J. Myostatin regulates cell survival during C2C12 myogenesis. Biochem Biophys Res Commun 2001;280(2):561-6.

124. Cao F, Wagner RA, Wilson KD, Xie X, Fu JD, Drukker M, Lee A, Li RA, Gambhir SS, Weissman IL and others. Transcriptional and functional profiling of human embryonic stem cell-derived cardiomyocytes. PLoS ONE 2008;3(10):e3474.

125. Liu J, Fu JD, Siu CW, Li RA. Functional sarcoplasmic reticulum for calcium handling of human embryonic stem cell-derived cardiomyocytes: insights for driven maturation. Stem Cells 2007;25(12):3038-44.

126. Binah O, Dolnikov K, Sadan O, Shilkrut M, Zeevi-Levin N, Amit M, Danon A, Itskovitz-Eldor J. Functional and developmental properties of human embryonic stem cells-derived cardiomyocytes. J Electrocardiol 2007;40(6 Suppl):S192-6.

127. Laflamme MA, Gold J, Xu C, Hassanipour M, Rosler E, Police S, Muskheli V, Murry CE. Formation of human myocardium in the rat heart from human embryonic stem cells. Am J Pathol 2005;167(3):663-71.

128. Gai H, Leung EL, Costantino PD, Aguila JR, Nguyen DM, Fink LM, Ward DC, Ma Y. Generation and characterization of functional cardiomyocytes using induced pluripotent stem cells derived from human fibroblasts. Cell Biol Int 2009.

129. Leschik J, Stefanovic S, Brinon B, Puceat M. Cardiac commitment of primate embryonic stem cells. Nat Protoc 2008;3(9):1381-7.

130. Gerull B, Heuser A, Wichter T, Paul M, Basson CT, McDermott DA, Lerman BB, Markowitz SM, Ellinor PT, MacRae CA and others. Mutations in the desmosomal protein plakophilin-2 are common in arrhythmogenic right ventricular cardiomyopathy. Nat Genet 2004;36(11):1162-4.

131. Hirschy A, Schatzmann F, Ehler E, Perriard JC. Establishment of cardiac cytoarchitecture in the developing mouse heart. Dev Biol 2006;289(2):430-41.

132. Kottke MD, Delva E, Kowalczyk AP. The desmosome: cell science lessons from human diseases. J Cell Sci 2006;119(Pt 5):797-806.

133. Huber O. Structure and function of desmosomal proteins and their role in development and disease. Cell Mol Life Sci 2003;60(9):1872-90.

134. Peters NS, Severs NJ, Rothery SM, Lincoln C, Yacoub MH, Green CR. Spatiotemporal relation between gap junctions and fascia adherens junctions during postnatal development of human ventricular myocardium. Circulation 1994;90(2):713-25.

135. Macfelda K, Kapeller B, Wilbacher I, Losert UM. Behavior of cardiomyocytes and skeletal muscle cells on different extracellular matrix components--relevance for cardiac tissue engineering. Artif Organs 2007;31(1):4-12.

136. Suzuki A, Iwama A, Miyashita H, Nakauchi H, Taniguchi H. Role for growth factors and extracellular matrix in controlling differentiation of prospectively isolated hepatic stem cells. Development 2003;130(11):2513-24.

137. Bach AD, Beier JP, Stern-Staeter J, Horch RE. Skeletal muscle tissue engineering. J Cell Mol Med 2004;8(4):413-22.

138. Reubinoff BE, Pera MF, Fong CY, Trounson A, Bongso A. Embryonic stem cell lines from human blastocysts: somatic differentiation in vitro. Nat Biotechnol 2000;18(4):399-404.

139. Schuldiner M, Yanuka O, Itskovitz-Eldor J, Melton DA, Benvenisty N. Effects of eight growth factors on the differentiation of cells derived from human embryonic stem cells. Proc Natl Acad Sci U S A 2000;97(21):11307-12.

140. Tibbitt MW, Anseth KS. Hydrogels as extracellular matrix mimics for 3D cell culture. Biotechnol Bioeng 2009;103(4):655-63.

141. Seif-Naraghi SB, Salvatore MA, Schup-Magoffin PJ, Hu DP, Christman KL. Design and characterization of an injectable pericardial matrix gel: a potentially autologous scaffold for cardiac tissue engineering. Tissue engineering. Part A 2010;16(6):2017-27.

142. Christman KL, Singelyn JM, Salvatore M, Schup-Magoffin PJ, Hu DP, Johnson T, Bartels K, DeMaria AN, Dib N. Catheter-Deliverable Hydrogel Derived from Decellularized Ventricular Extracellular Matrix Increases Cardiomyocyte Survival and Preserves Cardiac Function Post-Myocardial Infarction. Journal of the American College of Cardiology 2011;57(14):E2017-E2017.

143. DeQuach JA, Mezzano V, Miglani A, Lange S, Keller GM, Sheikh F, Christman KL. Simple and high yielding method for preparing tissue specific extracellular matrix coatings for cell culture. PLoS One 2010;5(9):e13039.

144. Bhang SH, Kim JH, Yang HS, La WG, Lee TJ, Kim GH, Kim HA, Lee M, Kim BS. Combined gene therapy with hypoxia-inducible factor-1alpha and heme oxygenase-1 for therapeutic angiogenesis. Tissue engineering. Part A 2011;17(7-8):915-26.

145. Bach AD, Arkudas A, Tjiawi J, Polykandriotis E, Kneser U, Horch RE, Beier JP. A new approach to tissue engineering of vascularized skeletal muscle. Journal of cellular and molecular medicine 2006;10(3):716-26.

146. Christman KL, Vardanian AJ, Fang Q, Sievers RE, Fok HH, Lee RJ. Injectable fibrin scaffold improves cell transplant survival, reduces infarct expansion, and induces neovasculature formation in ischemic myocardium. Journal of the American College of Cardiology 2004;44(3):654-60.

147. Bruey JM, Kantarjian H, Ma W, Estrov Z, Yeh C, Donahue A, Sanders H, O'Brien S, Keating M, Albitar M. Circulating Ki-67 index in plasma as a biomarker and prognostic indicator in chronic lymphocytic leukemia. Leukemia research 2010;34(10):1320-4.

148. Scholzen T, Gerdes J. The Ki-67 protein: from the known and the unknown. Journal of cellular physiology 2000;182(3):311-22.

149. Diniz G, Aktas S, Turedi A, Temir G, Ortac R, Vergin C. Telomerase reverse transcriptase catalytic subunit expression and proliferation index in Wilms tumor. Tumour biology : the journal of the International Society for Oncodevelopmental Biology and Medicine 2011;32(4):761-7.

150. Cooper RN, Tajbakhsh S, Mouly V, Cossu G, Buckingham M, Butler-Browne GS. In vivo satellite cell activation via Myf5 and MyoD in regenerating mouse skeletal muscle. J Cell Sci 1999;112 (Pt 17):2895-901.

151. Megeney LA, Kablar B, Garrett K, Anderson JE, Rudnicki MA. MyoD is required for myogenic stem cell function in adult skeletal muscle. Genes Dev 1996;10(10):1173-83.

152. Yamamoto DL, Csikasz RI, Li Y, Sharma G, Hjort K, Karlsson R, Bengtsson T. Myotube formation on micro-patterned glass: intracellular organization and protein distribution in C2C12 skeletal muscle cells. J Histochem Cytochem 2008;56(10):881-92.

153. Hidestrand M, Richards-Malcolm S, Gurley CM, Nolen G, Grimes B, Waterstrat A, Zant GV, Peterson CA. Sca-1-expressing nonmyogenic cells contribute to fibrosis in aged skeletal muscle. J Gerontol A Biol Sci Med Sci 2008;63(6):566-79.

154. Belch JJ, Topol EJ, Agnelli G, Bertrand M, Califf RM, Clement DL, Creager MA, Easton JD, Gavin JR, 3rd, Greenland P and others. Critical issues in peripheral arterial disease detection and management: a call to action. Archives of internal medicine 2003;163(8):884-92.

155. Sprengers RW, Lips DJ, Moll FL, Verhaar MC. Progenitor cell therapy in patients with critical limb ischemia without surgical options. Annals of surgery 2008;247(3):411-20.

156. Lawall H, Bramlage P, Amann B. Stem cell and progenitor cell therapy in peripheral artery disease. A critical appraisal. Thrombosis and haemostasis 2010;103(4):696-709.

157. Fadini GP, Agostini C, Avogaro A. Autologous stem cell therapy for peripheral arterial disease meta-analysis and systematic review of the literature. Atherosclerosis 2010;209(1):10-7.

158. Lee J, Bhang SH, Park H, Kim BS, Lee KY. Active blood vessel formation in the ischemic hindlimb mouse model using a microsphere/hydrogel combination system. Pharmaceutical research 2010;27(5):767-74.

159. Silva EA, Mooney DJ. Spatiotemporal control of vascular endothelial growth factor delivery from injectable hydrogels enhances angiogenesis. Journal of thrombosis and haemostasis : JTH 2007;5(3):590-8.

160. Kong HJ, Kim ES, Huang YC, Mooney DJ. Design of biodegradable hydrogel for the local and sustained delivery of angiogenic plasmid DNA. Pharmaceutical research 2008;25(5):1230-8.

161. Jay SM, Shepherd BR, Bertram JP, Pober JS, Saltzman WM. Engineering of multifunctional gels integrating highly efficient growth factor delivery with endothelial cell transplantation. The FASEB journal : official publication of the Federation of American Societies for Experimental Biology 2008;22(8):2949-56.

162. Doi K, Ikeda T, Marui A, Kushibiki T, Arai Y, Hirose K, Soga Y, Iwakura A, Ueyama K, Yamahara K and others. Enhanced angiogenesis by gelatin hydrogels incorporating basic fibroblast growth factor in rabbit model of hind limb ischemia. Heart and vessels 2007;22(2):104-8.

163. Badylak SF, Freytes DO, Gilbert TW. Extracellular matrix as a biological scaffold material: Structure and function. Acta biomaterialia 2009;5(1):1-13.

164. Badylak SF, Gilbert TW. Immune response to biologic scaffold materials. Seminars in immunology 2008;20(2):109-16.

165. Sundararaghavan HG, Metter RB, Burdick JA. Electrospun fibrous scaffolds with multiscale and photopatterned porosity. Macromolecular bioscience 2010;10(3):265-70.

166. Jeon O, Krebs M, Alsberg E. Controlled and sustained gene delivery from injectable, porous PLGA scaffolds. Journal of biomedical materials research. Part A 2011;98(1):72-9.

167. Banker G, Goslin K. Culturing Nerve Cells: The MIT Press; 1998.

168. Wada MR, Inagawa-Ogashiwa M, Shimizu S, Yasumoto S, Hashimoto N. Generation of different fates from multipotent muscle stem cells. Development 2002;129(12):2987-95.

169. Kanisicak O, Mendez JJ, Yamamoto S, Yamamoto M, Goldhamer DJ. Progenitors of skeletal muscle satellite cells express the muscle determination gene, MyoD. Developmental biology 2009;332(1):131-41.

170. Lee JY, Qu-Petersen Z, Cao B, Kimura S, Jankowski R, Cummins J, Usas A, Gates C, Robbins P, Wernig A and others. Clonal isolation of muscle-derived cells capable of enhancing muscle regeneration and bone healing. The Journal of cell biology 2000;150(5):1085-100.

171. Christman KL, Lee RJ. Biomaterials for the treatment of myocardial infarction. J Am Coll Cardiol 2006;48(5):907-13.

172. Christman KL, Fok HH, Sievers RE, Fang Q, Lee RJ. Fibrin glue alone and skeletal myoblasts in a fibrin scaffold preserve cardiac function after myocardial infarction. Tissue engineering 2004;10(3-4):403-9.

173. Huang NF, Yu J, Sievers R, Li S, Lee RJ. Injectable biopolymers enhance angiogenesis after myocardial infarction. Tissue engineering 2005;11(11-12):1860-6.

174. Lu WN, Lu SH, Wang HB, Li DX, Duan CM, Liu ZQ, Hao T, He WJ, Xu B, Fu Q and others. Functional improvement of infarcted heart by co-injection of embryonic stem cells with temperature-responsive chitosan hydrogel. Tissue engineering. Part A 2009;15(6):1437-47.

175. Davis ME, Motion JP, Narmoneva DA, Takahashi T, Hakuno D, Kamm RD, Zhang S, Lee RT. Injectable self-assembling peptide nanofibers create intramyocardial microenvironments for endothelial cells. Circulation 2005;111(4):442-50.

176. Padin-Iruegas ME, Misao Y, Davis ME, Segers VF, Esposito G, Tokunou T, Urbanek K, Hosoda T, Rota M, Anversa P and others. Cardiac progenitor cells and biotinylated insulin-like growth factor-1 nanofibers improve endogenous and exogenous myocardial regeneration after infarction. Circulation 2009;120(10):876-87.

177. Kofidis T, Lebl DR, Martinez EC, Hoyt G, Tanaka M, Robbins RC. Novel injectable bioartificial tissue facilitates targeted, less invasive, large-scale tissue restoration on the beating heart after myocardial injury. Circulation 2005;112(9 Suppl):I173-7.

178. Konakci KZ, Bohle B, Blumer R, Hoetzenecker W, Roth G, Moser B, Boltz-Nitulescu G, Gorlitzer M, Klepetko W, Wolner E and others. Alpha-Gal on bioprostheses: xenograft immune response in cardiac surgery. European journal of clinical investigation 2005;35(1):17-23.

179. Flynn LE. The use of decellularized adipose tissue to provide an inductive microenvironment for the adipogenic differentiation of human adipose-derived stem cells. Biomaterials 2010;31(17):4715-24.

180. Baiguera S, Jungebluth P, Burns A, Mavilia C, Haag J, De Coppi P, Macchiarini P. Tissue engineered human tracheas for in vivo implantation. Biomaterials 2010;31(34):8931-8.

181. Macchiarini P, Jungebluth P, Go T, Asnaghi MA, Rees LE, Cogan TA, Dodson A, Martorell J, Bellini S, Parnigotto PP and others. Clinical transplantation of a tissue-engineered airway. Lancet 2008;372(9655):2023-30.

182. Chen YJ, Chung MC, Jane Yao CC, Huang CH, Chang HH, Jeng JH, Young TH. The effects of acellular amniotic membrane matrix on osteogenic differentiation and ERK1/2 signaling in human dental apical papilla cells. Biomaterials 2012;33(2):455-63.

183. Wilshaw SP, Kearney J, Fisher J, Ingham E. Biocompatibility and potential of acellular human amniotic membrane to support the attachment and proliferation of allogeneic cells. Tissue engineering. Part A 2008;14(4):463-72.

184. Wilshaw SP, Kearney JN, Fisher J, Ingham E. Production of an acellular amniotic membrane matrix for use in tissue engineering. Tissue engineering 2006;12(8):2117-29.

185. Mirsadraee S, Wilcox HE, Watterson KG, Kearney JN, Hunt J, Fisher J, Ingham E. Biocompatibility of acellular human pericardium. The Journal of surgical research 2007;143(2):407-14.

186. Flynn L, Prestwich GD, Semple JL, Woodhouse KA. Adipose tissue engineering with naturally derived scaffolds and adipose-derived stem cells. Biomaterials 2007;28(26):3834-42.

187. Hopper RA, Woodhouse K, Semple JL. Acellularization of human placenta with preservation of the basement membrane: a potential matrix for tissue engineering. Annals of plastic surgery 2003;51(6):598-602.

188. Baiguera S, Gonfiotti A, Jaus M, Comin CE, Paglierani M, Del Gaudio C, Bianco A, Ribatti D, Macchiarini P. Development of bioengineered human larynx. Biomaterials 2011;32(19):4433-42.

189. Chen AY, Yu C, Bodley A, Peng LF, Liu LF. A new mammalian DNA topoisomerase I poison Hoechst 33342: cytotoxicity and drug resistance in human cell cultures. Cancer research 1993;53(6):1332-7.

190. Lutolf MP, Hubbell JA. Synthetic biomaterials as instructive extracellular microenvironments for morphogenesis in tissue engineering. Nature biotechnology. Volume 23; 2005. p 47-55.

191. DeQuach JA, Mezzano V, Miglani A, Lange S, Keller GM, Sheikh F, Christman KL. Simple and high yielding method for preparing tissue specific extracellular matrix coatings for cell culture. PLoS ONE. Volume 5; 2010. p e13039.

192. Young DA, Ibrahim DO, Hu D, Christman KL. Injectable hydrogel scaffold from decellularized human lipoaspirate. Acta biomaterialia; 2010.

193. Seif-Naraghi SB, Salvatore MA, Schup-Magoffin PJ, Hu DP, Christman KL. Design and characterization of an injectable pericardial matrix gel: a potentially autologous scaffold for cardiac tissue engineering. Tissue Engineering Part A; 2010.

194. Stenger DA, Pike CJ, Hickman JJ, Cotman CW. Surface determinants of neuronal survival and growth on self-assembled monolayers in culture. Brain Res. Volume 630; 1993. p 136-47.

195. Ruoslahti E. Brain extracellular matrix. Glycobiology 1996;6(5):489-92.

196. Singelyn JM, DeQuach JA, Seif-Naraghi SB, Littlefield RB, Schup-Magoffin PJ, Christman KL. Naturally derived myocardial matrix as an injectable scaffold for cardiac tissue engineering. Biomaterials. Volume 30; 2009. p 5409-16.

197. Yuan SH, Martin J, Elia J, Flippin J, Paramban RI, Hefferan MP, Vidal JG, Mu Y, Killian RL, Israel MA and others. Cell-surface marker signatures for the isolation of neural stem cells, glia and neurons derived from human pluripotent stem cells. PLoS One;6(3):e17540.

198. Zeng X, Cai J, Chen J, Luo Y, You Z-B, Fotter E, Wang Y, Harvey B, Miura T, Backman C and others. Dopaminergic differentiation of human embryonic stem cells. Stem Cells. Volume 22; 2004. p 925-40.

199. Mizushima S, Nagata S. pEF-BOS, a powerful mammalian expression vector. Nucleic Acids Res 1990;18(17):5322.

200. Yuan SH, Qiu Z, Ghosh A. TOX3 regulates calcium-dependent transcription in neurons. Proc Natl Acad Sci U S A 2009;106(8):2909-14.

201. Wu JI, Lessard J, Olave IA, Qiu Z, Ghosh A, Graef IA, Crabtree GR. Regulation of dendritic development by neuron-specific chromatin remodeling complexes. Neuron 2007;56(1):94-108.

202. Griffin GD, Flanagan-Cato LM. Sex differences in the dendritic arbor of hypothalamic ventromedial nucleus neurons. Physiol Behav 2009;97(2):151-6.

203. Qian L, Saltzman WM. Improving the expansion and neuronal differentiation of mesenchymal stem cells through culture surface modification. Biomaterials. Volume 25; 2004. p 1331-7.

204. Czyz J, Wobus A. Embryonic stem cell differentiation: the role of extracellular factors. Differentiation. Volume 68; 2001. p 167-74.

205. Venstrom KA, Reichardt LF. Extracellular matrix. 2: Role of extracellular matrix molecules and their receptors in the nervous system. FASEB J. Volume 7; 1993. p 996-1003.

206. Pavlov I, Lauri S, Taira T, Rauvala H. The role of ECM molecules in activity-dependent synaptic development and plasticity. Birth Defects Res C Embryo Today. Volume 72; 2004. p 12-24.

207. Goetz AK, Scheffler B, Chen H-X, Wang S, Suslov O, Xiang H, Brüstle O, Roper SN, Steindler DA. Temporally restricted substrate interactions direct fate and specification of neural precursors derived from embryonic stem cells. Proc Natl Acad Sci USA. Volume 103; 2006. p 11063-8.

208. Edgar D, Timpl R, Thoenen H. The heparin-binding domain of laminin is responsible for its effects on neurite outgrowth and neuronal survival. The EMBO Journal. Volume 3; 1984. p 1463-8.

209. Ma W, Tavakoli T, Derby E, Serebryakova Y, Rao MS, Mattson MP. Cell-extracellular matrix interactions regulate neural differentiation of human embryonic stem cells. BMC Dev Biol. Volume 8; 2008. p 90.

210. Gilbert T, Sellaro T, Badylak S. Decellularization of tissues and organs. Biomaterials; 2006.

211. Grauss RW, Hazekamp MG, van Vliet S, Gittenberger-de Groot AC, DeRuiter MC. Decellularization of rat aortic valve allografts reduces leaflet destruction and extracellular matrix remodeling. J Thorac Cardiovasc Surg. Volume 126; 2003. p 2003-10.

212. Lumpkins SB, Pierre N, McFetridge PS. A mechanical evaluation of three decellularization methods in the design of a xenogeneic scaffold for tissue engineering the temporomandibular joint disc. Acta Biomater. Volume 4; 2008. p 808-16.

213. Smalheiser NR, Crain SM, Reid LM. Laminin as a substrate for retinal axons in vitro. Brain Res. Volume 314; 1984. p 136-40.

214. Ushakova GA, Nikonenko IR, Nikonenko AG, Skibo GG. Extracellular matrix heparin induces alteration of the cell adhesion during brain development. Neurochem Int. Volume 40; 2002. p 277-83.

215. Gilbert TW, Freund JM, Badylak SF. Quantification of DNA in biologic scaffold materials. J Surg Res. Volume 152; 2009. p 135-9.

216. Lin HJ, O'Shaughnessy TJ, Kelly J, Ma W. Neural stem cell differentiation in a cell-collagen-bioreactor culture system. Brain Res Dev Brain Res. Volume 153; 2004. p 163-73.

217. Rall W. Electrophysiology of a dendritic neuron model. Biophysical Journal. Volume 2; 1962. p 145-67.

218. Woerly S, Petrov P, Sykova E, Roitbak T, Simonova Z, Harvey AR. Neural tissue formation within porous hydrogels implanted in brain and spinal cord lesions: ultrastructural, immunohistochemical, and diffusion studies. Tissue Eng 1999;5(5):467-88.

219. Leor J, Amsalem Y, Cohen S. Cells, scaffolds, and molecules for myocardial tissue engineering. Pharmacol Ther 2005;105(2):151-63.

220. Uriel S, Labay E, Francis-Sedlak M, Moya ML, Weichselbaum RR, Ervin N, Cankova Z, Brey EM. Extraction and Assembly of Tissue-Derived Gels for Cell Culture and Tissue Engineering. Tissue Eng Part C Methods 2008.

221. Brown L. Cardiac extracellular matrix: a dynamic entity. Am J Physiol Heart Circ Physiol 2005;289(3):H973-4.

222. Rosso F, Giordano A, Barbarisi M, Barbarisi A. From cell-ECM interactions to tissue engineering. J Cell Physiol 2004;199(2):174-80.